# ON THE SYNTHESIS OF A CLASS OF GEARED LINKAGE MECHANISMS

A THESIS SUBMITTED TO
THE GRADUATE SCHOOL OF NATURAL AND APPLIED SCIENCES
OF
MIDDLE EAST TECHNICAL UNIVERSITY

BY

VOLKAN PARLAKTAŞ

IN PARTIAL FULFILLMENT OF THE REQUIREMENTS
FOR
THE DEGREE OF DOCTOR OF PHILOSOPHY
IN
MECHANICAL ENGINEERING

MAY 2007

Approval of the Graduate School of Natural and Applied Sciences

Prof. Dr. Canan Özgen
Director

I certify that this thesis satisfies all the requirements as a thesis for the degree of Doctor of Philosophy.

Prof. Dr. Kemal İder
Head of Department

This is to certify that we have read this thesis and that in our opinion it is fully adequate, in scope and quality, as a thesis for the degree of Doctor of Philosophy.

Prof. Dr. Eres Söylemez
Supervisor

**Examining Committee Members**

| | | |
|---|---|---|
| Prof. Dr. S. Kemal İder | (METU, ME) | |
| Prof. Dr. Eres Söylemez | (METU, ME) | |
| Prof. Dr. Reşit Soylu | (METU, ME) | |
| Prof. Dr. Tuna Balkan | (METU, ME) | |
| Prof. Dr. Yaşar T. Hondur | (Gazi Unv., ME) | |

**I hereby declare that all information in this document has been obtained and presented in accordance with academic rules and ethical conduct. I also declare that, as required by these rules and conduct, I have fully cited and referenced all material and results that are not original to this work.**

Name, Last name: Parlaktaş, Volkan

Signature:

# ABSTRACT

ON THE SYNTHESIS OF A CLASS OF GEARED LINKAGE MECHANISMS

Parlaktaş, Volkan

Ph.D., Department of Mechanical Engineering

Supervisor : Prof. Dr. Eres Söylemez

May 2007, 160 pages

In this thesis, two types of geared linkages are studied in detail. One of the mechanisms is the geared five link mechanism for which the input and output shafts are collinear. The other is a two degree-of-freedom nine-link mechanism which is called the "geared adjustable stroke mechanism". The geared adjustable stroke mechanism uses the geared five link mechanism in its structure. The geared adjustable stroke mechanism has been used in practice, but neither of these mechanisms have been studied in the literature. Analysis procedures are developed and expressions for the transmission angles of the mechanisms are derived. A synthesis procedure is proposed and charts are prepared for the design of such mechanisms.

Keywords: Geared Linkages, Geared Five Link Mechanisms, Adjustable Stoke Mechanisms

# ÖZ

BİR SINIF DİŞLİ MEKANİZMA TASARIMI

Parlaktaş, Volkan
Doktora, Makina Mühendisliği Bölümü
Tez Yöneticisi : Prof. Dr. Eres Söylemez

Mayıs 2007, 160 sayfa

Bu çalışmada, iki tip dişli mekanizma detaylı olarak ele alınmıştır. Bunlardan birincisi; giriş çıkış milleri aynı doğrultuda olan dişli beş çubuk mekanizmasıdır. İkincisi ise, iki serbestlik derecesine sahip, dokuz uzuvlu "dişli ayarlanabilir deplasmanlı mekanizmadır". Dişli ayarlanabilir deplasmanlı mekanizma yapısında dişli beş çubuk mekanizmasını kullanmaktadır. Dişli ayarlanabilir deplasmanlı mekanizma pratikte kullanılmıştır. Literatürde bu iki mekanizmanın da analizi ve tasarımıyla ilgili çalışmalar bulunmamaktadır. Bu mekanizmaların kuvvet iletim açıları belirlenmiş ve analiz yöntemleri geliştirilmiştir. Ayrıca bu mekanizmalar için tasarım metodları önerilmiş ve tasarım abakları hazırlanmıştır.

Anahtar Kelimeler: Dişli Mekanizmalar, Dişli Beş Çubuk Mekanizmaları, Değişken Deplasmanlı Mekanizmalar

**To My Parents**

## ACKNOWLEDGMENTS

The author wishes to express his deepest gratitude to his supervisor Prof. Dr. Eres Söylemez for his guidance, advice, criticism, encouragements and insight throughout the research.

The author would also like to thank Dr. Engin Tanık for his suggestions and comments.

## TABLE OF CONTENTS

## LIST OF TABLES

TABLES

## LIST OF FIGURES

FIGURES

## LIST OF SYMBOLS

$\theta_{ij}$ : Angle between $i^{th}$ and $j^{th}$ links

$s_{ij}$ : Position of $j^{th}$ link

$c_{19}$ : Height of the output slider axis

$a_i$ : Length of the $i^{th}$ link

$d_2$ : Length of link 2 of the GASM

$r_j$ : Radii of the gear j

$R$ : Gear ratio between gears 3 and 5

$R_2$ : Gear ratio between gears 7 and 5

$k_1$ : The integration constant

$k_2$ : The phase angle

$\delta$ : Adjustment angle

$\mu_1$ : Transmission angle of the GFLM

$\mu_2$ : Second transmission angle of the GASM

$\alpha$ : Pressure angle between the gears

$\phi$ : Rotation of the arm from the folded position to the extended position

$\psi$ : Rotation of link 4 from the folded position to the extended position

$\theta$ : Position of the arm (link 2) when the GFLM is at the folded position

$\xi$ : Position of link 4 when the GFLM is at the folded position

$\beta$ : Rotation of link 3 from the folded position to the extended position

$\lambda$ : Ratio of the lengths of link 3 over 4

$\lambda_2$ : Ratio of the lengths of link 7 over 8

$\Delta\theta_{l5}$ : Rotation of link 5 from the folded position to the extended position

$\Delta\theta_{l7}$ : Rotation of link 5 from the folded position to the extended position

$\theta_{ljf}$ : Position of link j when the GASM is at the folded position

$\theta_{ljf}$ : Position of link j when the GASM is at the folded position

$\theta_{lje}$ : Position of link j when the GASM is at the extended position

$\Delta s$ : Ouput stroke of the GASM

$s$ : Distance between the max. X coord. and the min. X coord. of path of point E

$h$ : Distance between the max. Y coord. and the min. Y coord. of path of point E

$\vec{z}_p$ : Equation of the moving centrode in polar coordinates

$\vec{Z}_p$ : Equation of the fixed centrode in polar coordinates

$x_p$ , $y_p$ : Equations of the moving centrode in cartesian coordinates

$X_p$ , $Y_p$ : Equations of the fixed centrode in cartesian coordinates

$\gamma$ : Diameter of the inflection circle

$\vec{C}$ : Center of the inflection circle

$\vec{I}$ : Inflection circle

$\vec{IP}$ : Inflection pole

$\zeta$ : Slope of the centrodes

$\upsilon$ : Angle between the X axis and the pole normal

PN : Pole normal

PT : Pole tangent

$\omega_{1j}$ : Angular velocity of the link j

$\alpha_{1j}$ : Angular acceleration of link j

$\ddot{s}_{19}$ : Acceleration of link 9

# CHAPTER 1

# INTRODUCTION

Geared linkages are useful mechanisms, which can be formed by combining planar linkages with one or more pairs of gears. Geared linkage mechanisms are suitable for obtaining large output motions, pilgrim step motions, and dwell motions with increased transmission characteristics.

This dissertation, presents in detail studies of two types of geared mechanisms. One of these is the geared adjustable stroke mechanism (GASM) and it is shown in Figure 1.1. Although it has been used in practice [1, 2], theory on its analysis and synthesis is not available in literature.

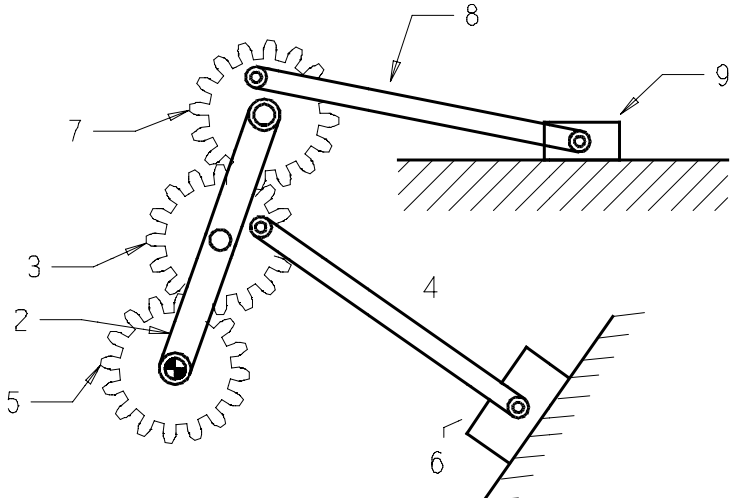


Figure 1.1 The Geared Adjustable Stroke Mechanism

This mechanism possesses two degrees-of-freedom. Link 6 is the stroke adjustment link and it can be positioned by an adjusting screw. The input is applied to link 5, and the output is obtained at link 9.

The GASM is investigated and it is observed that it will be useful to divide the problem into three parts and generalize each part.

In the first part, links 7, 8 and 9 are neglected and the mechanism is considered to be formed by the links 2, 3, 4, 5, and 6. When link 6 is fixed at a certain position, the mechanism becomes a geared five-link mechanism (GFLM), as shown in Figure 1.2. The input is applied to the sun gear (link 5), and the output is obtained at the arm (link 2). Thus, the input and the output displacements are about the same rotation axis.

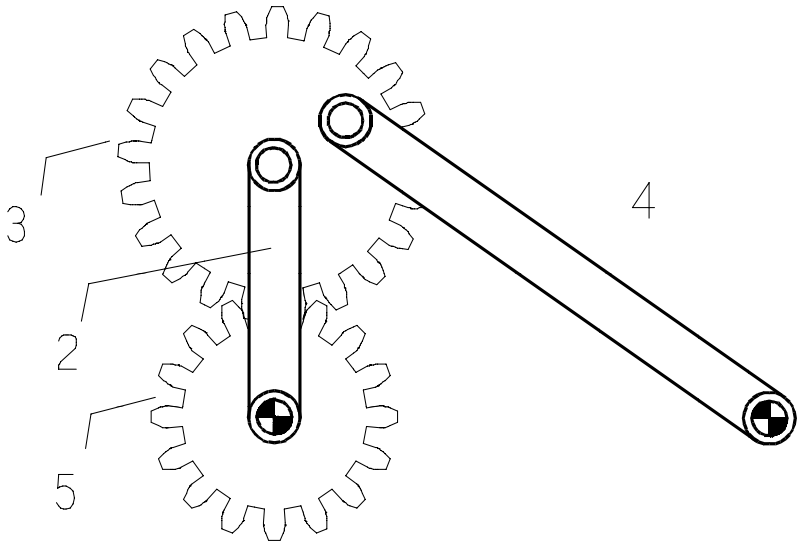


Figure 1.2 The Geared Five-Link Mechanism

The analysis and synthesis theory of this type of GFLM also is not available in literature. The motion characteristic of the GASM is defined by the arm (link2), and the arm is actuated by the GFLM. Hence, initially an analysis procedure is developed and an expression for the transmission angle of the GFLM is determined. Then, an optimum synthesis procedure is developed and design charts are prepared for such mechanisms.

In the second part, link 6 of the GASM is fixed at a certain position. Consequently, the GASM becomes an eight-link mechanism. The rotation of the input link produces

a large-stroke reciprocating motion of the output link. As the stroke increases the movability and the transmission angles of the mechanism becomes more critical. First of all, an analysis procedure is developed and transmission angles are determined for such mechanisms. Then, several methods have been developed to obtain mechanisms which can produce large strokes. Furthermore, an optimum synthesis procedure for maximum possible strokes is developed and corresponding design charts are prepared.

The third part of the problem is concerned with the stroke adjustment. The output stroke can be adjusted just by changing the position of link 6 by an actuator, even during the operation. As a result, considerable flexibility is introduced to the mechanism and the capacity of the mechanism is increased. In adjustable stroke mechanisms usually maximum variation in the stroke is desirable. A method for stroke adjustment is developed by changing the position of the link 6 and design charts for adjustment are prepared.

# CHAPTER 2

## SURVEY of the RELATED LITERATURE

The kinematic and dynamic syntheses of geared five-bar linkages have been studied extensively. Neumann [3] classified the geared mechanisms as shown in Figure 2.1 and obtained their output motions as functions of the inputs.

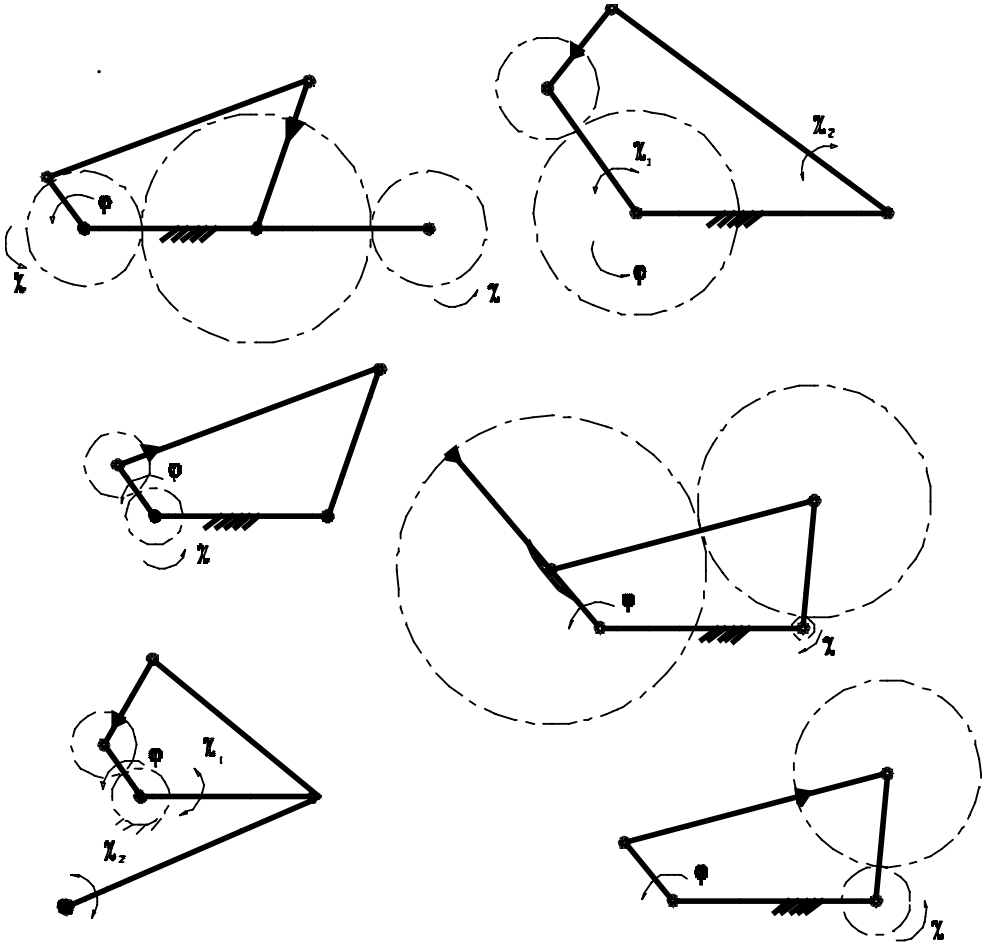

Figure 2.1 Classification of Geared Mechanisms due to Neumann [3]

Neumann [4] searched for the type of mechanism, which could produce the largest output oscillation among from the others and prepared design charts for this type of mechanism. This mechanism is a crank-rocker type as shown in Figure 2.2. Neumann [5] also investigated its dynamic characteristics and compared it with a six-link mechanism which generated the same motion.

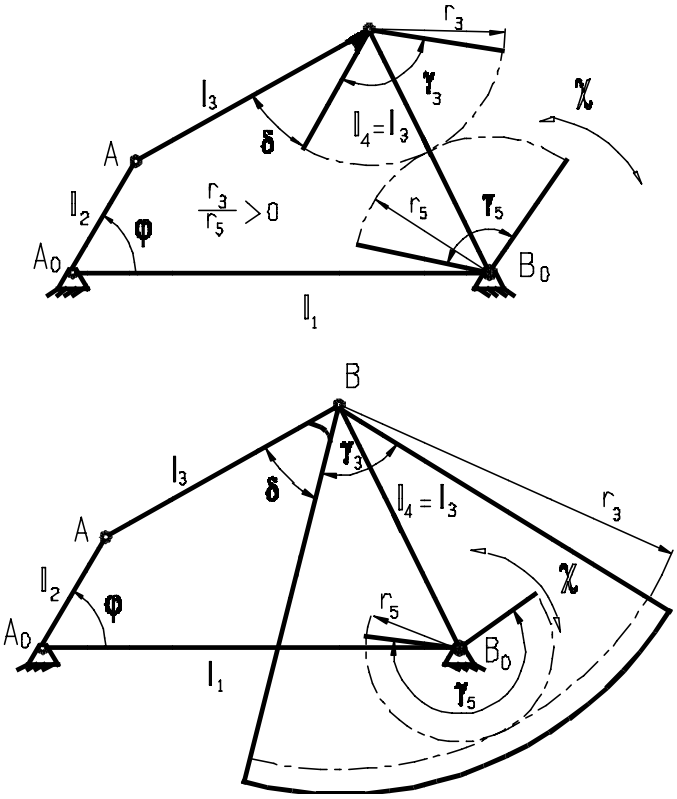


Figure 2.2 Crank-Rocker Type Geared Five-Link Mechanisms [4]

Volmer, J., Riedel, H., and Rissman, E., [6] studied geared five-link mechanisms and obtained a pilgrim step motion by adding an internal gear train to the crank of the four-bar mechanisms. Volmer, J., and Meiner, C., also obtained pilgrim step motion by adding an internal gear train to the crank of slider-crank mechanisms [7, 8]. These mechanisms are shown in Figures 2.3 and 2.4.

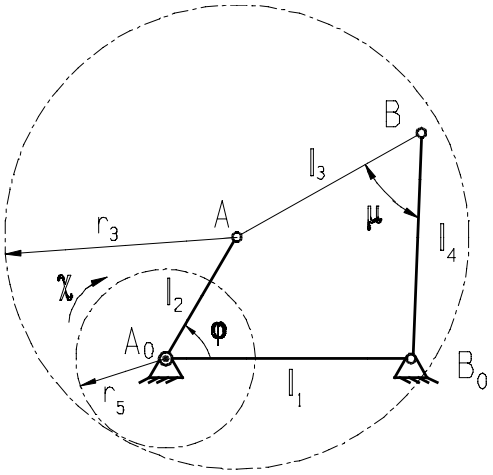


Figure 2.3 Pilgrim Step Motion via a Geared Five-Link Mechanism

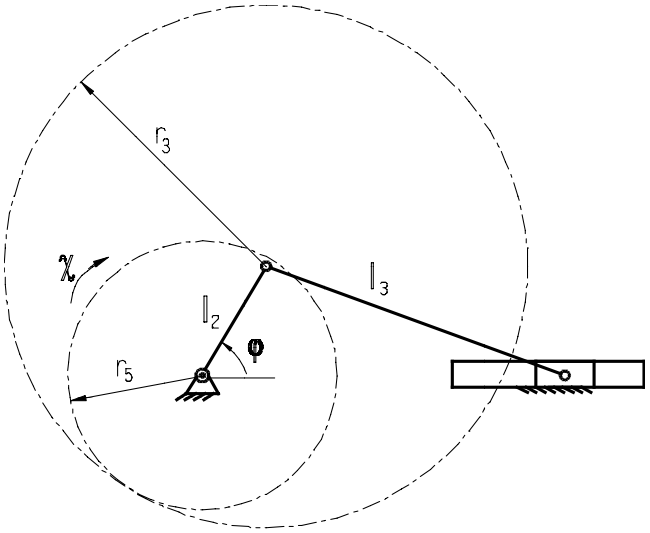


Figure 2.4 Pilgrim Step Motion via a Geared Slider-Crank Mechanism

Yüksel and Söylemez [9] studied several types of geared five-link mechanism and prepared design charts for the mechanisms generating pilgrim step motion.

Erdman and Sandor [10] synthesized a geared five-bar function generator. Geared linkage function generators are extensively studied in the literature [11, 12, 13]. A typical geared five-bar function generator is show in Figure 2.5.

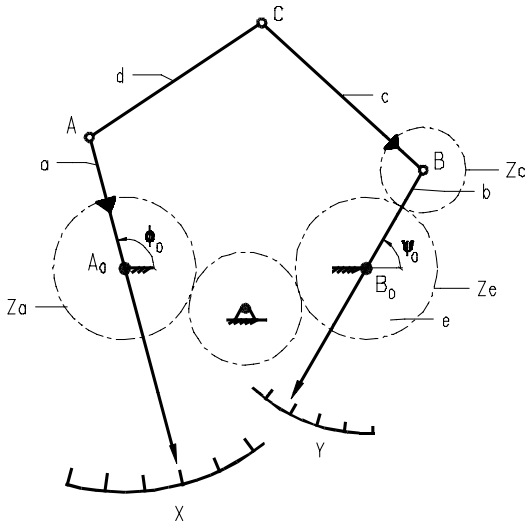


Figure 2.5 A Typical Geared Five-Bar Function Generator

W. Lee and Freudenstein [14] designed geared 5-bar mechanisms for unlimited crank rotations and optimum transmission, Figure 2.6. Rao [15] synthesized geared planar 4-bar linkages and cams to generate function of two variables. Li and Cao [16] synthesized geared planar 5-bar linkages to obtain dwell.

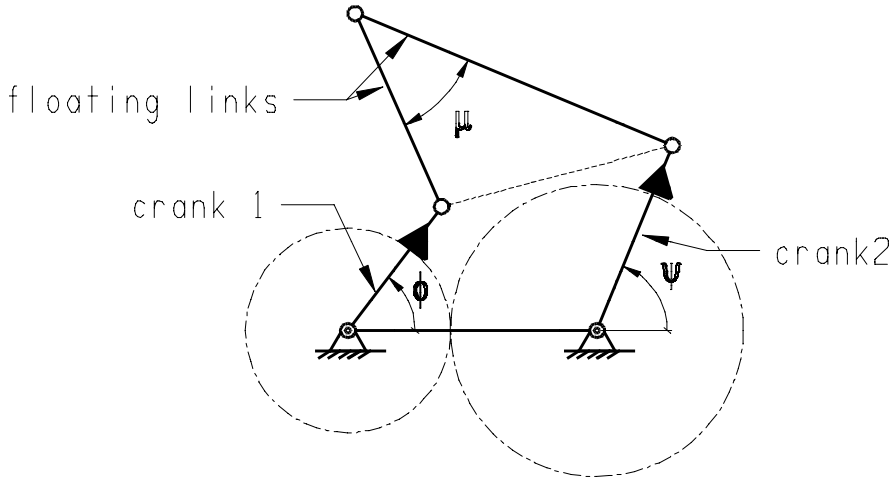


Figure 2.6 A Geared Five-Bar Mechanism Due to Lee and Freudenstein

Robots are extremely capable of accommodating variations within a given task, but if these variations are limited, adjustable mechanisms can also accomplish the same variations.

Hong and Erdman [17] described a new method for the synthesis of adjustable four-bar linkages, both in planar and spherical form. They used fixed ground pivots and an adjustable length for input and output links.

Sodhi and Russel [18] presented a new technique for synthesizing planar four-bar mechanisms for multi-phase motion generation with tolerances. This method is an extension of the adjustable RRSS motion generation synthesis methods developed by these authors [19, 20]. Sodhi and Russel [21] also presented a method to design planar five-bar mechanisms to achieve multiple phases of prescribed rigid body path points. By prescribing the angular positions of one driving link with respect to synthesized moving pivot positions of the other driving link, the positions of both driving links are synchronized. The same authors also presented methods for designing slider-crank mechanisms to achieve multiphase motion generation, path and function generation [22, 23].

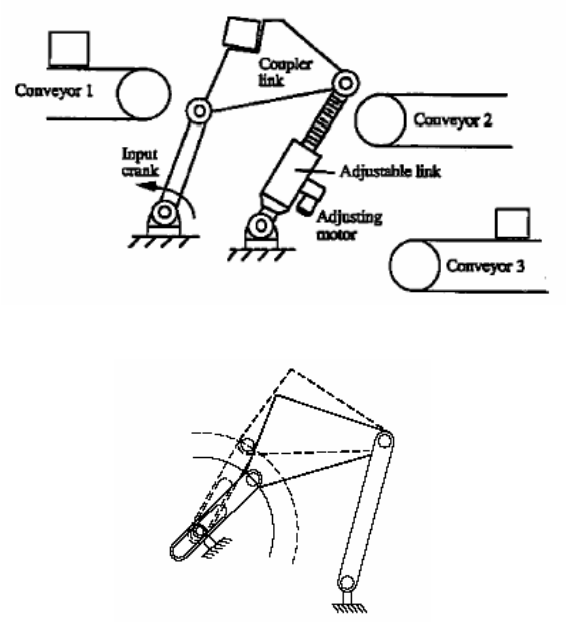


Figure 2.7 Adjustable Four-Bar Linkages

McGovern and Sandor [24, 25] presented methods to synthesize adjustable mechanisms for function and path generation using complex variables. Ahmad and Waldron [26] outlined synthesis techniques of adjustable 4-bar mechanisms for motion generation with driven side-link pivot adjustment. Zhou and Ting [27] analyzed the path flexibility of adjustable slider–crank linkages and set up an optimal synthesis method.

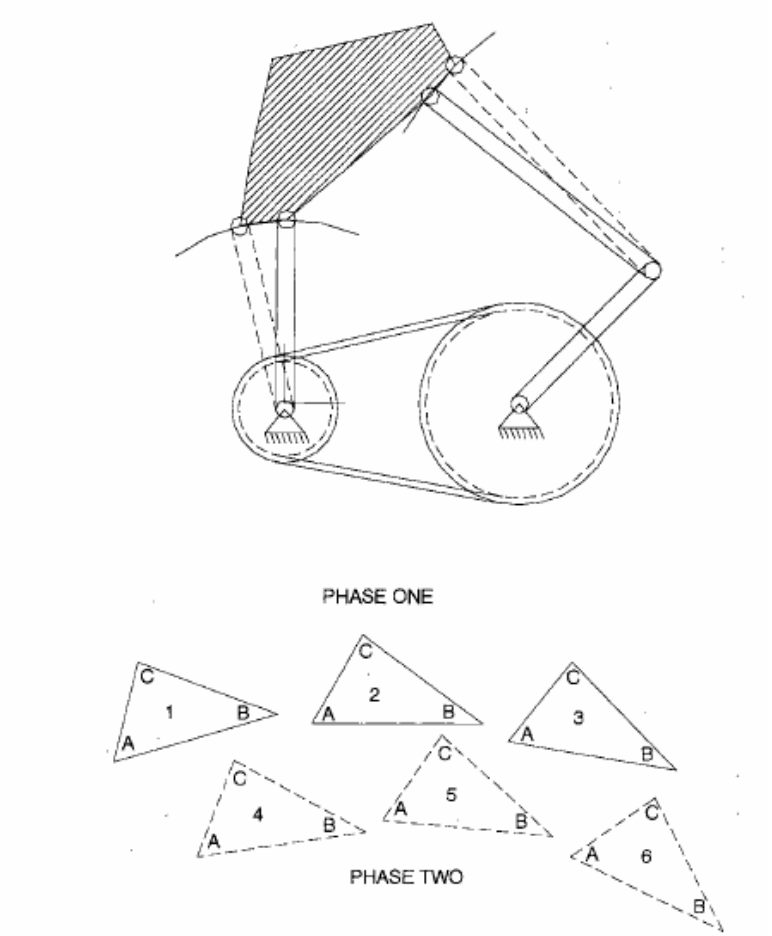


Figure 2.8 An Adjustable Five-Bar Linkage

Kohli and Soni [28] proposed a synthesis technique to design for varieties of synthesis problems for seven-link mechanisms with two degrees of freedom. Mruthyunjaya [29] presented a graphical method for synthesis of the general, seven-

link, two degree-of-freedom plane linkage to generate functions of two variables. The method is based on point position reduction and permits the synthesis of the linkage to satisfy up to six arbitrarily selected precision positions (Fig.2.9).

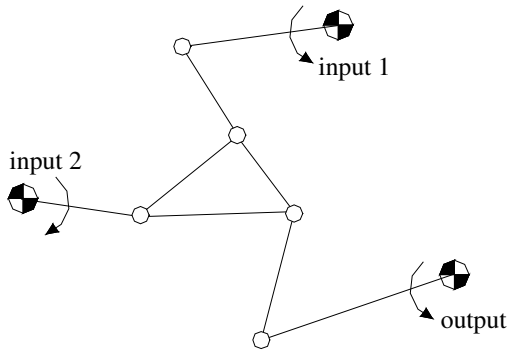


Figure 2.9 General Two Degree-of-Freedom Linkage

Handra-Luca [30] discussed the basic principles of linkages with adjustable output oscillations, and, showed how to design six-bar linkages with adjustable output oscillations. In Figure 2.10 one such mechanism is shown. The mechanism is made up of 4-bar $O_1ABO_2$ to which $CDO_3$ has been added. The input link is $O_1A$ (crank) and the output link is $DO_3$ (rocker). Displacing the fixed joint $O_2$ to different positions causes a variation in the magnitude of the oscillation.

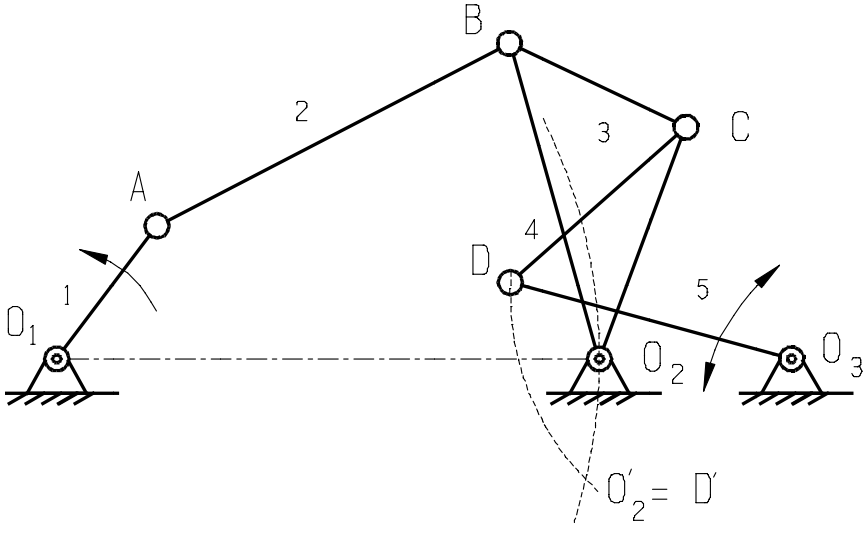


Figure 2.10 An Adjustable Oscillation Linkage [30]

In order not to alter the link lengths of the 4-bar mechanism, the joint $O_2$ is rotated about center $O_1$ with the radius $O_1O_2$. At a certain phase the joint $O_2$ overlaps D ($O_2^{/}$ = $D^{/}$) thus the output link remains at rest for a rotation of the crank.

For the mechanisms shown in Fig.2.11, the link $O_1O_2$ is rotated around $O_1$. When $O_2$ coincides with the sliding joint of link-5, the rocker will remain stationary. The oscillation angle of the output link increases as $O_2$ gets further from $O_2^{/}$.

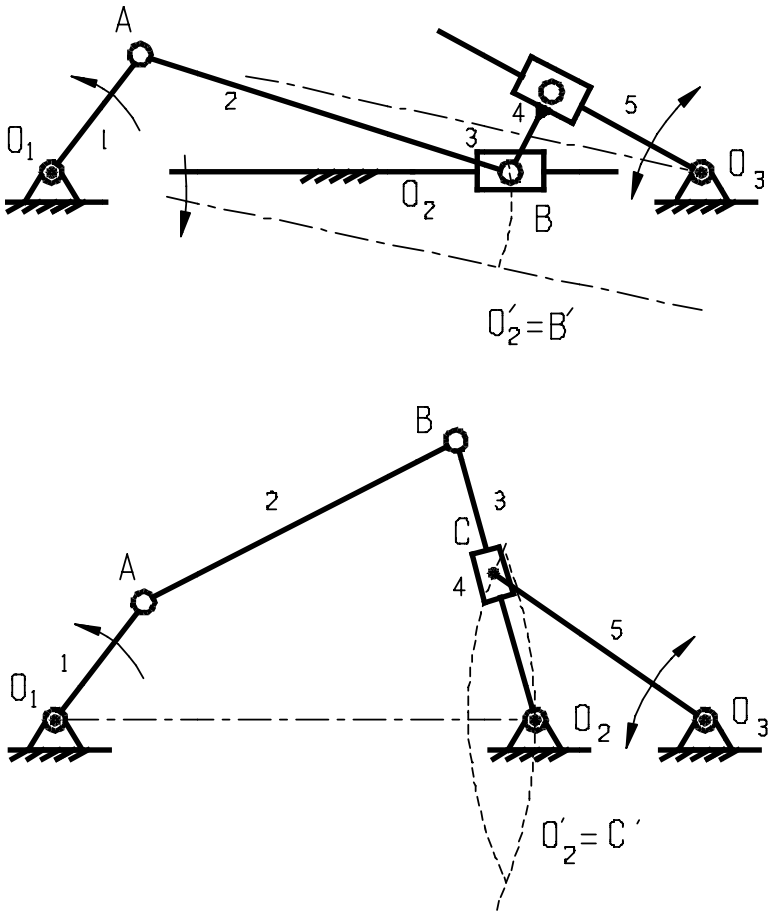


Figure 2.11 Adjustable Oscillation Mechanisms [30]

Akmeşe and Söylemez [31] synthesized serially connected two four-bar mechanisms, which performs variable output-link oscillation, Figure 2.12. By changing the

position of the link AD, the output-link oscillation is changed. Since the control-link AD is the fixed link of the first four-bar mechanism, the proportions of the first four-bar mechanism doesn't change.

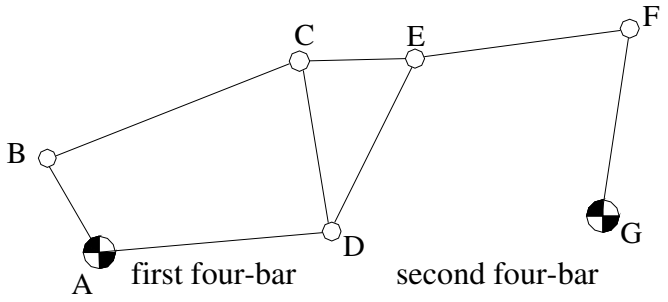


Figure 2.12 The Adjustable Oscillation Four-Bar Mechanism [31]

Tanık and Söylemez [32] developed a synthesis procedure for two different types of seven-link mechanisms. These mechanisms work as six-link mechanisms for different positions of the control-link to achieve the required output oscillations, Figure 2.13.

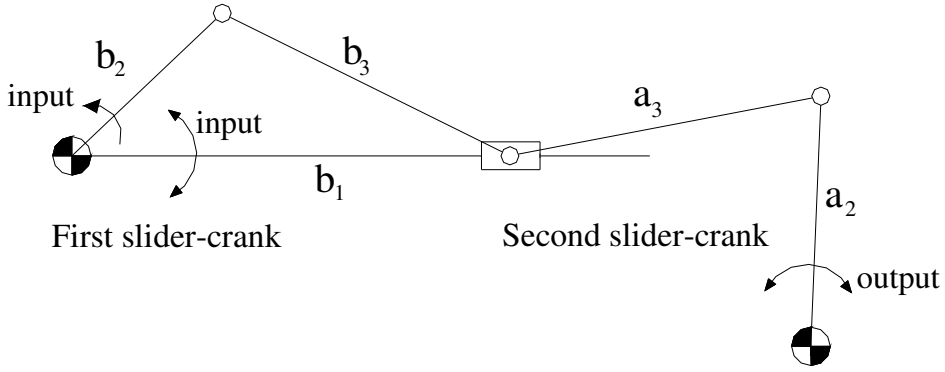


Figure 2.13 The Adjustable Oscillation Seven-Link Mechanism [32]

Kireçci, Dülger and Gültekin [33] used a seven-link, two degree-of-freedom mechanism, for variable oscillation at output, Figure 2.14. The input link is link-2,

the output link is link 7 and the translational adjustment at link 5 provides variable oscillation. The adjustment control system is mounted on link 4, which is driven by a servomotor.

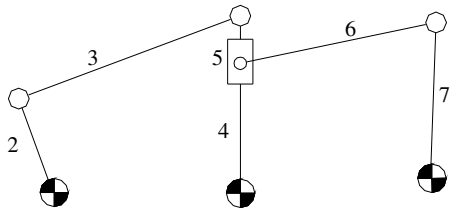


Figure 2.14 Variable Oscillation Seven-Link Mechanism [33]

# CHAPTER 3

# KINEMATIC ANALYSIS and SYNTHESIS of the GEARED FIVE-LINK MECHANISM

## 3.1 Introduction

### 3.1.1 Enumeration of Geared Five-Link Mechanisms

Geared five-link mechanisms have two basic kinematic topologies. They are shown in Figures 3.1 and 3.2 irrespective of the fixed link.

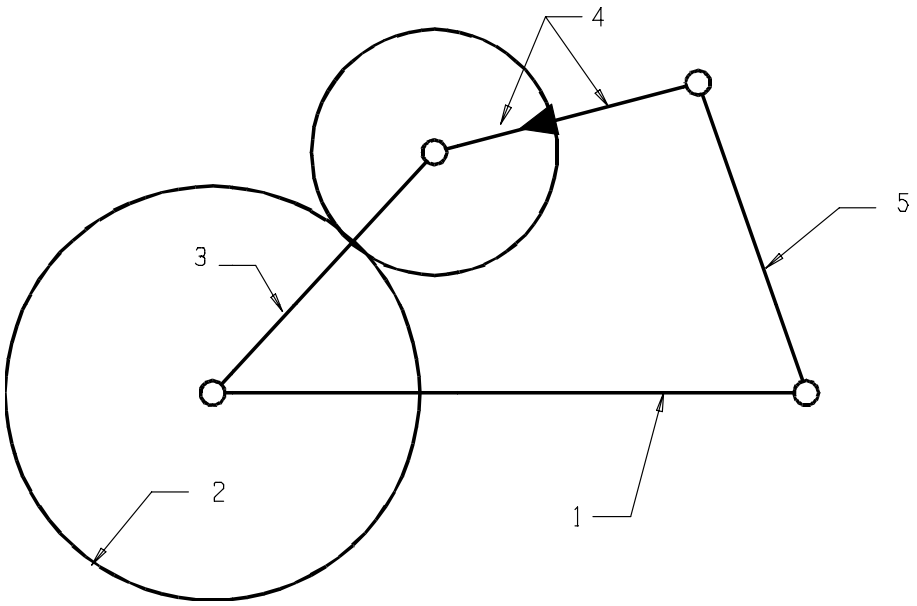


Figure 3.1 Topology Type A

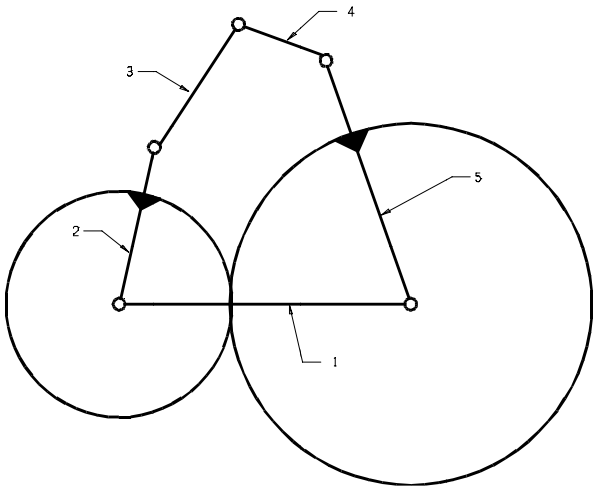


Figure 3.2 Topology Type B

The mechanism studied in this work has a topology type A. Different mechanisms can be obtained by fixing links 1 to 5 in structure type A. Moreover, by changing the input and output links, different motions can be achieved. These mechanisms can be summarized as:

**a)** Link 1 Fixed

Table 3.1 Possible Input-Output Links when Link 1 Fixed

| Input | Output |
|---|---|
| 2 | 3 |
| 2 | 5 |
| 5 | 2 |
| 5 | 3 |
| 3 | 2 |
| 3 | 5 |

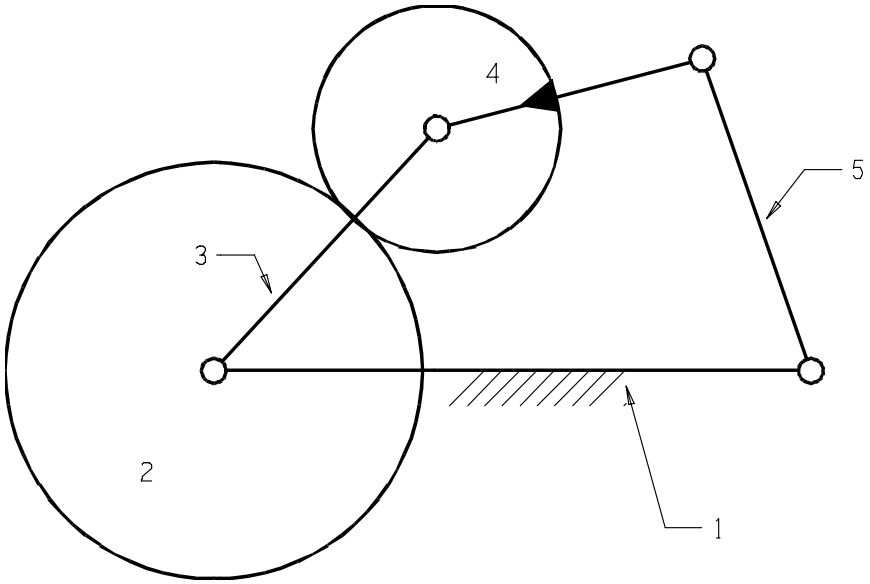


Figure 3.3 Mechanism Type A1

In Fig.3.4, an application of mechanism type A1 (input-3, output-2) is shown. A cycloidal motion for dwell is obtained by this mechanism [34].

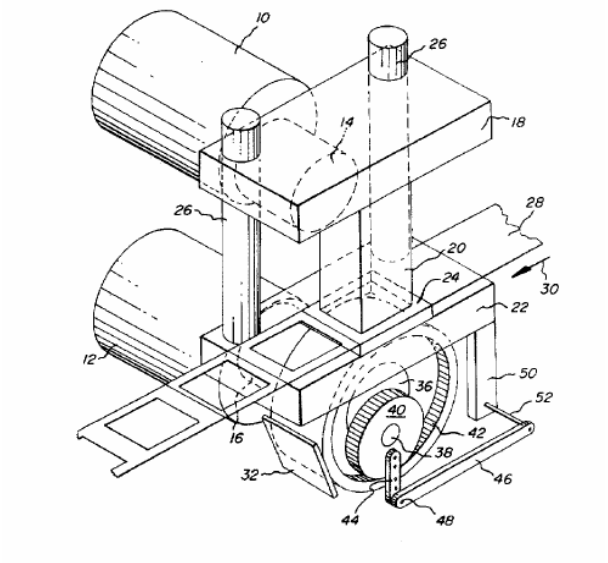


Figure 3.4 “Variable Dwell Cycloidal Indexing Device”

**b)** Link 2 Fixed

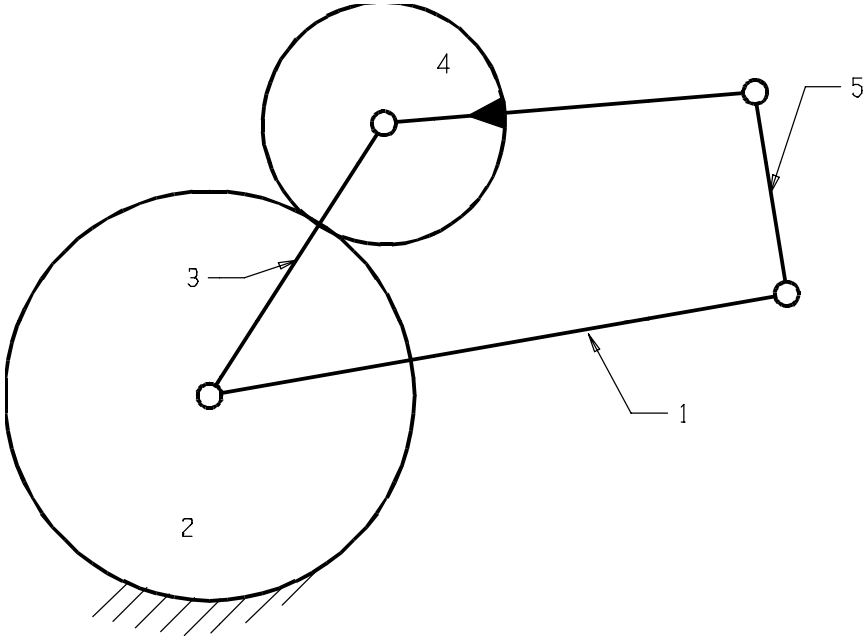


Figure 3.5 Mechanism Type A2

Table 3.2 Possible Input-Output Links when Link 2 Fixed

| Input | Output |
|---|---|
| 3 | 1 |

This kind of mechanism is used for obtaining cycloidal drive motion.

**c)** Link 3 Fixed

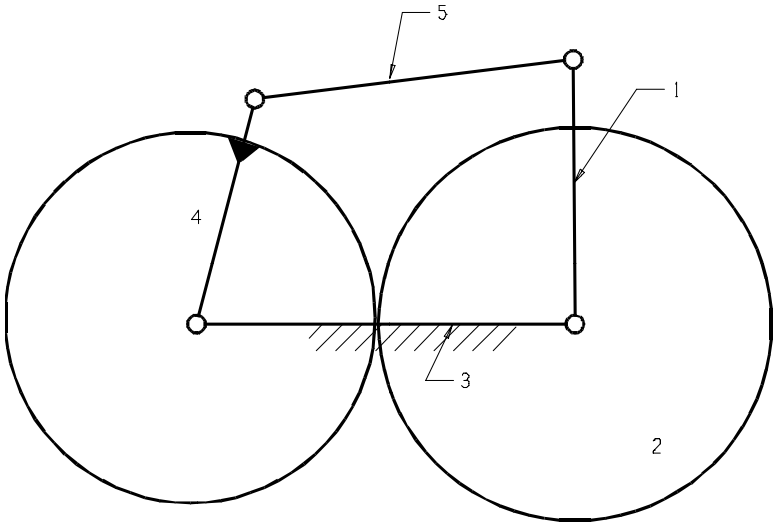


Figure 3.6 Mechanism Type A3

This mechanism is basically a four-bar with a simple gear train in series.

**d)** Link 4 Fixed

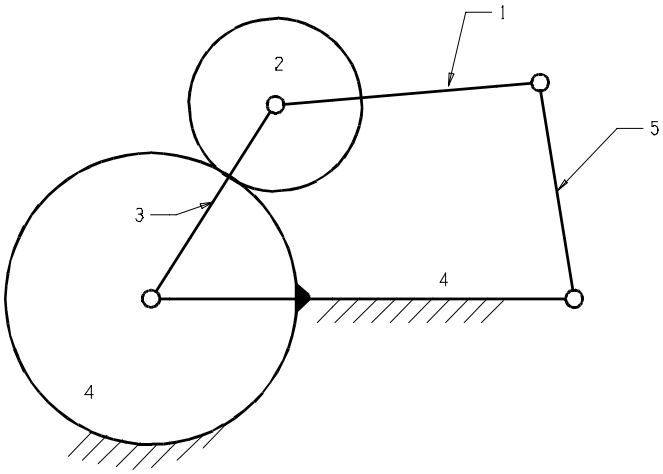


Figure 3.7 Mechanism Type A4

This mechanism is similar to Type A2.

**e)** Link 5 Fixed

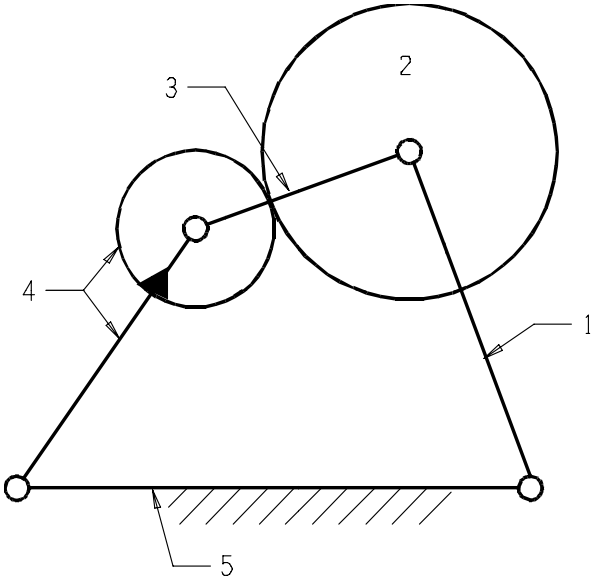


Figure 3.8 Mechanism Type A5

This is a four-bar mechanism with a floating gear.

In order to obtain different input-output functions, instead of external gears internal gears can also be used in some of these mechanisms, Fig. 3.9. Such mechanisms have found application for pilgrim step motion in which there is a momentary dwell or reversal of motion for a continuous input or for large output oscillations.

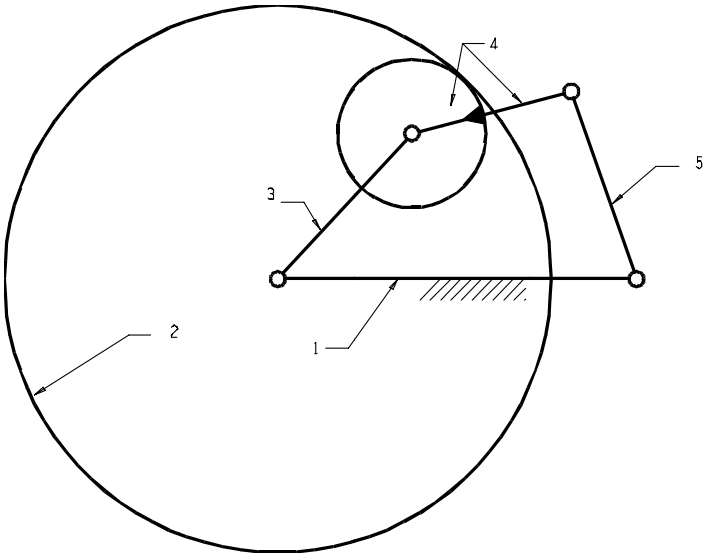


Figure 3.9 Mechanism Type A1 with Internal Gear

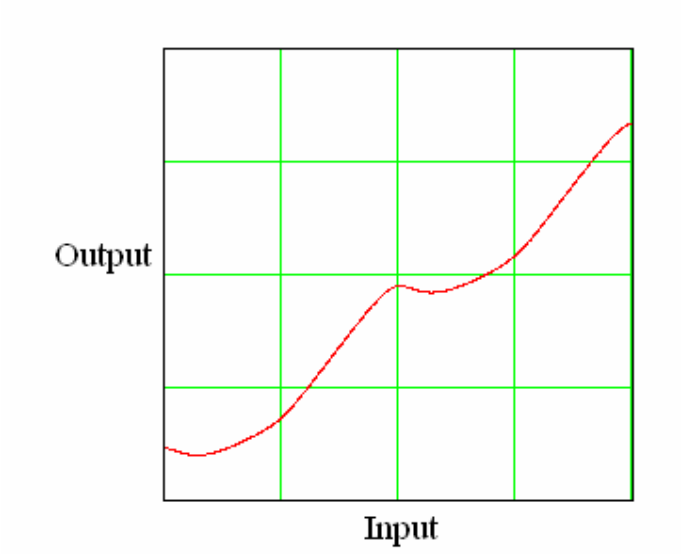


Figure 3.10 A Pilgrim Step Motion

### 3.2 Geared Five-Link Mechanism Type A1

A single degree-of freedom, type A1 GFLM is shown in Figure 3.11. The gears and link 2 form a planetary gear train, where link 5 is the sun gear, link 3 is the planet gear, and link 2 is the arm. The input torque is applied to the sun gear, and the output link is the arm. Thus, the input and the output displacements are about the same rotation axis. As link 5 rotates continuously, link 3 also makes a full rotation and links 2 and 4 oscillate.

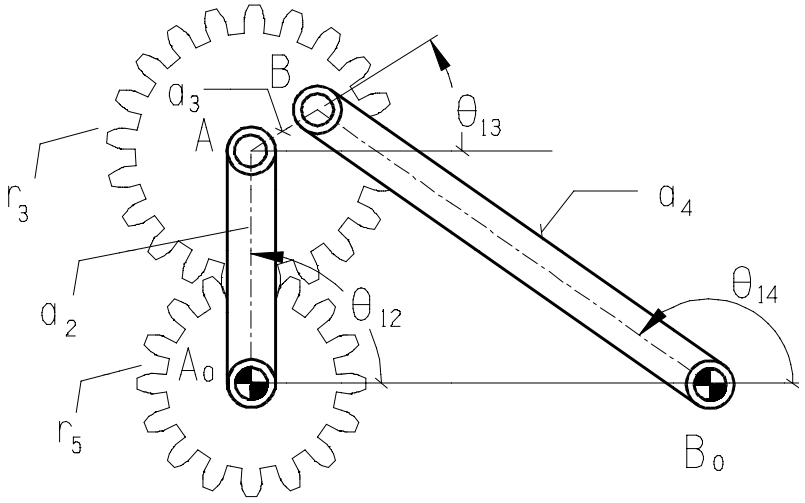


Figure 3.11 A Geared Five-Link Mechanism Type A1

### 3.3 Motion Analysis of the Geared Five-Link Mechanism

Consider the loop formed by the links:

$$\vec{A_o A} + \vec{AB} = \vec{A_o B_o} + \vec{B_o B}$$

In complex numbers the vector loop equation is:

$$(r_5 + r_3)e^{i\theta_{12}} + a_3 e^{i\theta_{13}} = a_1 + a_4 e^{i\theta_{14}} \tag{3.1}$$

There is another loop formed by links 2, 3 and 5, where one of the joints is the gear pair. This is a planetary gear arrangement. The velocity ratio between the links is given by:

$$-\frac{r_3}{r_5}=\frac{\omega_{15}-\omega_{12}}{\omega_{13}-\omega_{12}} \tag{3.2}$$

Integrating equation (3.2),

$$\theta_{13}=(\frac{R+1}{R})\theta_{12}-\frac{\theta_{15}}{R}+k_1 \tag{3.3}$$

where, the gear ratio $R = r_3/r_5$ and $k_1$ is a constant.

Equation (3.3) can be used in equation (3.1) to eliminate $\theta_{13}$. Then this equation can be multiplied by its complex conjugate to obtain a relationship between $\theta_{15}$ and $\theta_{12}$, which leads a 4th order polynomial equation. A closed form relationship between the input and the output could not be reached by this method.

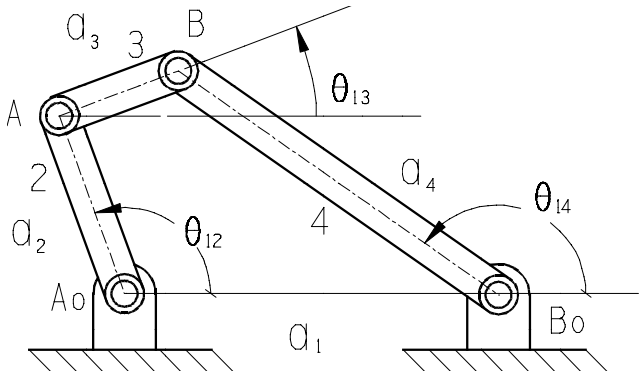


Figure 3.12 A Four-Bar Mechanism Whose Coupler Link is the Input

In order to obtain a simpler motion analysis method for the GFLM, let us assume the angular rotation of link 3 to be the input. Continuous rotation of the input link (5) results in a continuous rotation of link 3. In such a case, the mechanism can be

analyzed as a four-bar mechanism with the coupler link as the input, and the angular rotations of links 2 and 4 can be determined in terms of the angular rotation of the coupler.

The loop closure equation for the mechanism is:

$$\vec{A_o A} + \vec{AB} = \vec{A_o B_o} + \vec{B_o B}$$

In complex numbers the vector loop equation and its complex conjugate can be written as:

$$a_2 e^{i\theta_{12}} + a_3 e^{i\theta_{13}} = a_1 + a_4 e^{i\theta_{14}} \tag{3.4}$$

$$a_2 e^{-i\theta_{12}} + a_3 e^{-i\theta_{13}} - a_1 = a_4 e^{-i\theta_{14}} \tag{3.5}$$

Multiplying (3.4) by (3.5) and rearranging terms, the relationship between $\theta_{13}$ and $\theta_{12}$ can be obtained as:

$$\theta_{12} = 2.\tan^{-1}\left(\frac{-B \mp \sqrt{B^2 - 4.A.C}}{2.A}\right) \tag{3.6}$$

where,

$A = K_1 - K_2 \cos\theta_{13} + K_3 - K_4 \cos\theta_{13}$

$B = 2K_2 \sin\theta_{13}$

$C = K_1 + K_2 \cos\theta_{13} - K_3 - K_4 \cos\theta_{13}$

$K_1 = a_1^2 + a_2^2 + a_3^2 - a_4^2$

$K_2 = 2a_2 a_3$

$K_3 = 2a_1 a_2$

$K_4 = 2a_1 a_3$

For every value of $\theta_{13}$, there are two values of $\theta_{12}$ as shown in Fig. 3.13. Depending on the form of assembly, one of the solutions can be eliminated.

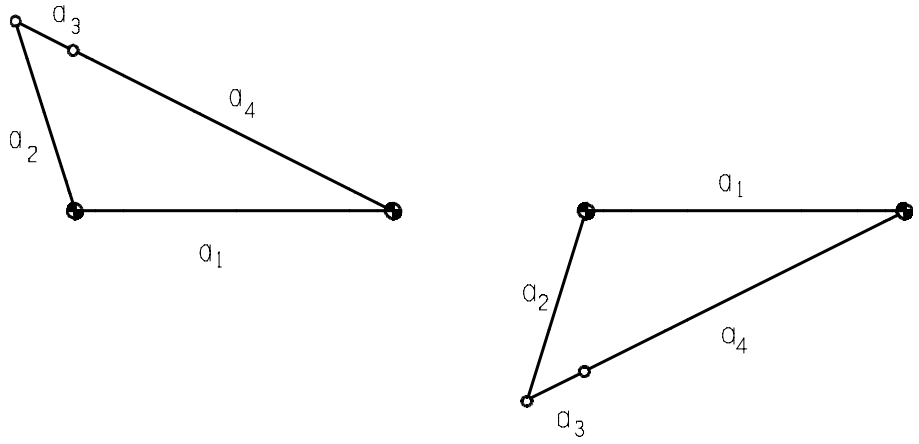


Figure 3.13 Forms of Assembly

$\theta_{14}$ can be obtained from Eq.3.4 after determining $\theta_{12}$.

The mechanism is analyzed as a four-bar mechanism where the input is from the coupler link (link 3), which makes a full rotation, and the output is link 2. The four-bar mechanism is double-rocker type according to Grasshof's rule. Sum of the lengths of the shortest and the longest links is less than the sum of the two intermediate links, the shortest link makes a full rotation, and the link opposite the shortest link is the frame.

The relationship between $\theta_{13}$ and $\theta_{12}$ is obtained in Eq 3.6, so rotation of the output link (2) is determined in terms of the angular rotation of the coupler. However, since the input link is link 5, rotation of the output link (2) must be determined in terms of the input link (5), so the relationship between $\theta_{15}$ and $\theta_{12}$ must be obtained. Therefore, from Eq. 3.3, $\theta_{15}$ can be obtained in terms of $\theta_{13}$ and $\theta_{12}$:

$$\frac{\theta_{15}}{R} = (\frac{R+1}{R})\theta_{12} - \theta_{13} + k_1$$

where, the gear ratio, $R = r_3/r_5$, and $k_1$ is a constant. Note that, $r_3+r_5 = a_2$ .

### 3.4 Transmission Angle of the Geared Five-Link Mechanism

The transmission angle of a mechanism is defined as [35]:

$$\tan(\mu) = \frac{\text{force component acting on the output link tending to produce output rotation}}{\text{force component tending to apply pressure on the driven link bearings}}$$

Neglecting the mass of the links, the free-body diagrams of the links of the mechanism will be as shown in Fig. 3.14. Where, $T_i$ is the input torque applied to link 5, $T_o$ is the output torque at link 2, and $\alpha$ is the pressure angle of the gears. The transmission angle of the mechanism can be obtained as:

$$\tan(\mu) = \frac{F_{32t}}{F_{32n}}$$

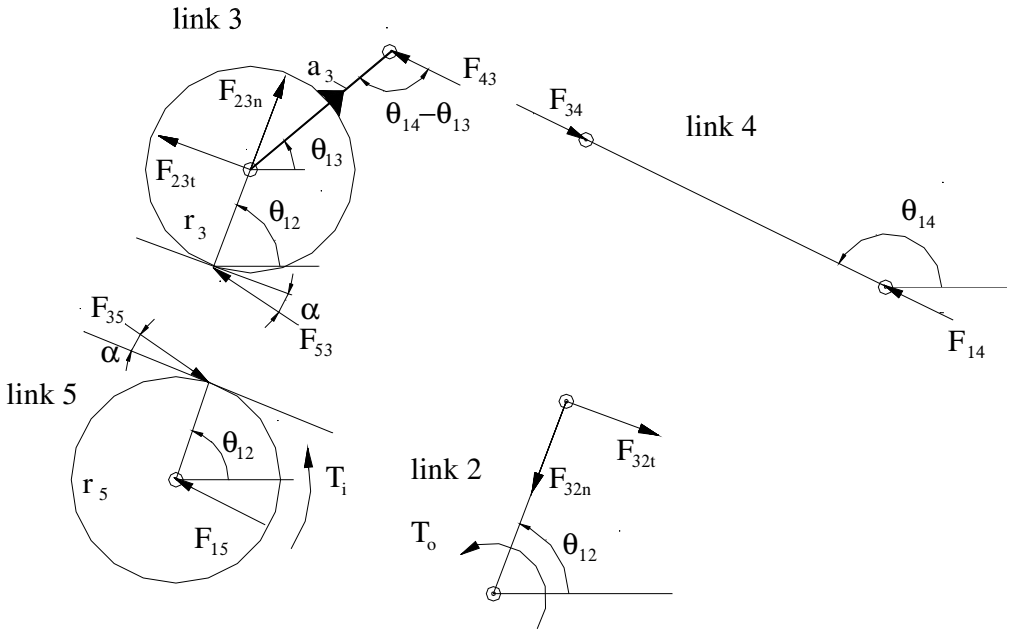


Figure 3.14 Free-Body Diagrams of the Links

From the free-body diagrams of the links, $F_{32t}$ and $F_{32n}$ can be obtained, manipulating these equations, transmission angle can be determined as:

$$\tan(\mu) = \frac{-\frac{a_3}{r_3}\sin(\theta_{14}-\theta_{13}) - \sin(\theta_{14}-\theta_{12})}{\frac{a_3}{r_3}\tan(\alpha)\sin(\theta_{14}-\theta_{13}) + \cos(\theta_{14}-\theta_{12})} \tag{3.7}$$

A very interesting property is observed in the transmission characteristics of the mechanism. If the direction of rotation of the input link 5 is changed, then the transmission angle of the mechanism alters since the direction of the force between the gears 3 and 5 changes (Fig.3.15). In this case, the transmission angle will be given by:

$$\tan(\mu) = \frac{-\frac{a_3}{r_3}\sin(\theta_{14}-\theta_{13}) - \sin(\theta_{14}-\theta_{12})}{-\frac{a_3}{r_3}\tan(\alpha)\sin(\theta_{14}-\theta_{13}) + \cos(\theta_{14}-\theta_{12})} \tag{3.8}$$

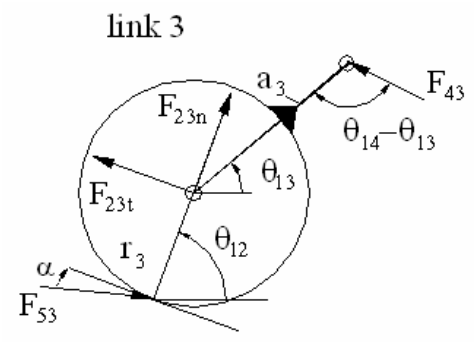


Figure 3.15 Free-Body Diagram of Link 3

Attempts at finding examples on dependence of transmission angle on the direction of rotation in the literature were unsuccessful. However, for this type of GFLM, direction of rotation of the input link significantly affects transmission angle. A mechanism which has proper transmission angle values in one rotation direction can even lock if the direction of rotation of the input is reversed.

### 3.5 Synthesis of the Geared Five-Link Mechanism

It is mentioned that the mechanism is analyzed as a four-bar mechanism where the input is from the coupler link (link 3), which makes a full rotation, and the output is link 2. The four-bar mechanism is double-rocker type according to Grasshof's rule. A synthesis procedure is devised by using the same logic. The problem is considered in two parts. The first part is the synthesis problem in which one must determine four-bar mechanisms with double-rocker proportions that must have a given swing angle ($\phi$) and a corresponding rotation of link 4 ($\psi$). There is an infinite set of solutions for this part of the problem. The second part of the problem is concerned with the optimization. Out of the infinite possible set of solutions obtained in the first part, one must determine a particular mechanism whose maximum transmission angle deviation from $90^o$ is a minimum. The transmission angle optimization is performed for several gear ratios.

The extended and folded positions of the mechanism are shown in Fig. 3.16. When links 3 and 4 are at the extended position, link 2 is at the forward position and when links 3 and 4 are at the folded position, link 2 is at the fully withdrawn position.

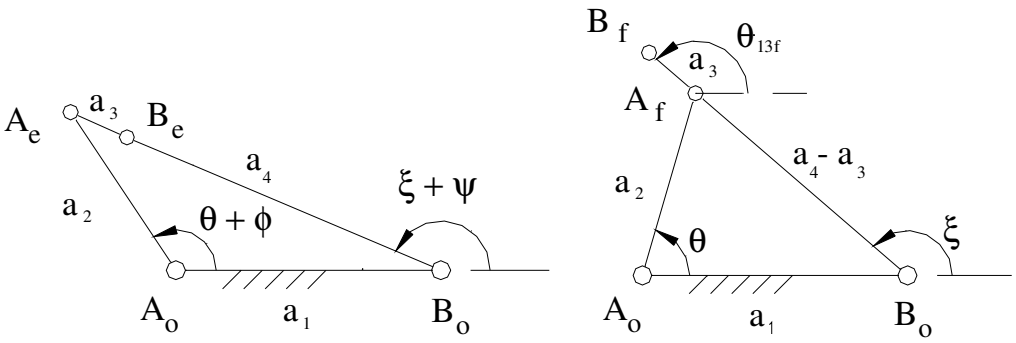


Figure 3.16 Dead-Center Positions of the GFLM

$\theta$ is the position of the arm (link 2) when the mechanism is at the folded position. $\phi$ is the rotation of the arm from the folded position to the extended position. In other words, $\phi$ is the output swing angle. $\xi$ corresponds to the folded position of link 4, where $\xi = \theta_{13f}$. $\psi$ is the rotation of link 4 from the folded position to the extended

position, where $\xi + \psi = \theta_{13e} - \pi$. If $\psi$ is equal to zero, then the mechanism is symmetric with respect to link 3 (the rotation of link 3 between the dead centers is $180^o$). The loop closure equations for the folded and extended positions of the mechanism can be written as [36]:

$$a_2.e^{i\theta} = a_1 + (a_4 - a_3)e^{i\xi} \tag{3.9}$$

$$a_2.e^{i(\theta+\phi)} = a_1 + (a_4 + a_3)e^{i(\xi+\psi)} \tag{3.10}$$

One can define $Z_1$, $Z_2$ and $\lambda$ as:

$$Z_1 = a_2.e^{i\theta}$$

$$Z_2 = a_4 e^{i\xi}$$

$$\lambda = \frac{a_3}{a_4}$$

Without a loss of generality fixed link can be chosen as unity,

$$a_1 = 1$$

Then, equations (3.9) and (3.10) can be written in normalized form as:

$$Z_1 - Z_2(1-\lambda) = 1 \tag{3.11}$$

$$Z_1 e^{i\phi} - Z_2 e^{i\psi}(1+\lambda) = 1 \tag{3.12}$$

These complex equations are linear in terms of the unknowns $Z_1$ and $Z_2$. Then $Z_1$ and $Z_2$ can be solved in terms of $\lambda$, $\phi$, and $\psi$ as:

$$Z_1 = \frac{(1-\lambda)-(1+\lambda)e^{i\psi}}{(1-\lambda)e^{i\phi}-(1+\lambda)e^{i\psi}} \tag{3.13}$$

$$Z_2 = \frac{1-e^{i\phi}}{(1-\lambda)e^{i\phi}-(1+\lambda)e^{i\psi}} \tag{3.14}$$

As $\lambda$ changes from -∞ to +∞, $Z_1$ and $Z_2$ describe a curve which is the loci of the tip of the vectors $A_oA_f$ and $B_oB_f$. These loci are two circles for any given value of $\phi$ and $\psi$. In Fig. 3.17, these two circles are shown for the values of $\phi = 50^o$ and $\psi = 10^o$, note that in order to draw two circles with the same reference frame, the vector $1+ Z_2$ is drawn instead of $Z_2$. A line can be drawn from (0,0), which is $A_o$, at an angle $\theta$ with respect to $A_oB_o$. $A_f$ is the intersection point of this line and the $Z_1$ circle. Another line can be drawn from $B_o$ at angle $\xi$ with respect to $A_oB_o$ which intersects the circles at $A_f$ and $B_f$, respectively. This corresponds to the folded position of the mechanism, where the link lengths are, $A_oA_f = a_2$, $A_fB_f = a_3$, $B_oB_f = a_4$ and $A_oB_o = a_1 = 1$.

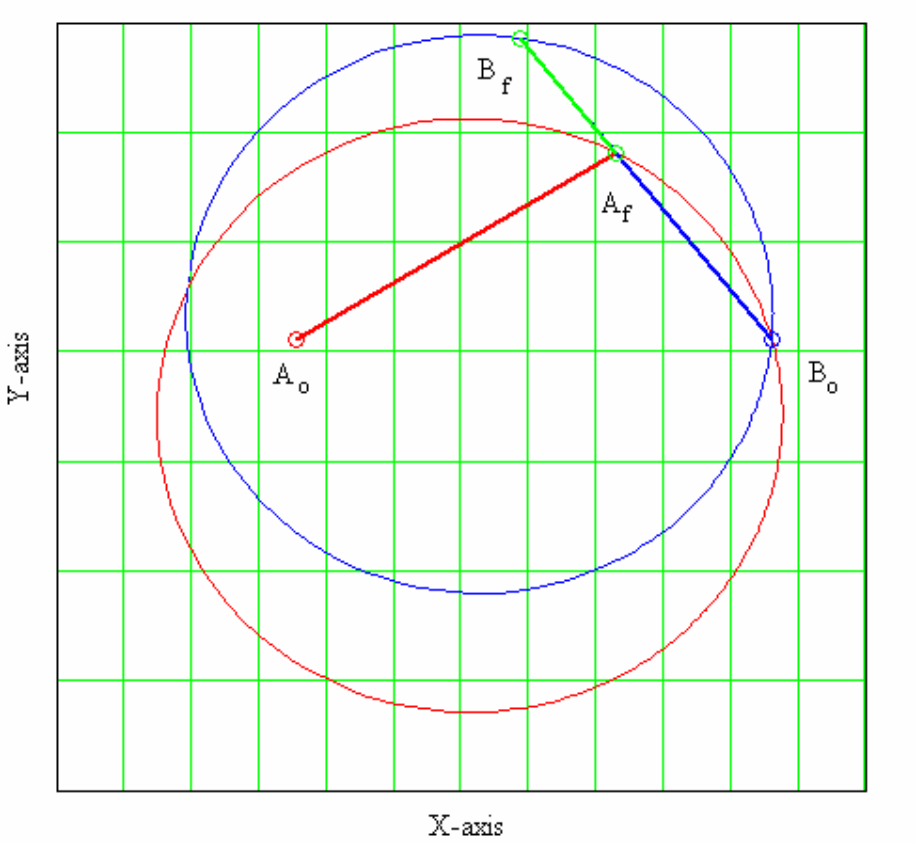


Figure 3.17 $Z_1$ and $Z_2$ Circles for the Values of $\phi = 50^o$ and $\psi = 10^o$

Analytically, link lengths can be determined as:

$$a_2 = \sqrt{Z_1 \bar{Z}_1} \tag{3.15}$$

$$a_4 = \sqrt{Z_2 \bar{Z}_2} \tag{3.16}$$

$$a_3 = \sqrt{a_4^2 \lambda^2} \tag{3.17}$$

$$a_1 = 1$$

The link lengths are functions of the free parameter $\lambda$, the given swing angle $\phi$, and corresponding rotation of link 4 $\psi$. For a given $\phi$ and $\psi$, there is a set of solutions with respect to the free parameter $\lambda$. In Fig.3.18 a different solution for the same $\phi$ and $\psi$ is shown.

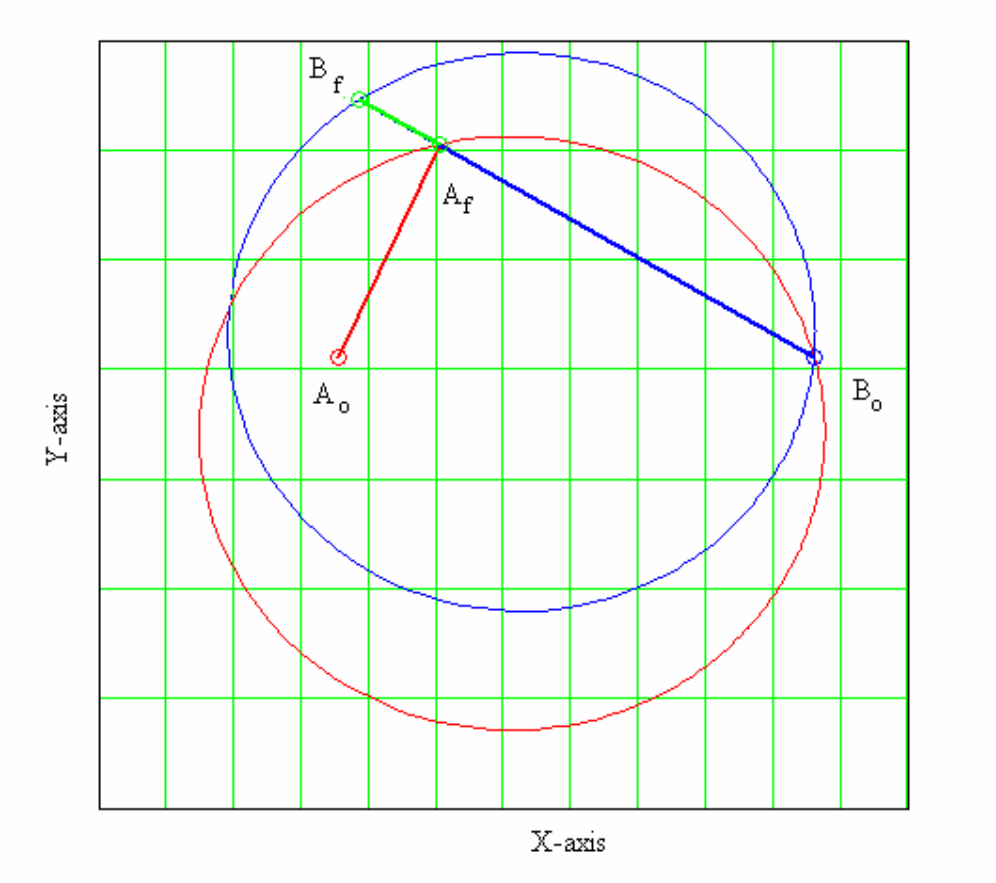


Figure 3.18 A Different Solution for $\phi = 50^o$ and $\psi = 10^o$

A necessary but not sufficient condition for double-rocker proportions is:

$$0 < |\lambda| < 1$$

In order to obtain double-rocker proportions there are limits on swing angle and corresponding rotation of link 4 as:

$$0 < \phi < 180 \text{ and } \frac{\phi}{2} - 90^o < \psi < \frac{\phi}{2} + 90^o$$

### 3.6 Transmission Angle Optimization

Among the set of solutions for a given swing angle and corresponding rotation of link 4, the one must be selected for which the maximum deviation of the transmission angle from $90^o$ is a minimum. In other words, for a given $\phi$ and $\psi$, the optimum $\lambda$ parameter must be selected corresponding to that for which the maximum deviation of the transmission angle from $90^o$ is a minimum. Therefore, a parametric optimization routine is developed and design charts for the optimum geared five-link mechanisms are prepared by using MATLAB.

According to the direction of rotation of the input, the transmission angle of the GFLM changes. That condition leads to two different optimum mechanisms which have same output swing angle and corresponding crank rotation. Therefore, transmission angle optimization is performed for both of the input directions of rotation and two sets of design charts are prepared. Moreover, transmission angle optimization is performed for several gear ratios and the corresponding design charts are also prepared.

### 3.7 Design Charts for the Geared Five-Link Mechanism

In Figure 3.19, a design chart is displayed for a gear ratio of unity and cw rotation of the input gear (link 5). The Y-axis represents the output swing angle, $\phi$, and the X-

axis represents the corresponding rotation of link 4, $\psi$. The full lines represent the optimum $\lambda$ parameter ($\lambda$=$a_3/a_4$), and the dotted lines represent the maximum deviation of the transmission angle from 90° for the corresponding mechanisms.

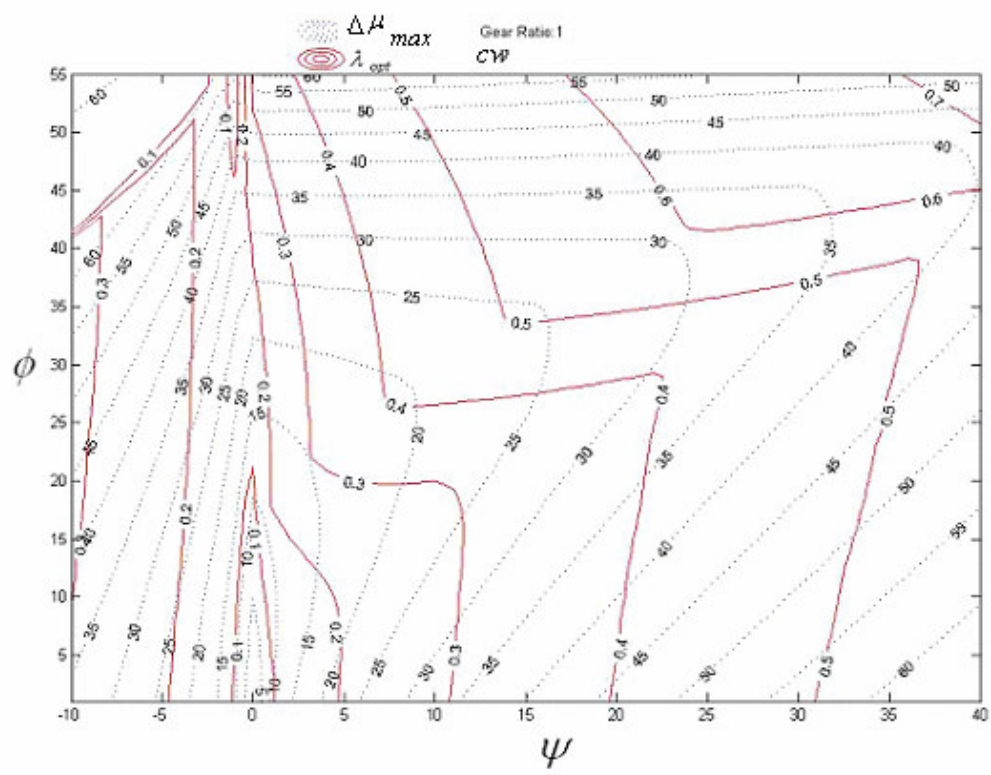


Figure 3.19 Design Chart for Gear Ratio = 1, CW Input Rotation

It can be observed that when the output swing angle reaches 50°, transmission angle deviation from 90° becomes 45°. It can also be observed that transmission characteristics of the mechanisms deteriorate drastically for negative values of $\psi$. It is mentioned before there are two different optimum mechanisms for a given $\phi$ and $\psi$ according to the direction of rotation of the input. Therefore, design charts are prepared for both cw and ccw rotation of the input. In figure 3.20, a design chart for gear ratio of unity and ccw rotation of the input is shown. Note that $\lambda_{opt}$ values are different from the ones in Fig.3.19 for the same $\phi$ and $\psi$. Also note that for some values of $\psi$, output swing angle of 55° can be obtained with a 45° deviation of transmission angle from 90°.

The gear ratio significantly affects the transmission angle of the mechanisms. It is observed that as the gear ratio ($r_3/r_5$) increases, the transmission angle improves and mechanisms with 70$^o$ output swing angle can be obtained (Fig. 3.21). On the other hand, if the gear ratio is decreased the transmission characteristics deteriorate.

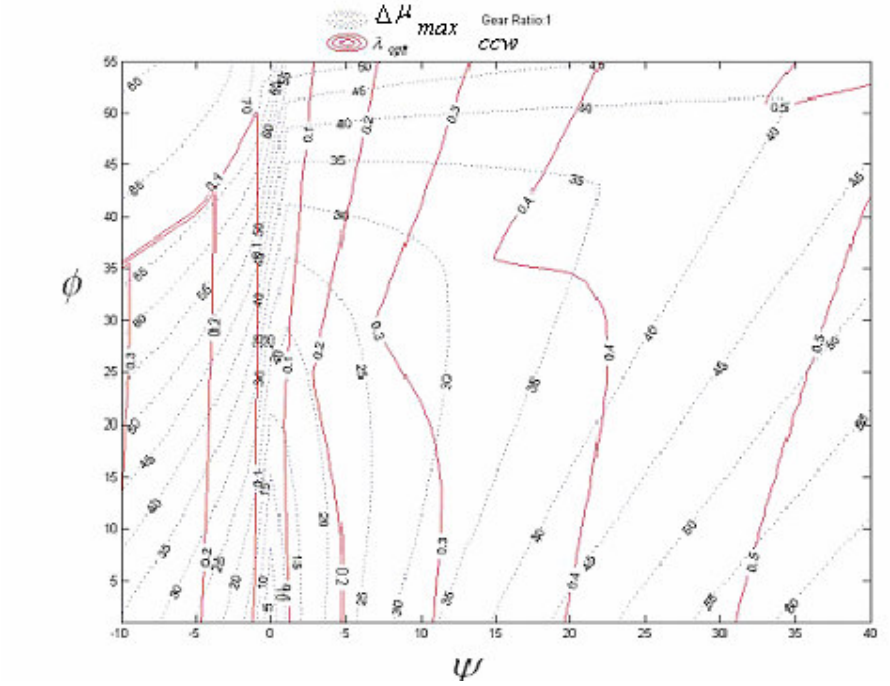


Figure 3.20 Design Chart for Gear Ratio = 1, CCW Input Rotation

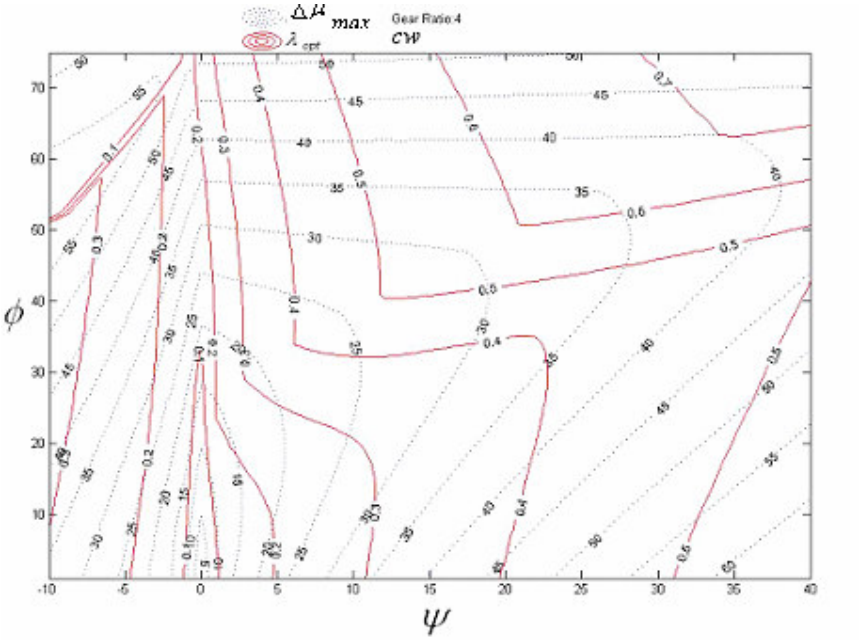


Figure 3.21 Design Chart for Gear Ratio = 4, CW Input Rotation

Design charts for different gear ratios and input rotations are displayed in Appendix A.

### 3.8 Time Ratio of the Geared Five-Link Mechanisms

After the synthesis of the GFLM it is observed that the mechanisms obtained are mostly quick-return mechanisms. Consequently, conditions of obtaining centric geared five-link mechanisms are investigated.

$\phi$ is defined as the rotation of the arm from the folded position to the extended position, in other words $\phi$ is the output swing angle. And $\psi$ is the rotation of link 4 from the folded position to the extended position. Consequently, $\beta$ is the rotation of link 3 from the folded position to the extended position. If the rotation of the input is chosen as cw, then the rotation of link 3 is ccw (Fig3.22). Therefore, $\beta$ can be obtained as:

$$\beta = \psi + \pi \tag{3.18}$$

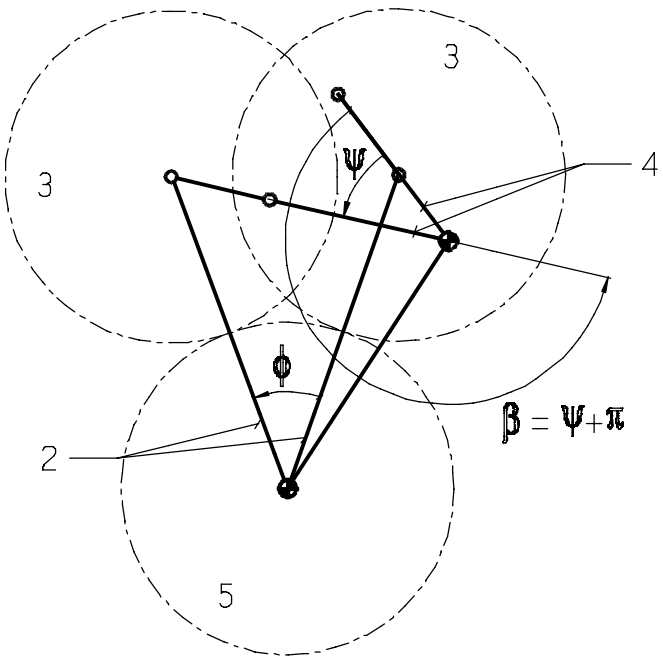


Figure 3.22 A Geared Five-Link Mechanism At Dead-Centers

If $\psi = 0$, then the mechanism is symmetric with respect to link 3, since the rotation of link 3 between the dead centers is $180^o$ (Fig. 3.23).

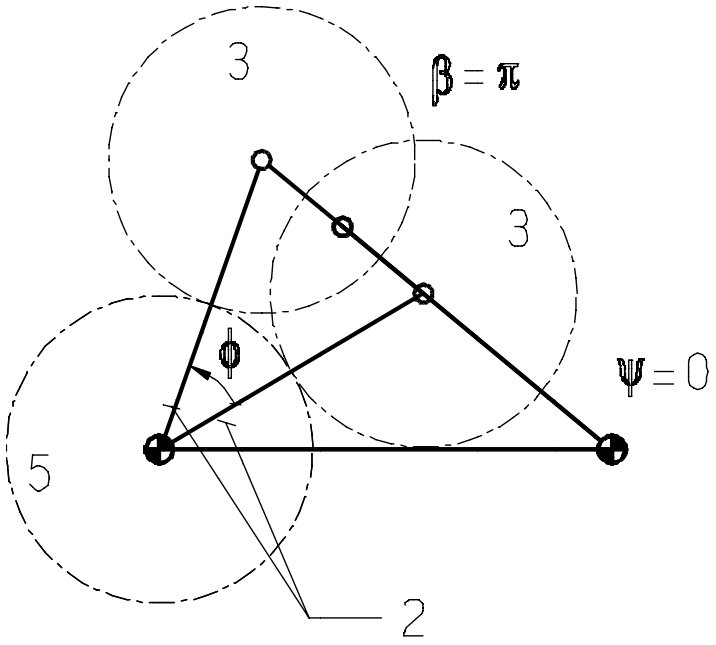


Figure 3.23 A Geared Five-Link Mechanism where $\beta = \pi$

When the input is applied to link 5, the relationship between $\theta_{15}$, and $\theta_{12}$ and $\theta_{13}$ is obtained from Eq 3.3 as:

$$\frac{\theta_{15}}{R} = (\frac{R+1}{R})\theta_{12} - \theta_{13} + k_1$$

This equation can be rewritten for a gear ratio of unity as:

$$\theta_{15} = 2\theta_{12} - \theta_{13} + k_1 \tag{3.19}$$

Therefore, the rotation of link 5 from the folded position to the extended position can be determined from Eq 3.19 as:

$$\Delta\theta_{15} = 2\phi - \beta \tag{3.20}$$

The time ratio of the mechanism is equal to unity if the rotation of link 5 from the folded position to the extended position ($\Delta\theta_{15}$) is equal to $\pm\pi$. Consequently, if $\beta = \pi$ ($\psi = 0$), centric mechanisms can not be obtained. Equation (3.20) can also be written as:

$$\Delta\theta_{15} = 2\phi - \pi - \psi \tag{3.21}$$

From Eq.3.21, it can be seen that in order to obtain centric mechanisms, $\psi$ must be equal to $2\phi$, but from the related design chart (Fig 3.19) it can be observed that this condition can barely be satisfied when $\phi \cong 12^o$ because of the transmission angle. Therefore, it is not possible to obtain centric mechanisms when output swing angle is greater then $12^o$.

If, the gear ratio is equal to two, $\frac{r_3}{r_5} = 2$, then from Eq.3.3:

$$\theta_{15} = 3\theta_{12} - 2\theta_{13} + k_1 \tag{3.22}$$

and

$$\Delta\theta_{15} = 3\phi - 2\pi - 2\psi \tag{3.23}$$

In order to obtain centric mechanisms, $\Delta\theta_{15}$ must be $-2\pi$, so $\psi$ must be equal to $\frac{3\phi}{2}$, but from the related design chart it can be observed that this condition can barely be satisfied when $\phi \cong 17^o$ because of the transmission angle. Therefore, it is not possible to obtain centric mechanisms when output swing angle is greater then $17^o$ for a gear ratio of 2.

Similarly, as the gear ratio increases up to 4, centric mechanisms can be obtained up to $\phi \cong 22^o$. Therefore, it can be concluded that for an acceptable transmission angle, centric mechanisms can be obtained when the output swing angle is very small.

**Design Example 3.1**

The purpose of this example is to illustrate the use of the design charts and to display the output motions and the transmission angles of the designed mechanisms. For a given swing angle, $\phi$ = 40°, and corresponding $\psi$ = 10°, the optimum value of $\lambda$ parameter is determined to be 0.46 from the corresponding design chart (Fig.3.19, input rotation is cw). The corresponding maximum deviation of transmission angle from 90° is 30°. The link lengths can be determined from Equations 3.13-17 as:

$a_1 = 1$, $a_2 = 0.907$, $a_3 = 0.306$, $a_4 = 0.665$

Then, the motion of the output link and the transmission angle will be shown as:

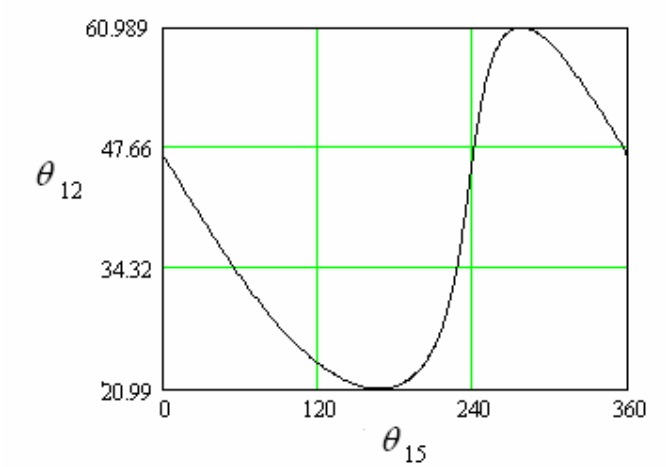


Figure 3.24 Motion of the Output Link for $\phi$ = 40°, $\psi$ = 10°, and $\lambda_{opt}$ = 0.46

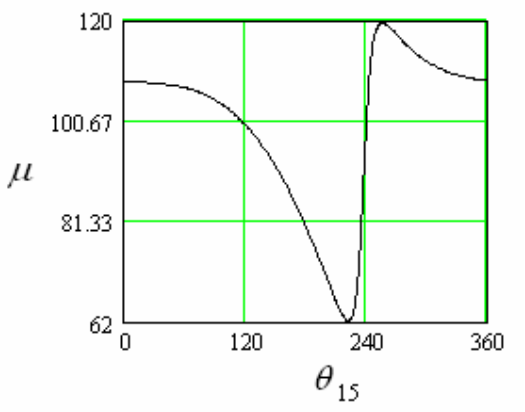


Figure 3.25 Transmission Angle of the Mechanism for $\phi$ = 40°, $\psi$ = 10°, $\lambda_{opt}$ = 0.46

If the rotation of input link is ccw, for the same $\phi$ and $\psi$, the optimum $\lambda$ value of 0.3 can be read from the corresponding design chart (Fig 3.20). The corresponding maximum deviation of transmission angle is $32^o$. The link lengths can be determined from Equations 3.13-17 as:

$a_1 = 1$, $a_2 = 0.801$, $a_3 = 0.264$, $a_4 = 0.88$

Then, the motion of the output link and the transmission angle will be shown as:

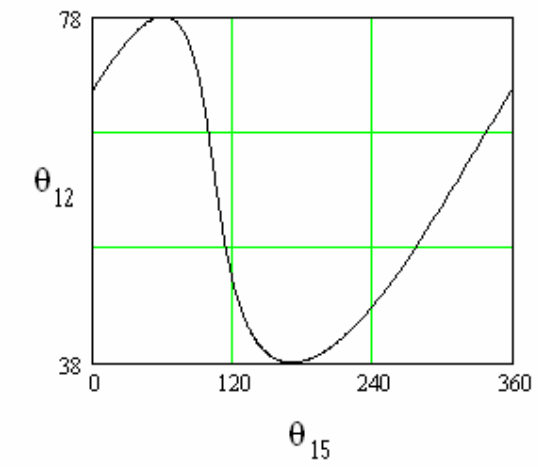


Figure 3.26 Motion of the Output Link for $\phi = 40^o$, $\psi = 10^o$, and $\lambda_{opt} = 0.3$

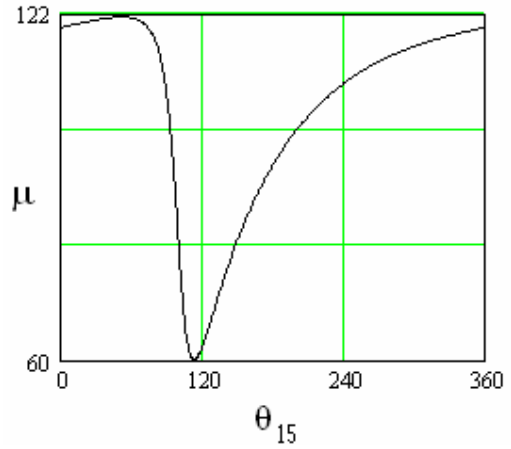


Figure 3.27 Transmission Angle of the Mechanism for $\phi = 40^o$, $\psi = 10^o$, and $\lambda_{opt} = 0.3$

### 3.9 Velocity and Acceleration Analysis of the Geared Five-Link Mechanism

The first derivatives of the loop closure equation and its complex conjugate (Eq. 3.4 and Eq. 3.5) are:

$$a_2 e^{i\theta_{12}} \dot{\theta}_{12} - a_4 e^{i\theta_{14}} \dot{\theta}_{14} = -a_3 e^{i\theta_{13}} \dot{\theta}_{13} \tag{3.24}$$

$$-a_2 e^{-i\theta_{12}} \dot{\theta}_{12} + a_4 e^{-i\theta_{14}} \dot{\theta}_{14} = a_3 e^{-i\theta_{13}} \dot{\theta}_{13} \tag{3.25}$$

From Eq.3.24 and 3.25, the angular velocity of the arm (link 2) is determined as a function of the angular velocity of link 3:

$$\omega_{12} = \frac{-a_3 \sin(\theta_{13} - \theta_{14})}{a_2 \sin(\theta_{12} - \theta_{14})} \omega_{13} \tag{3.26}$$

From Eq.3.2 the angular velocity of link 3 can be obtained as a function of the angular velocity of link 2 is and the input link 5 as:

$$\omega_{13} = \frac{(R+1)\omega_{12} - \omega_{15}}{R} \tag{3.27}$$

From Eq.3.26 and 3.27 the angular velocity of link 2 can be determined as:

$$\omega_{12} = \frac{K\omega_{15}}{K(R+1) - R} \tag{3.28}$$

where

$$K = \frac{-a_3 \sin(\theta_{13} - \theta_{14})}{a_2 \sin(\theta_{12} - \theta_{14})}$$

Analyses are performed for a constant input velocity which is equal to unity ( $\omega_{15} = \mp 1$ rad/s).

After determining $\omega_{12}$, $\omega_{13}$ can be obtained from Eq.3.27, then velocity of link 4 can be determined as:

$$\omega_{14} = \frac{a_3 \sin(\theta_{12} - \theta_{13})}{a_4 \sin(\theta_{12} - \theta_{14})} \omega_{13} \tag{3.29}$$

The first derivative of Eq. 3.27 is:

$$\alpha_{13} = \left( \frac{R+1}{R} \right) \alpha_{12} \tag{3.30}$$

Then, from the second derivatives of the loop closure equation and its complex conjugate and from Eq. 3.30, angular accelerations of link 2 and link 4 can be determined as:

$$\alpha_{12} = \frac{-a_2 \omega_{12}{}^2 \cos(\theta_{12} - \theta_{14}) + a_4 \omega_{14}{}^2 - a_3 \omega_{13}{}^2 \cos(\theta_{13} - \theta_{14})}{a_2 \sin(\theta_{12} - \theta_{14}) + 2a_3 \sin(\theta_{13} - \theta_{14})} \tag{3.31}$$

$$\alpha_{14} = \frac{-a_2 \omega_{12}{}^2 + a_4 \omega_{14}{}^2 \cos(\theta_{12} - \theta_{14}) - a_3 \omega_{13}{}^2 \cos(\theta_{12} - \theta_{13}) + a_3 \alpha_{13} \sin(\theta_{12} - \theta_{13})}{a_4 \sin(\theta_{12} - \theta_{14})} \tag{3.32}$$

**Design Example 3.2**

The purpose of this example is to display the angular velocity and the angular acceleration of the output link of the mechanism designed in Ex.3.1 (cw input rotation). In Figure 3.28, the position and the angular velocity of the output link ($\phi$ = 40°, $\psi$ = 10°, and $\lambda$opt = 0.46) are shown.

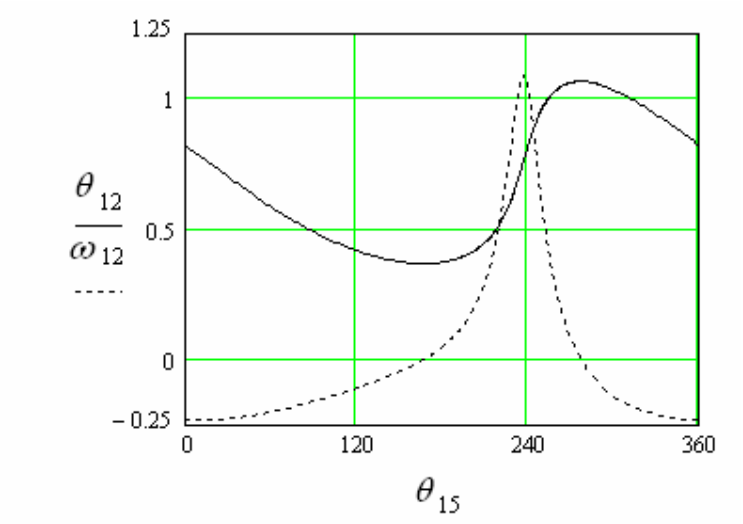


Figure 3.28 Motion and Angular Velocity of the Output Link

In Figure 3.29, the angular velocity and the angular acceleration of the output link of the mechanism are shown.

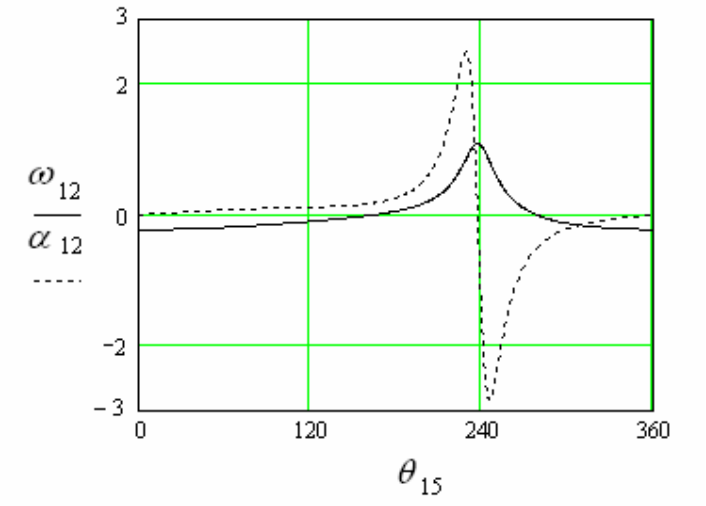


Figure 3.29 Angular Velocity and Acceleration of the Output Link

**Design Example 3.3**

The purpose of this example is to show that for several cases approximately a constant angular velocity can be obtained at the output link during the working cycle. In Figure 3.30, the motion and the angular velocity of the output link of the mechanism for a given swing angle $\phi = 40^o$, corresponding $\psi = 0^o$, and $\lambda$opt = 0.209 are shown. During the working cycle approximately a constant velocity is obtained.

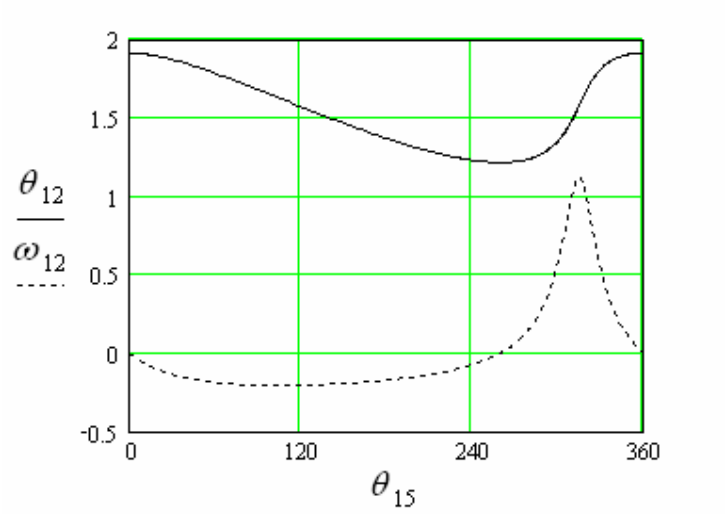


Figure 3.30 Motion and Angular Velocity of the Output Link for $\phi = 40^o$, $\psi = 0^o$

However, as $\psi$ increases this condition vanishes as shown in Fig. 3.31 ($\phi = 40^o$, $\psi = 10^o$, $\lambda$opt = 0.46) and Fig. 3.32 ($\phi = 40^o$, $\psi = 40^o$, $\lambda$opt = 0.55).

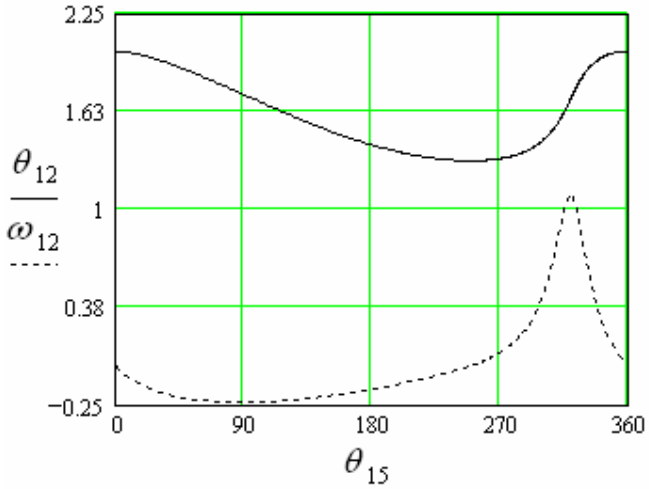


Figure 3.31 Motion and Angular Velocity of the Output Link for $\phi = 40^o$, $\psi = 10^o$

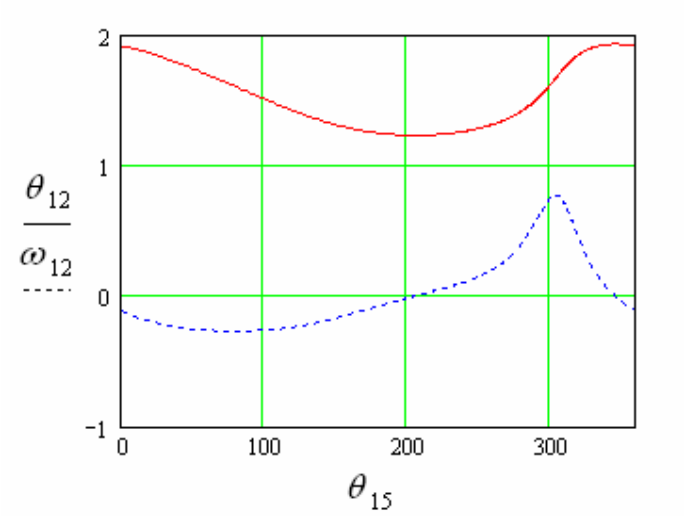


Figure 3.32 Motion and Angular Velocity of the Output Link for $\phi = 40^{o}$, $\psi = 40^{o}$

# CHAPTER4

# KINEMATIC ANALYSIS and SYNTHESIS of the GEARED ADJUSTABLE STROKE MECHANISM

## 4.1 Introduction

An adjustable stroke mechanism is shown in Fig. 4.1. Link 6 is assumed to be fixed at a certain position. The link lengths are defined as:

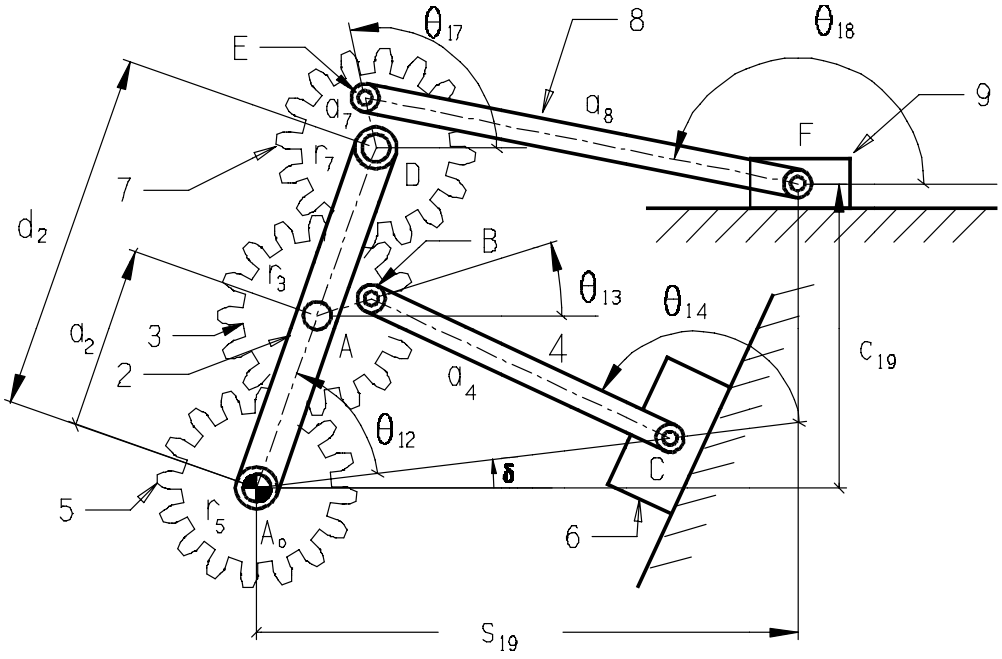


Figure 4.1 The Geared Adjustable Stroke Mechanism

$A_oC = a_1$, $A_oA = a_2$, $AB = a_3$, $BC = a_4$, $DE = a_7$, $EF = a_8$,

$d_2 = r_5 + 2r_3 + r_7$ where $r_5$, $r_3$ and $r_7$ are the pitch radii of gears 5, 3 and 7 respectively.

The vertical distance between $A_o$ and F is $c_{19}$. The position of link 9 is given by the position parameter $s_{19}$, as shown. $\delta$ is the angle between the X-axis and $A_oC$, which will be called "adjustment angle". The unknown position parameters are $\theta_{12}$, $\theta_{14}$, $\theta_{17}$, $\theta_{18}$, $c_{19}$ and $s_{19}$.

### 4.2 Motion Analysis of the Geared Adjustable Stroke Mechanism

One can write the loop closure equations for the mechanism:

$$(r_5 + r_3)e^{i(\theta_{12}+\delta)} + a_3 e^{i\theta_{13}} = a_1 e^{i\delta} + a_4 e^{i(\theta_{14}+\delta)} \tag{3.1}$$

$$(r_5 + 2r_3 + r_7)e^{i(\theta_{12}+\delta)} + a_7 e^{i\theta_{17}} = s_{19} + ic_{19} + a_8 e^{i\theta_{18}} \tag{4.1}$$

$\theta_{12}$ and $\theta_{14}$ are obtained as a function of the input, $\theta_{15}$, in Chapter 3. Analysis of the complete mechanism involves the relationship between $s_{19}$, $\theta_{17}$, and $\theta_{18}$ as a function of $\theta_{15}$.

The velocity ratio between the gears 3, 7 and the arm (link 2) is:

$$-\frac{r_7}{r_3} = \frac{\omega_{13} - \omega_{12}}{\omega_{17} - \omega_{12}} = -R_2 \tag{4.2}$$

Integrating equation (4.2), $\theta_{17}$ can be determined as:

$$\theta_{17} = \frac{(R_2 + 1)(\theta_{12} + \delta) - \theta_{13} + k_2}{R_2} \tag{4.3}$$

where, $k_2$ is the integration constant, which will be called "phase angle", and $R_2$ is the gear ratio ($r_7/r_3$).

Equation (4.1) and its complex conjugate can be written as:

$$d_2 e^{i(\theta_{12}+\delta)} + a_7 e^{i\theta_{17}} - s_{19} - ic_{19} = a_8 e^{i\theta_{18}} \tag{4.4}$$

$$d_2 e^{-i(\theta_{12}+\delta)} + a_7 e^{-i\theta_{17}} - s_{19} + ic_{19} = a_8 e^{-i\theta_{18}} \tag{4.5}$$

where,

$$d_2 = r_5 + 2r_3 + r_7$$

Multiplying equation (4.4) by equation (4.5), eliminating $\theta_{18}$, one can obtain the position of the output link, $s_{19}$, in terms of $\theta_{12}$ and $\theta_{17}$ as:

$$s_{19} = \frac{-D \mp \sqrt{D^2 - 4.E}}{2} \tag{4.6}$$

where,

$$D = -2d_2 \cos(\theta_{12} + \delta) - 2a_7 \cos(\theta_{17})$$

$$E = d_2^2 + a_7^2 + {c_{19}}^2 + 2d_2 a_7 \cos(\theta_{12} + \delta - \theta_{17}) - 2c_{19} d_2 \sin(\theta_{12} + \delta) - 2c_{19} a_7 \sin(\theta_{17}) - a_8^2$$

$\theta_{18}$ can be determined from equation (4.4) after $s_{19}$ is solved.

### 4.3 Transmission Angle of the Geared Adjustable Stroke Mechanism

When the complete mechanism is considered, there are two critical transmission angles. The first transmission angle is defined for the geared five-link mechanism in Chapter 3 as:

$$\tan(\mu_1) = \frac{-\frac{a_3}{r_3}\sin(\theta_{14}-\theta_{13}) - \sin(\theta_{14}-\theta_{12})}{\pm\frac{a_3}{r_3}\tan(\alpha)\sin(\theta_{14}-\theta_{13}) + \cos(\theta_{14}-\theta_{12})}$$

The second transmission angle is between the output link 9 and link 8, similar to that of the slider crank mechanisms.

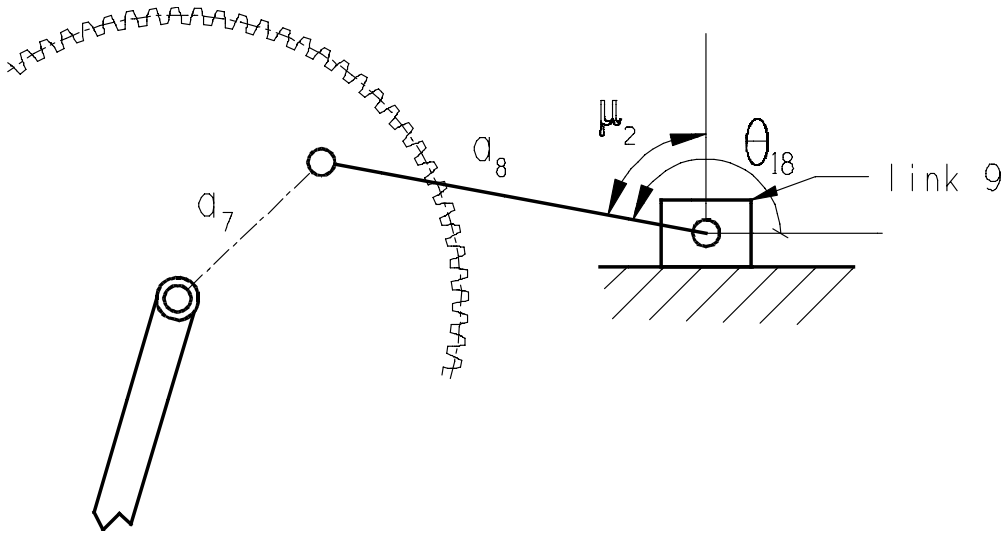


Figure 4.2 Second Transmission Angle of the Geared Adjustable Stroke Mechanism

Then,

$$\mu_2 = \theta_{18} - \frac{\pi}{2} \tag{4.7}$$

### 4.4 Synthesis of the Geared Adjustable Stroke Mechanism

In an adjustable stroke mechanism usually maximum variation in the stroke is required. For this purpose, initially the aim is to obtain mechanisms which perform a large stroke since as the stroke increases the movability and the transmission angle of the mechanism become more critical. Once a large stroke is obtained, by changing the position of the adjustment link, the stroke will be decreased. Several methods have been developed to obtain mechanisms which can produce large strokes. These methods are mentioned in the following parts of this chapter.

### 4.5 Dead-Center Synthesis of the Geared Adjustable Stroke Mechanism

At first, a synthesis procedure is derived by use of dead-centers of the GASM. It is mentioned in Chapter 3 when links 3 and 4 are at the extended position, link 2 is at the forward position and when links 3 and 4 are at the folded position, link 2 is at the fully withdrawn position. These positions are the dead-center positions of the geared five-link mechanism. If links 7 and 8 are at the extended position when links 3 and 4 are at the folded position, then output link 9 is at the forward position. Moreover, if links 7 and 8 are at the folded position when links 3 and 4 are at the extended position, then output link 9 is at the fully withdrawn position. These positions are the dead-center positions of the GASM. At the dead center positions the velocity of the output link is equal to zero. The velocity equation of the output link can be obtained for a constant input angular velocity as:

$$\dot{s}_{19} = -\frac{d_2 \sin(\theta_{12} - \theta_{18})\omega_{12} - a_7 \sin(\theta_{17} - \theta_{18})}{\cos\theta_{18}}$$

When the GFLM is at the dead-centers, the velocity of the arm ($w_{12}$) is equal to zero. Therefore, if $\sin(\theta_{17} - \theta_{18})$ is equal to zero when the GFLM is at the dead-centers, then the velocity of the output link ($\dot{s}_{19}$) is equal to zero. Thus, when the GFLM is at the dead-centers, in addition, if $\theta_{17} = \theta_{18}$ or $\theta_{17} = \theta_{18} + \pi$ the GASM is also at the dead-center position (Figure 4.3).

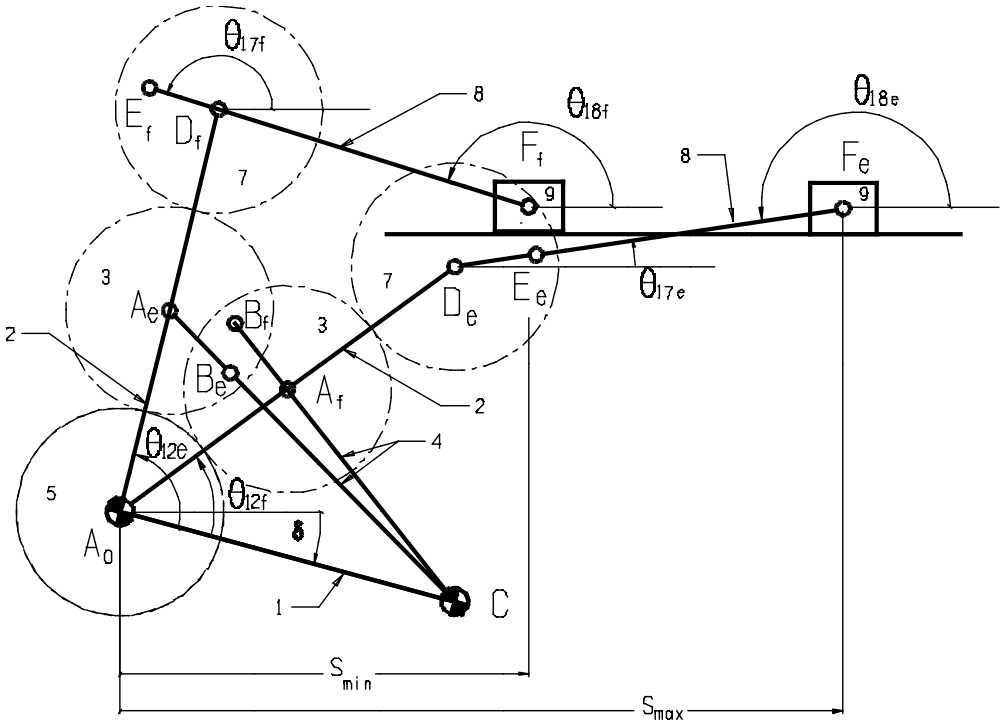


Figure 4.3 The Extended and Folded Positions of the GASM

At first, use of the gear ratio, $R_2 = r_7/r_3$, as a design parameter for the maximization of the stroke was considered ($R_1$=1). However, it is observed that if $R_2 = ½$, a pilgrim step motion is obtained. If $R_2$ is not an integer and $R_2 \neq ½$, then the output motion will complete a cycle after several cycles of the input link rotation (Appendix E). If $R_2$ is an integer greater than unity ($R_2$ = n, where n>1), then the output motion will complete a cycle after n*360$^o$ of the input link rotations, and a pilgrim step motion is obtained. Consequently, for the desired output reciprocating motion, $R_2$ must be equal to unity.

From the synthesis of the GFLM, it is known that, $\phi$ is the rotation of the arm from the folded position to the extended position ($\phi = \theta_{12e} - \theta_{12f}$), $\psi$ is the corresponding rotation of link 4 from the folded position to the extended position. $\beta$ is the rotation of link 3 from the folded position to the extended position ($\beta = \theta_{13e} - \theta_{13f}$). It is also obtained that, $\beta = \psi + \pi$.

For a given $\phi$, $\beta$, and $\lambda_{opt}$, link lengths of the GFLM can be obtained. The adjustment angle, $\delta$, is a free parameter. Then, the extended and folded positions of $\theta_{12,}$ and $\theta_{13}$ are determined as well. As mentioned above, the gear ratio $R_2$ is chosen equal to unity ($R_2 = 1$). Therefore, the length of the arm, $d_2$, can be determined as:

$$d_2 = r_5 + 3r_3$$

If the gear ratio $R_1$ is also chosen as unity ($R_1 = 1$), then, the length of the arm, $d_2$, is:

$$d_2 = 4r_5$$

So, the unknown parameters are $\theta_{17}$, $a_7$, $a_8$, $c_{19}$, $s_{19}$, and $k_2$. Since the dead-centers of the GFLM are determined, then the rotation of $\theta_{17}$ between the dead-center positions can be obtained. From equation (4.3) the extended and folded positions of $\theta_{17}$ can be written as:

$$\theta_{17e} = 2(\theta_{12f} + \delta) - \theta_{13f} + k_2 \tag{4.7}$$

$$\theta_{17f} = 2(\theta_{12e} + \delta) - \theta_{13e} + k_2 \tag{4.8}$$

$\Delta\theta_{17}$, the angle between the folded and extended positions of $\theta_{17}$ is:

$$\Delta\theta_{17} = \theta_{17f} - \theta_{17e} \tag{4.9}$$

Then, from Eq.(4.7) and Eq.(4.8):

$$\theta_{17f} - \theta_{17e} = 2\phi - \beta \tag{4.10}$$

Therefore, $\Delta\theta_{17}$ can be determined as:

$$\Delta\theta_{17} = 2\phi - \beta \tag{4.11}$$

Another free parameter, $\lambda_2$, is defined as:

$$\lambda_2 = \frac{a_7}{a_8} \tag{4.12}$$

One can write the equations for the dead-center positions (Fig 4 .4):

$$s_e = d_2 \cos(\theta_{12f} + \delta) + (a_7 + a_8)\cos\theta_{17e} \tag{4.13}$$

$$s_f = d_2 \cos(\theta_{12e} + \delta) + (a_7 - a_8)\cos\theta_{17f} \tag{4.14}$$

$$c_{19} = d_2 \sin(\theta_{12f} + \delta) + (a_7 + a_8)\sin\theta_{17e} \tag{4.15}$$

$$c_{19} = d_2 (\sin\theta_{12e} + \delta) + (a_7 - a_8)\sin\theta_{17f} \tag{4.16}$$

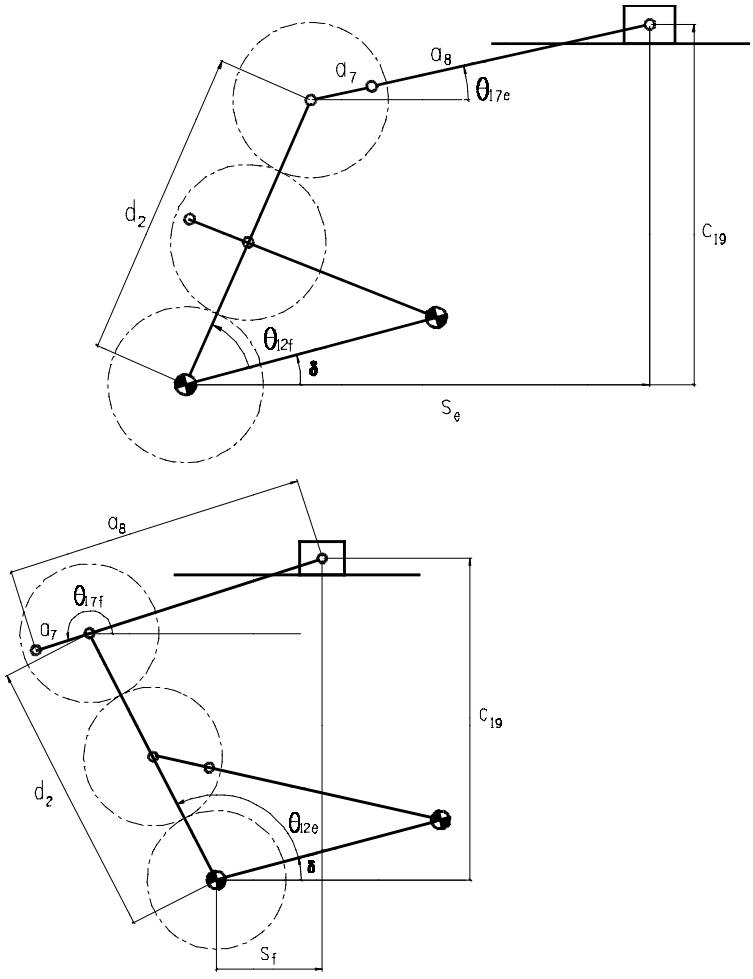


Figure 4.4 The Dead-Center Positions of the GASM

The output stroke of the mechanism is:

$$\Delta s = s_e - s_f$$

Then, for a desired stroke, $\Delta s$, the extended and folded positions of link 7 ($\theta_{17e}$ and $\theta_{17f}$) can be obtained from Equations 4.13-4.16 as:

$$\theta_{17f} = \tan^{-1}\left(\frac{K_2\cos\Delta\theta_{17} - K_3 - K_1K_2\sin\Delta\theta_{17}}{K_1K_3 - K_1K_2\cos\Delta\theta_{17} - K_2\sin\Delta\theta_{17}}\right) \tag{4.17}$$

$$\theta_{17e} = \theta_{17f} - \Delta\theta_{17} \tag{4.9}$$

$$K_1 = \frac{\Delta s - d_2\left(\cos(\theta_{12f}+\delta) - \cos(\theta_{12e}+\delta)\right)}{d_2\left(\sin(\theta_{12f}+\delta) - \sin(\theta_{12e}+\delta)\right)}$$

$$K_2 = \lambda_2 + 1$$

$$K_3 = \lambda_2 - 1$$

The phase angle, $k_2$, is:

$$k_2 = \theta_{17e} + \theta_{13f} - 2(\theta_{12f} + \delta) \tag{4.18}$$

The link lengths are:

$$a_8 = \frac{\Delta s - d_2\left(\cos(\theta_{12f}+\delta) - \cos(\theta_{12e}+\delta)\right)}{K_2\cos\theta_{17e} - K_3\cos\theta_{17f}} \tag{4.19}$$

$$a_7 = \lambda_2 a_8 \tag{4.20}$$

$$c_{19} = d_2\sin(\theta_{12f}+\delta) + \left(a_7 + a_8\right)\sin\theta_{17e} \tag{4.21}$$

Using this method, a closed-form solution for the link length proportions is obtained. However, the results show that solutions with permissible transmission characteristics can be determined in a limited region. The reason of this situation can be explained by the rotation of link 7 between the dead-centers. The rotation of link 7 is equal to the rotation of link 5 (input link). The velocity ratio between the gears 5, 7 and the arm (link 2) is:

$$\frac{\omega_{17} - \omega_{12}}{\omega_{15} - \omega_{12}} = 1$$

Integrating this equation:

$$\theta_{17} = \theta_{15} + k$$

In Chapter 3, it was shown that the use of centric geared five-link mechanisms was not feasible because of small swing angles and/or low transmission angle values. From four-bar and slider-crank mechanisms it is known that as the mechanisms gets further away from centricity, transmission angle deviation from $90^o$ increases. Similarly, as the rotation of link 7 between the dead-centers ($\Delta\theta_{17}$) gets further from $\pm 180^o$ obtaining solutions satisfying both of the dead-center positions with acceptable transmission characteristics becomes harder.

For example, if $\phi = 40^o$ and $\psi = 0^o$ ($\beta = 180^o$), then $\Delta\theta_{17} = -100^o$, if $\phi = 40^o$ and $\psi = 40^o$ ($\beta = 220^o$), then $\Delta\theta_{17} = -140^o$. After several trials it is seen that as $\psi < \phi - 20^o$ obtaining solutions with permissible transmission angle characteristics becomes harder.

Connecting rod $a_8$ and the height of the slider axis $c_{19}$ are chosen as unknown design parameters in this approach. However, they can be chosen according to design conditions. The reasons will be discussed in Sec 4.9.

**Design Example 4.1**

This example is to illustrate the use of dead-center synthesis of the GASM. Initially an optimum GFLM is chosen from the corresponding design chart (gear ratio is equal to unity and input rotation is cw). The oscillation of the arm (link 2) is, $\phi = 40^o$, corresponding rotation of link 4 is $\psi = 20^o$ (corresponding rotation of link 3 is, $\beta = 200^o$) and $\lambda_{opt} = 0.55$. Corresponding link lengths are: $a_1 = 1$, $a_2 = 1$, $a_3 = 0.331$, $a_4 = 0.601$. The free parameter $\delta$ is chosen as: $\delta = 105^o$. The motion of arm (link 2) is shown in Fig. 4.5.

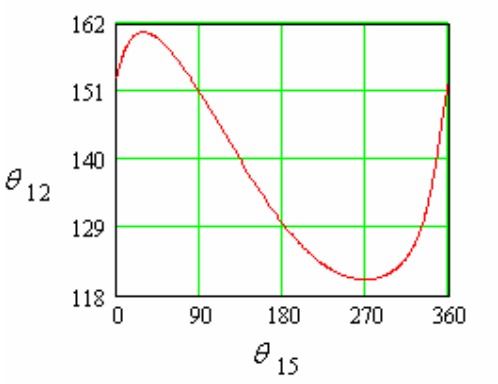


Figure 4.5 Motion of Link 2

Since the gear ratios are equal to unity, the length of the arm, $d_2$, is: $d_2 = 4r_3 = 2$

The rotation of $\theta_{17}$ between the dead-center positions is determined as:

$$\Delta\theta_{17} = 2.\phi - \beta = -120^o$$

The free parameter, $\lambda_2$ is chosen equal to 0.4. Then, for a desired stroke, $\Delta s = d_2$ the link lengths and $k_2$ are determined as:

$a_7 = 0.509$, $a_8 = 1.272$, $c_{19} = 1.179$, $k_2 = 124.1^o$

The output reciprocating motion is shown in Fig. 4.6.

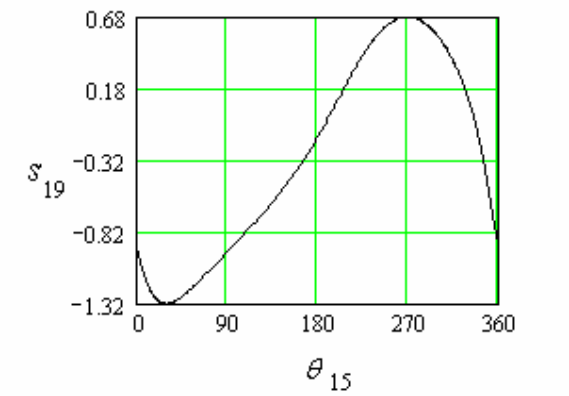


Figure 4.6 Displacement of Link 9

The second transmission angle, $\mu_2$:

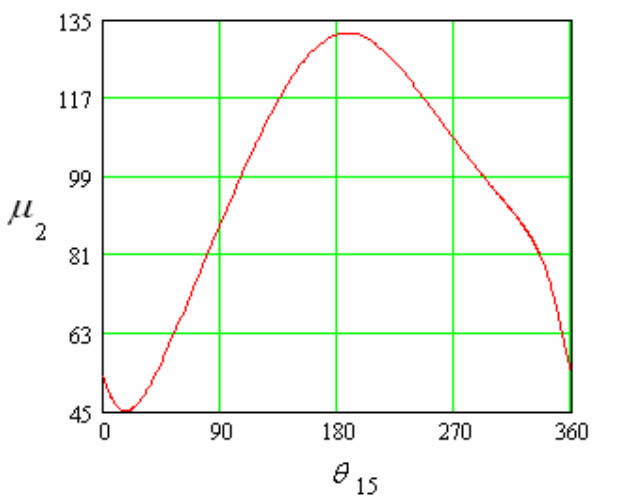


Figure 4.7 Second Transmission Angle of the Mechanism

The animation of the mechanism designed in Ex.4.1 is prepared and several positions are shown in the following figures.

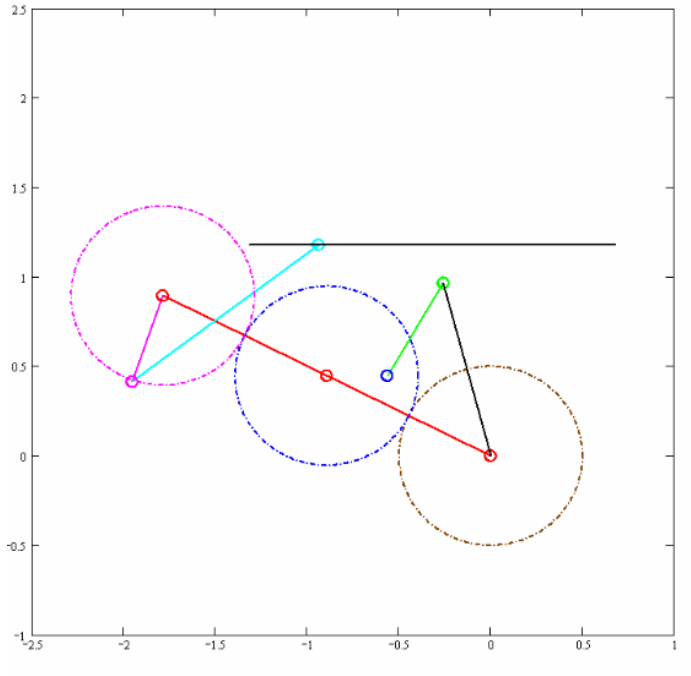


Figure 4.8 a. Input = $0^{o}$, Output = -0.94

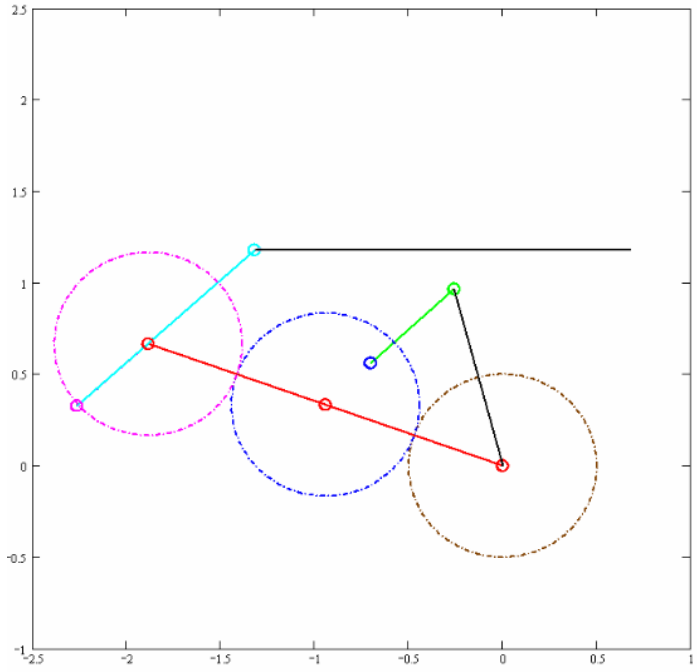


Figure 4.8 b. Input = $30.7^{o}$, Output = -1.32

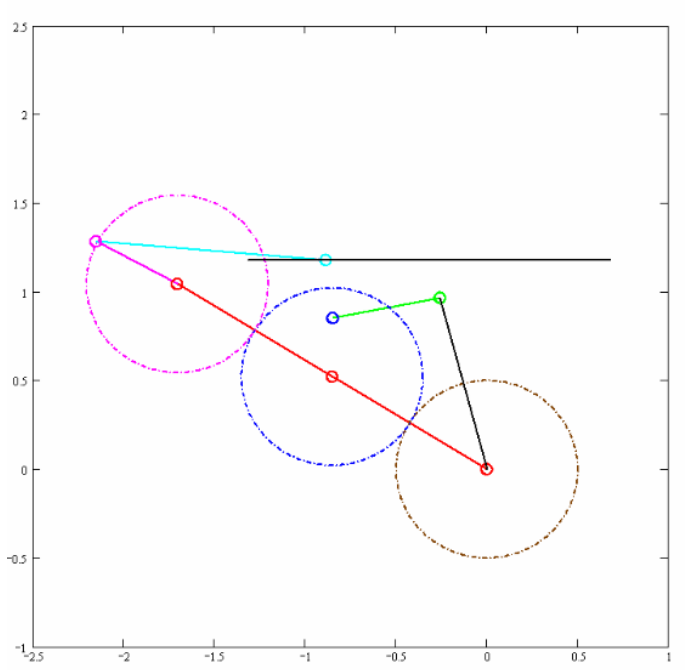


Figure 4.8 c. Input = 100$^{o}$, Output = -0.88

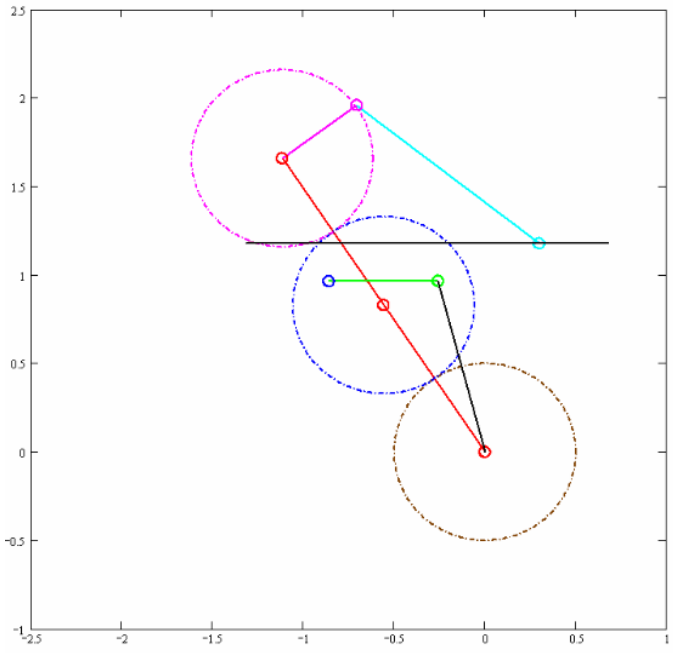


Figure 4.8 d. Input = 212$^{o}$, Output = 0.27

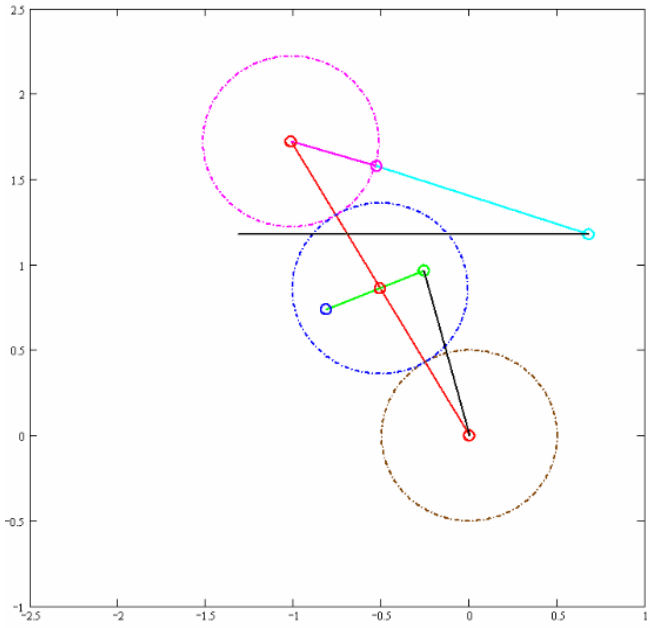


Figure 4.8 e. Input = 267$^{o}$, Output = 0.679

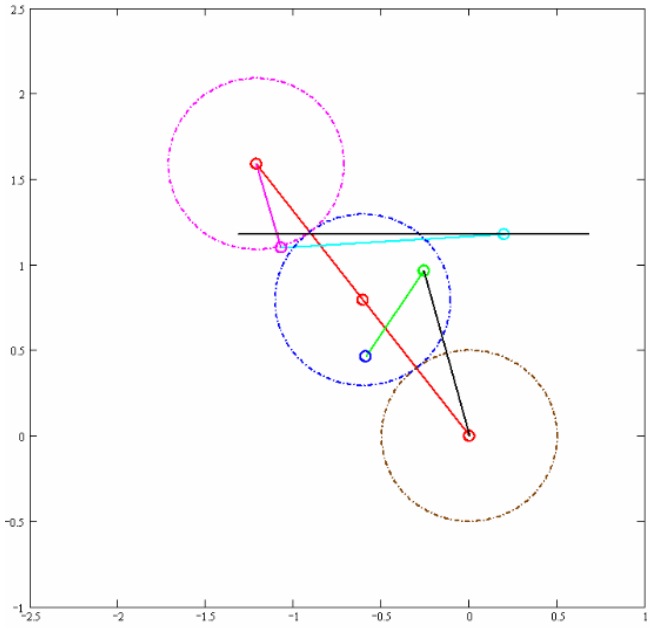


Figure 4.8 f. Input = 323$^{o}$, Output = 0.227

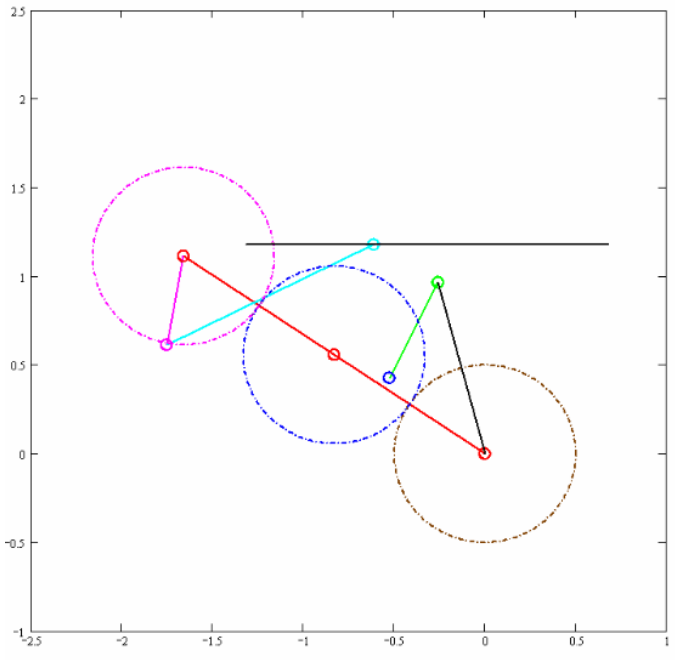


Figure 4.8 g. Input = 350$^{o}$, Output = -0.6

## 4.6 Synthesis of the Geared Adjustable Stroke Mechanism by Using the Inflection Circle of Link 7 at a Specified Position

It is known that these types of mechanisms are used in industry. An example of this is shown in Fig.4.9 [2]. It can be seen that links 7 and 8 are at the folded position when links 3 and 4 are at the extended position.

The link lengths, the phase angle $k_2$ and the adjustment angle $\delta$ are copied from the mechanism below and the mechanism is analyzed. It is observed that links 7 and 8 are not at the extended position when links 3 and 4 are at the folded position. In order to satisfy the second dead-center position, link 7 must rotate $180^o$ between the dead-centers. The rotation of link 7 is equal to rotation of link 5 (input link). This mechanism is not centric; the rotation of link 5 between the dead-centers is not equal to $180^o$. Therefore, this mechanism can not satisfy the second dead-center position.

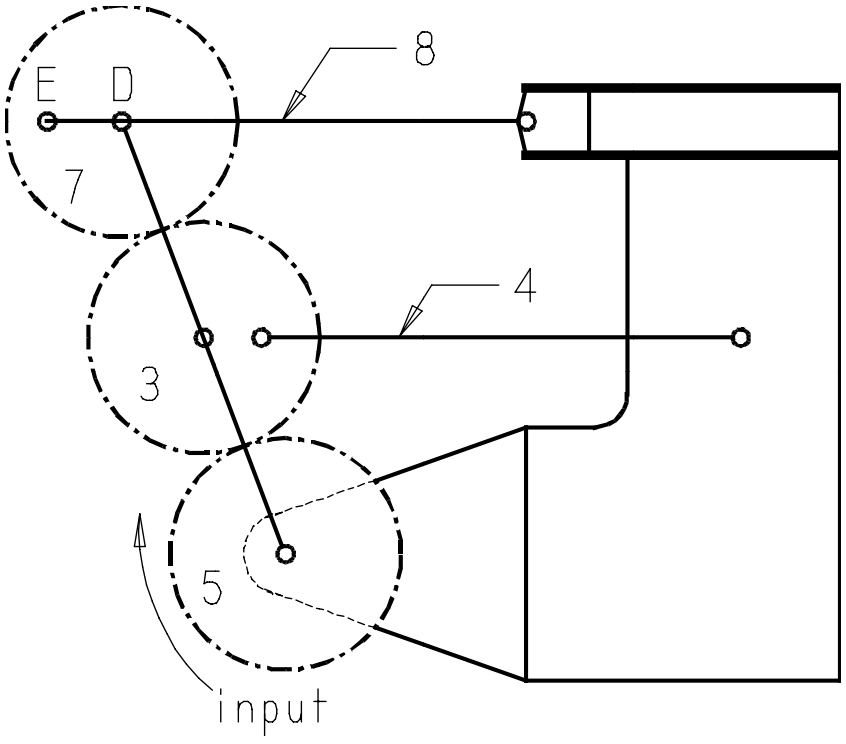


Figure 4.9 A Geared Adjustable Stroke Mechanism Used in Industry

The paths of points E and D are plotted as shown in Figure 4.10. The endpoint of the arm is point D, and the endpoint of the connecting-rod on the gear is point E.

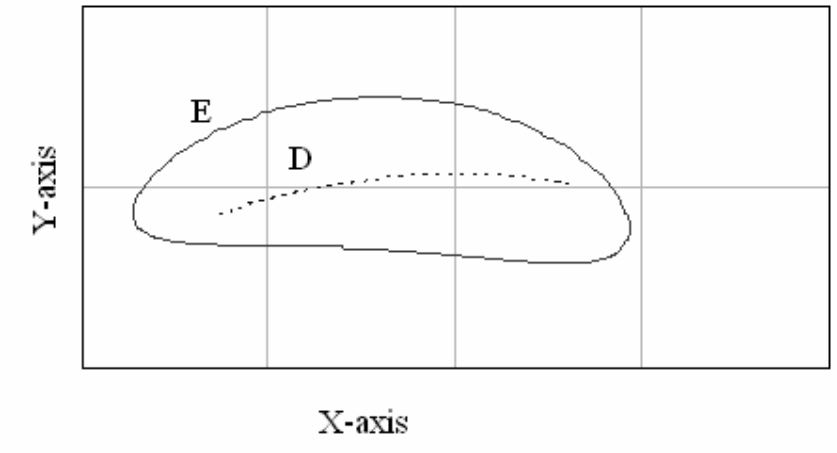


Figure 4.10 Paths of the Points E and D

The path of point E is very important, because the shape of this path is the major parameter for the stroke. The distance between the maximum X coordinate and the minimum X coordinate, *s*, is the major parameter for the output stroke. The distance between the maximum Y coordinate and the minimum Y coordinate (*h)* significantly affects the second transmission angle. For a large stroke, *s* must be increased, and for a better transmission angle, *h* should be decreased. Therefore, $d_2/s$ and $h/s$ should be decreased ($d_2$ is the arm).

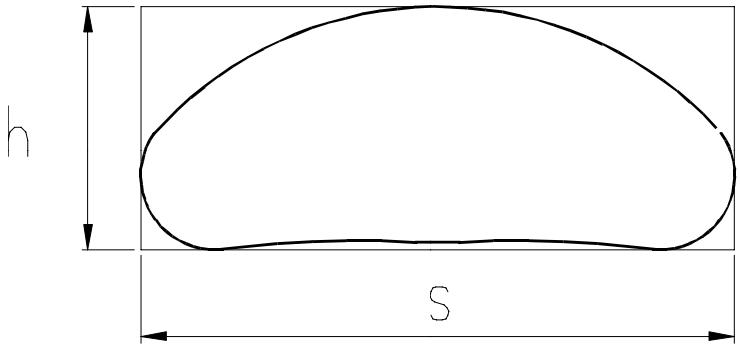


Figure 4.11 Path of the Point E, *s*, and *h*

By assigning different phase angles ($k_2$) from 0 to 2π, different paths of point E can be obtained from the mechanism, as shown in Fig. 4.12.

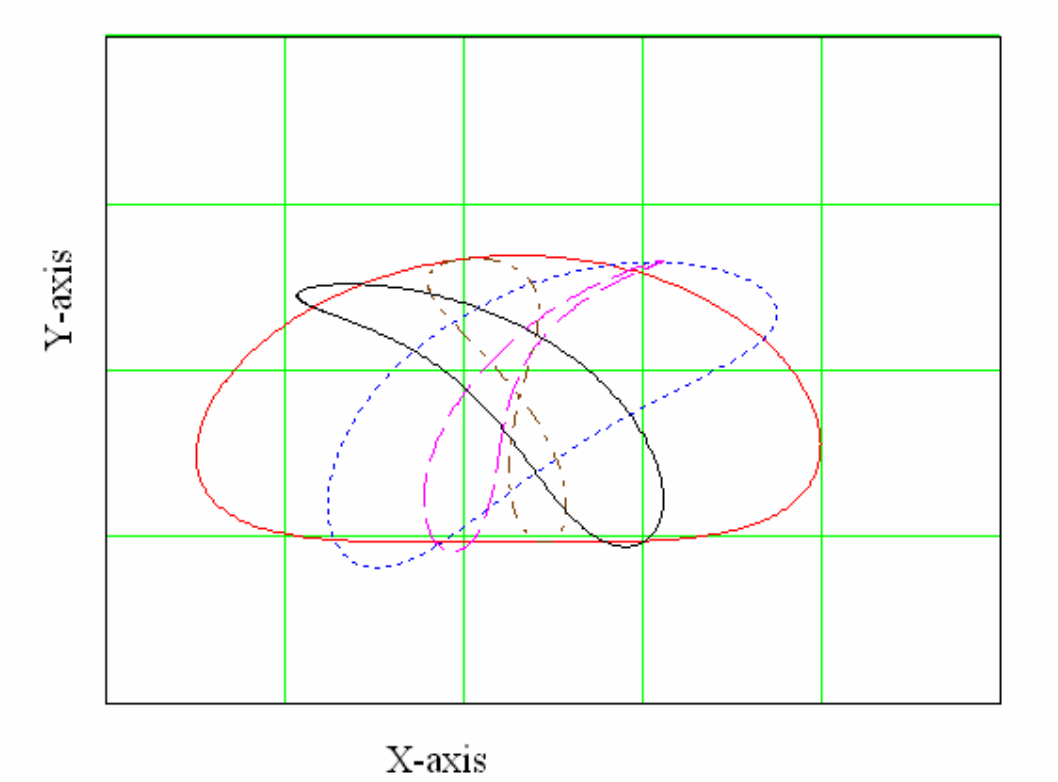


Figure 4.12 Several Paths of the Point E for Different Phase Angles

An interesting situation observed in the path of point E is that, as the lower portion of the path converges to a straight line, *s* increases. Therefore, in order to obtain a large output stroke, it is aimed to obtain an approximate straight line for the lower portion of the path of point E.

For this purpose, initially the motion is canonically represented and a procedure is developed to obtain the moving and fixed centrodes of link 7. Then, another procedure is developed to obtain the center of curvatures of moving and fixed centrodes and the inflection circle of link 7 throughout the complete cycle. Finally, a position is specified and the inflection pole at that position is chosen as point E.

### 4.7 Moving and Fixed Centrodes of Link 7

The equations of the moving and fixed centrodes can be obtained (Appendix B) both in polar and cartesian coordinates as:

In polar coordinates:

$$\vec{z}_p = -d_2 e^{i(\theta_{12}-\theta_{17})} \frac{d\theta_{12}}{d\theta_{17}} \tag{4.22}$$

$$\vec{Z}_p = d_2 e^{i\theta_{12}} (1-\frac{d\theta_{12}}{d\theta_{17}}) \tag{4.23}$$

In cartesian coordinates:

$$x_p = -d_2 \frac{d\theta_{12}}{d\theta_{17}} cos(\theta_{12}-\theta_{17}) \tag{4.24}$$

$$y_p = d_2 \frac{d\theta_{12}}{d\theta_{17}} \sin(\theta_{17}-\theta_{12}) \tag{4.25}$$

$$X_p = d_2 cos\,\theta_{12} \left(1-\frac{d\theta_{12}}{d\theta_{17}}\right) \tag{4.26}$$

$$Y_p = d_2 \sin\theta_{12} \left(1-\frac{d\theta_{12}}{d\theta_{17}}\right) \tag{4.27}$$

The only unknown in above equations is $\frac{d\theta_{12}}{d\theta_{17}}$ and it can be determined as:

$$\frac{d\theta_{12}}{d\theta_{17}} = \frac{K_2 \sin(-\theta_{12} + \theta_{17} - k_2) + K_4 \sin(2\theta_{12} - \theta_{17} + k_2)}{K_2 \sin(-\theta_{12} + \theta_{17} - k_2) + K_3 \sin\theta_{12} + 2K_4 \sin(2\theta_{12} - \theta_{17} + k_2)} \tag{4.28}$$

where

$$K_1 = a_1^2 + a_2^2 + a_3^2 - a_4^2$$

$$K_2 = 2a_2a_3$$

$$K_3 = 2a_1a_2$$

$$K_4 = 2a_1a_3$$

Then, the equations of the moving and fixed centodes can be obtained from Eqs.4.22-27. The equation of the moving centrode defines a curve, which is the locus of all instant centers with respect to the moving frame and the equation of the fixed centrode defines a curve, which is the locus of all instant centers with respect to the fixed frame. The motion of a moving plane can be obtained by the pure rolling of the moving centrode on the fixed centrode. The moving and fixed centrodes of a mechanism are plotted throughout a cycle as shown in Figure 4.13. The points of tangencies are the poles. Note that the moving centrode must be transformed to the fixed frame in order to plot the centrodes in the same reference frame.

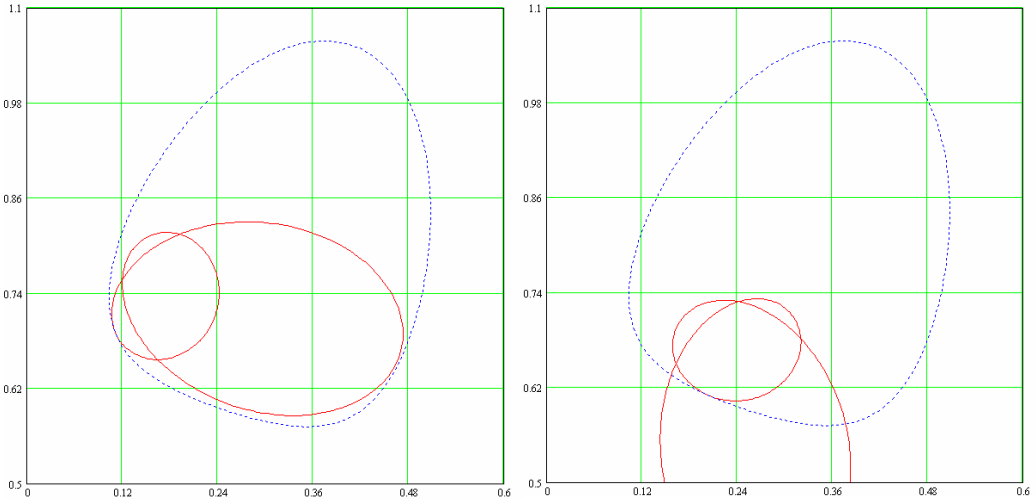

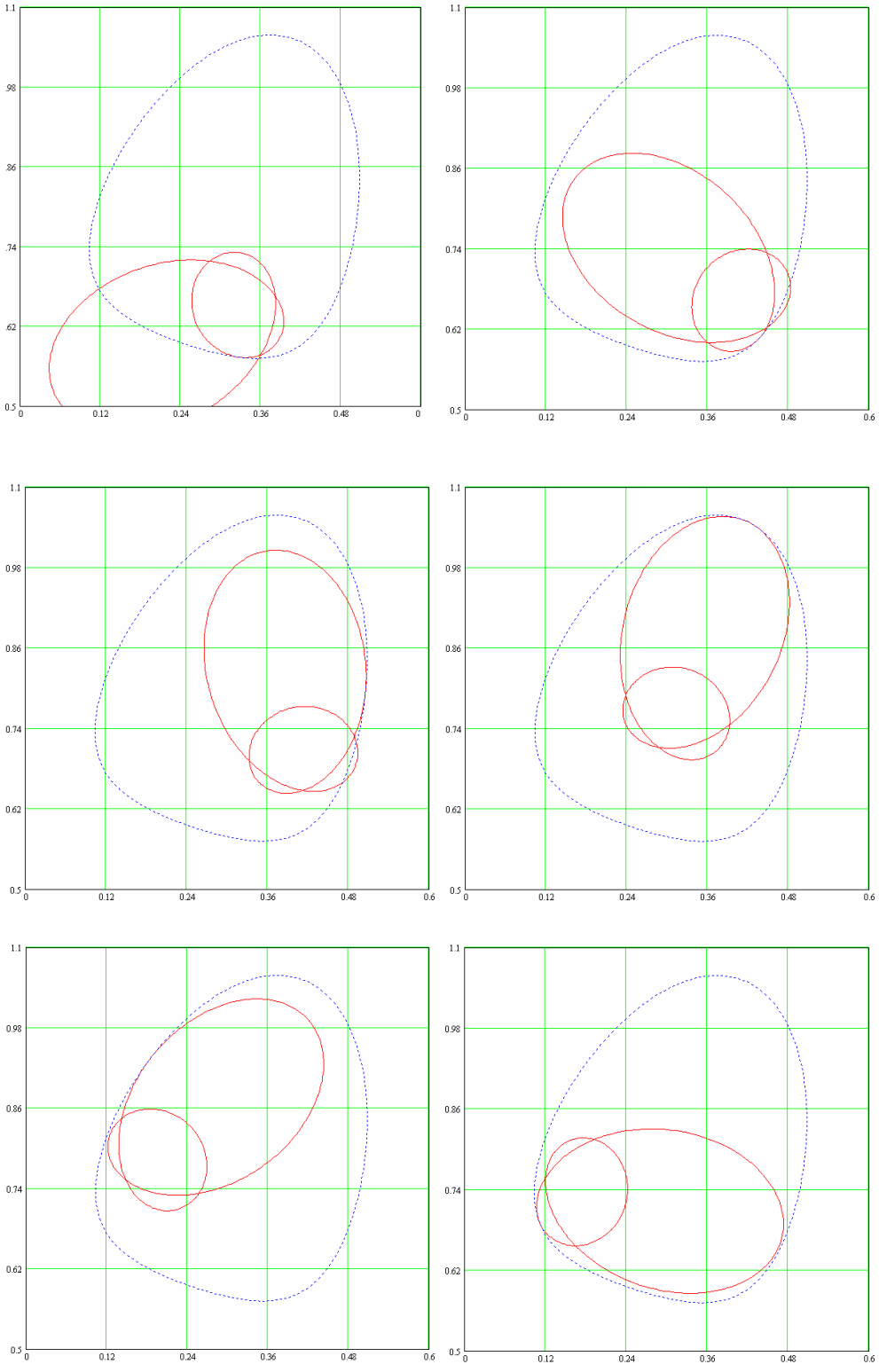

Figure 4.13 Moving and Fixed Centrodes of Link 7 throughout a Cycle

### 4.8 Center of Curvature of Fixed and Moving Centrodes of Link 7

It is aimed to obtain an approximate straight line for the lower part of the path of point E. For this reason, inflection circle of link 7 throughout the complete cycle can be obtained. In order to obtain the inflection circle diameter at each position, center of curvatures of the moving and fixed centrodes of link 7 at each position are determined (Appendix D).

### 4.9 Synthesis Procedure by Use of Inflection Circle

Initial design step is to choose an optimum GFLM from the related design charts. Consequently, link lengths $a_2$, $a_3$, $a_4$ are determined. When the gear ratios are specified, the length of the arm can be determined as well ($d_2 = r_5 + 2r_3 + r_7$). Then, link lengths $a_7$, $a_8$, the phase angle $k_2$, the adjustment angle $\delta$, and the slider axis $c_{19}$ have to be determined.

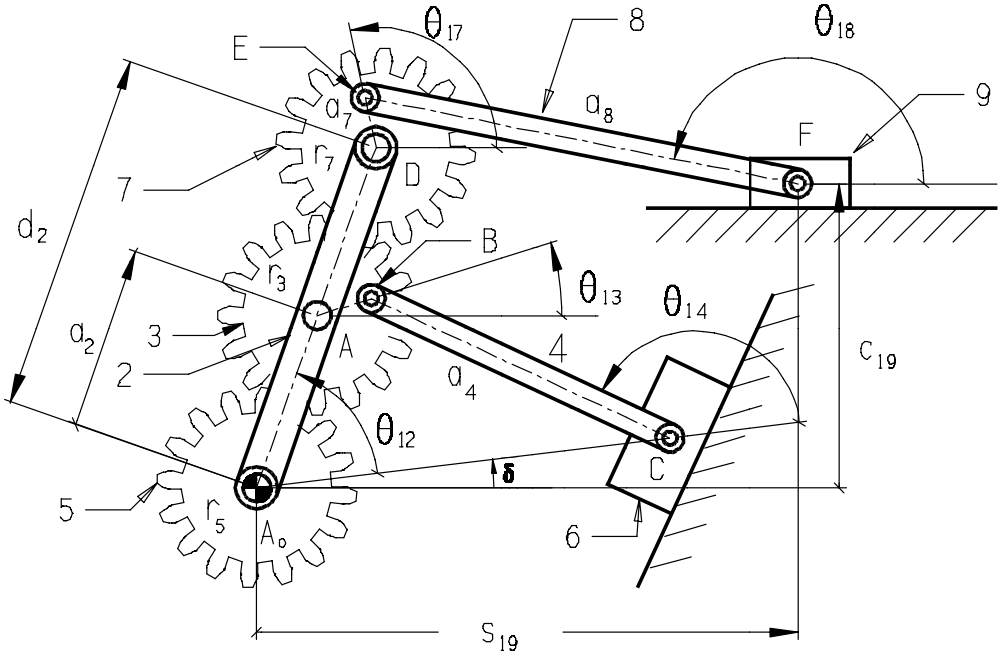


Figure 4.1 The Geared Adjustable Stroke Mechanism

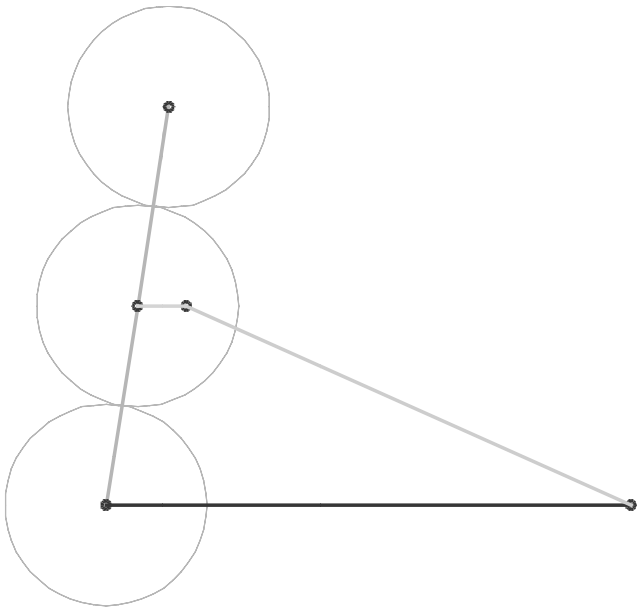

Figure 4.14 Determined Part of the Mechanism

Consequently, a GFLM with arm length $d_2$ is determined and a gear is attached to the endpoint of the arm (Fig. 4.14). The arm performs an oscillating motion. The mechanism can be analyzed and the motion of the arm can be determined (Fig.4.15). Then, the midpoint of this oscillation can be obtained.

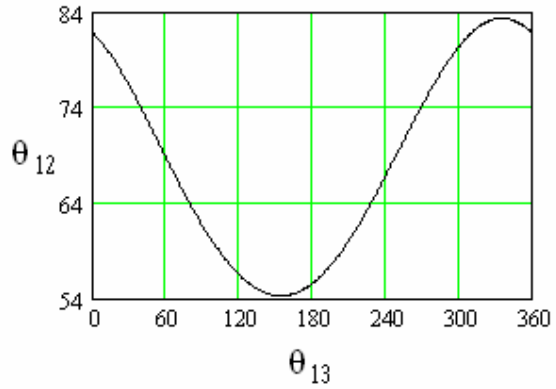


Fig.4.15 Motion of the Arm (Link 2) as a Function of Link 3

Arm passes from the midpoint two times, but the position that the arm passes from the midpoint during the quick-return cycle should be chosen (i.e. $\theta_{13}>\pi$) (Fig.4.16). The reason for this is, the desired approximate straight line is considered to be in this region, and this midpoint is approximately a symmetric position for the path of point E.

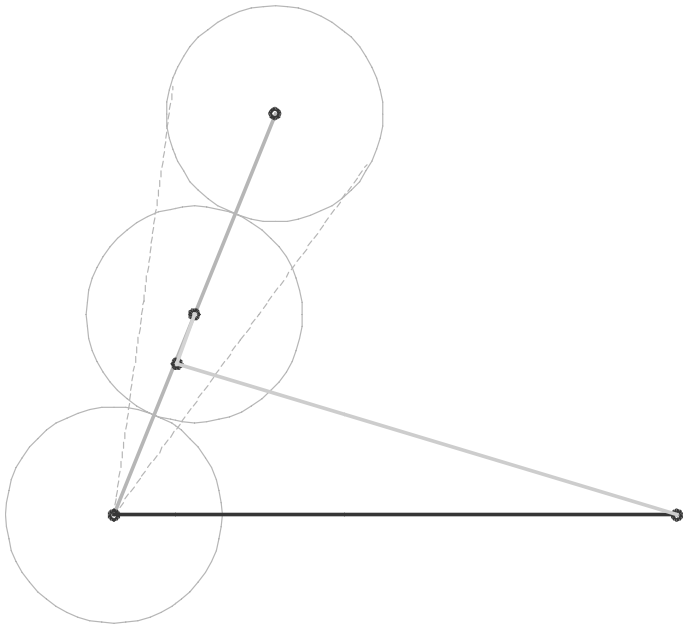

Fig. 4.16 Selected Position which the Arm Passes from the Midpoint

After obtaining the midpoint of the oscillation of the arm, the moving and fixed centrodes of link 7 are evaluated. After determining the moving and fixed centrodes, their center of curvatures are evaluated throughout the cycle. Then, the position which the arm passes from the midpoint is located.

For example, in Fig.4.17 the blue plot is the fixed centrode, the red plot is the moving centrode, the pink plot is the center of curvature of the fixed centrode, and the brown plot is the center of curvature of the moving centrode. The point of tangency of the moving and the fixed centrodes is the pole at the position located.

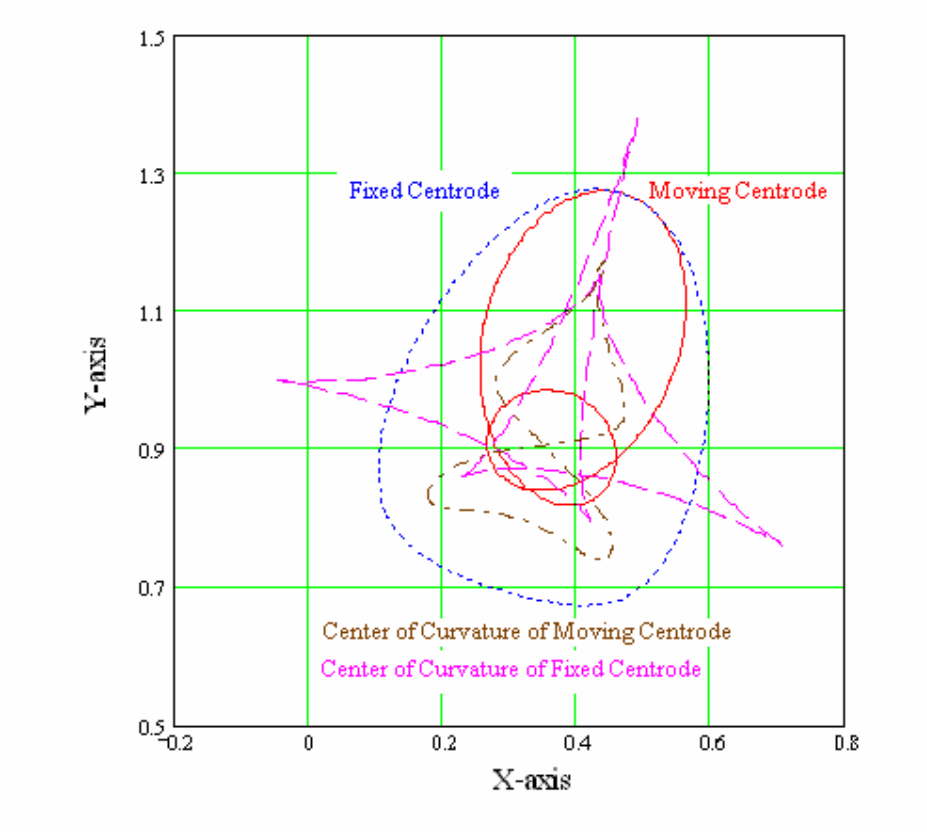


Fig. 4.17 Centrodes and Their Centers of Curvature of link 7 for a Geared Adjustable Stroke Mechanism

At the position located, the diameter of the inflection circle, $\gamma$, can be determined from the center of curvatures of the fixed and moving centrodes (Appendix C).

The center of the inflection circle is on the pole normal, and its radius is $\gamma/2$ (Fig. 4.18), so the center of the inflection circle can be determined as:

$$\vec{C} = \vec{Z}_p + \frac{\gamma}{2} e^{iv} \tag{4.29}$$

Therefore, the inflection circle can be determined as:

$$\vec{I} = \vec{C} + \frac{\gamma}{2} e^{i\Psi} \tag{4.30}$$

where

$$\Psi = 0^0 ... 360^0$$

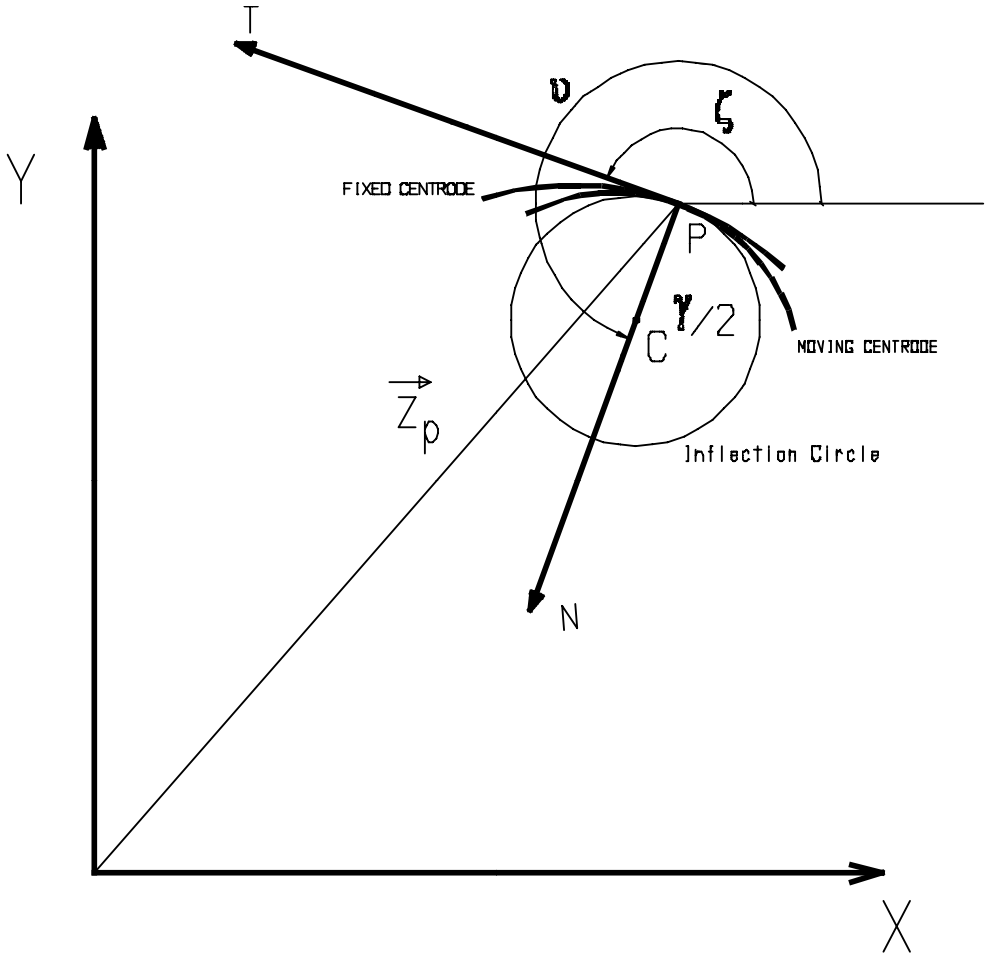


Fig.4.18 The Inflection Circle at the Located Position

At the located position the centrodes and the inflection circle are shown in Fig 4.19.

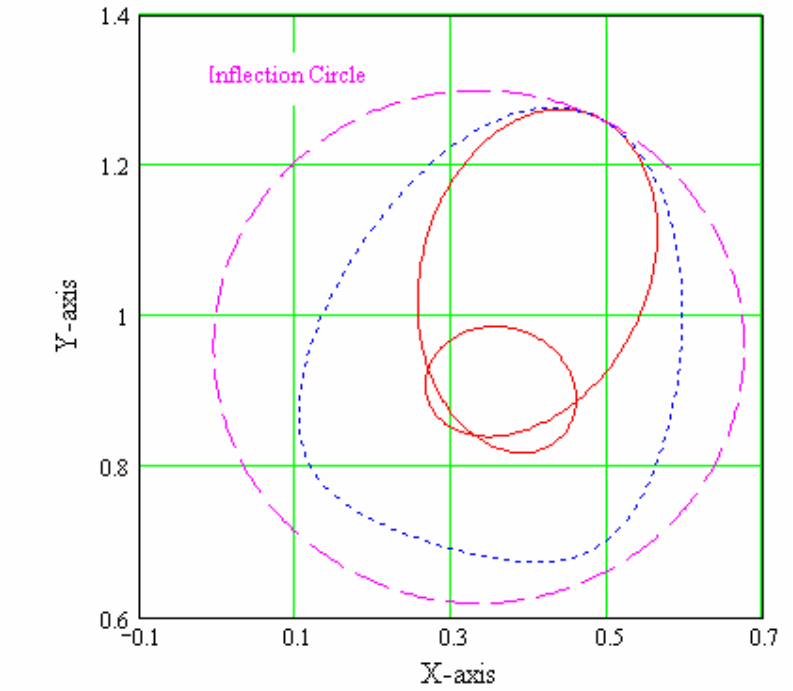


Fig. 4.19 The Centrodes and the Inflection Circle at the Located Position

After obtaining the inflection circle, a point will be determined on link 7 as point E, e.g. the attachment point of the connecting rod (link 8) to link 7. Since, the desired approximate straight line will be parallel to the slider axis (X-axis), the inflection pole will be chosen as the point E. The inflection pole is the intersection of the inflection circle and the pole normal and it can be determined as:

$$\vec{IP} = \vec{Z}_p + \gamma e^{i\upsilon} \tag{4.31}$$

The center of the link 7 is:

$$\vec{D} = d_2 e^{i\theta_{12}} \tag{4.32}$$

Therefore, the vector $\vec{DE}$ can be determined (Fig 4.20).

$$\vec{DE} = \vec{IP} - \vec{D} \tag{4.33}$$

The magnitude of this vector is the link length $a_7$, and the argument of this vector is the angle $\theta_{17}$, then the phase angle $k_2$ can be determined from Eq (4.3).

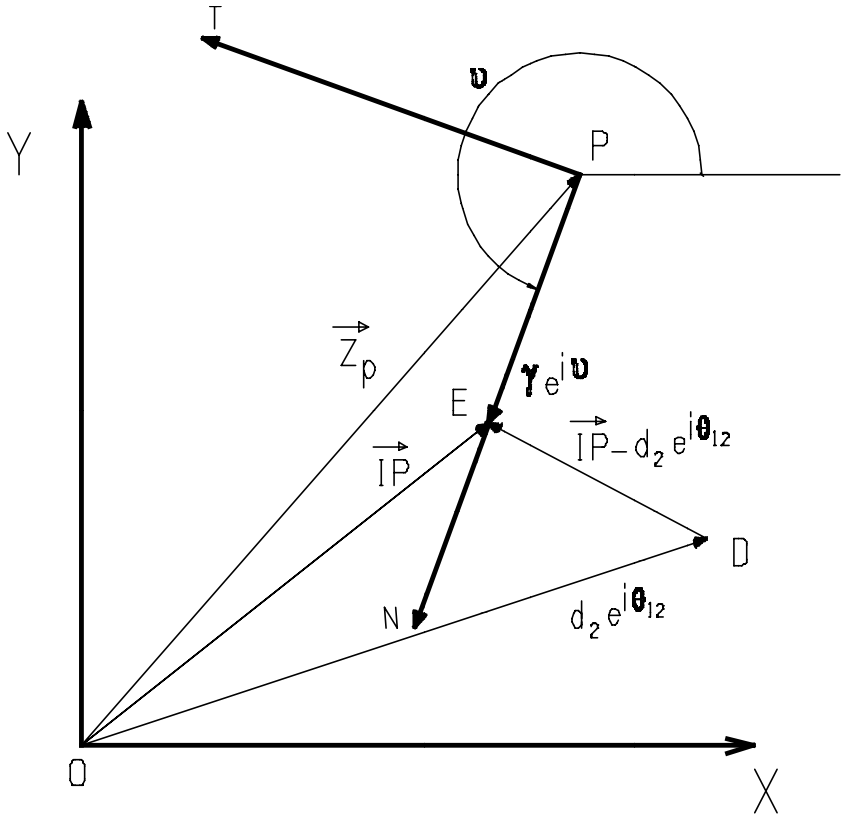


Fig. 4.20 Determination of the Point E

Since link length $a_7$, and the phase angle $k_2$ is determined, the resulting path of the point E can be seen in Fig. 4.21.

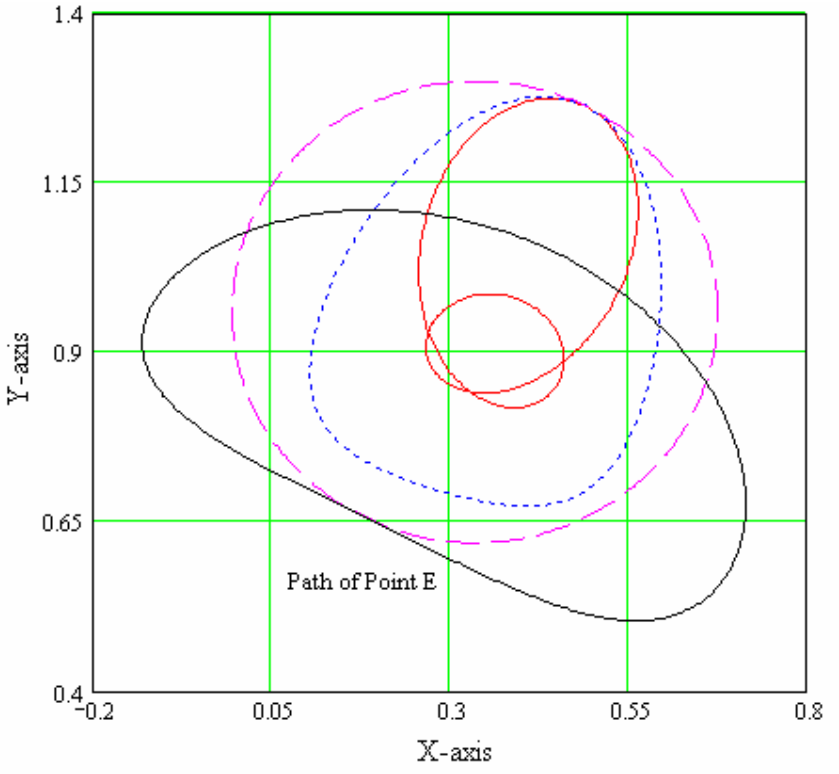


Fig. 4.21 Path of the Point E

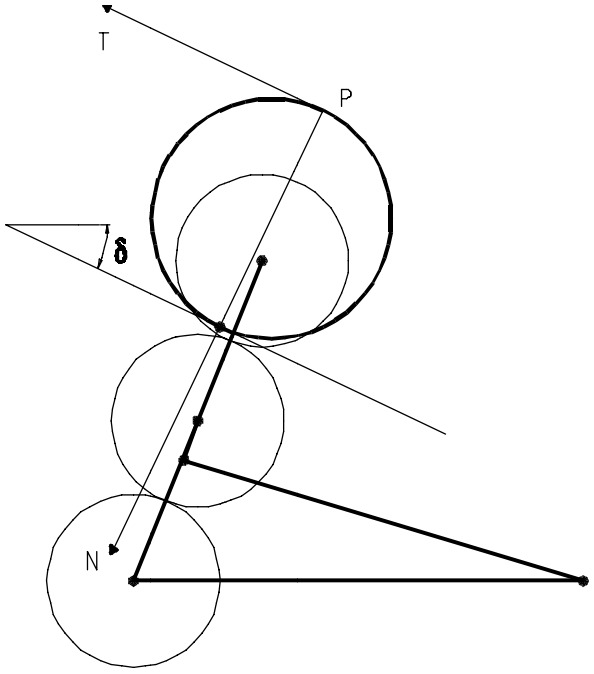


Fig.4.22 Straight Line Parallel to Pole Tangent

At the position located, the inflection circle and the inflection pole is shown in Fig. 4.22. Since the inflection pole is chosen as point E, the approximate straight line is parallel to the pole tangent. The angle between the X-axis and the pole tangent is, $\zeta$, which is the slope of the centrodes at the position. The slider axis was chosen to be X-axis. Therefore, the mechanism must be rotated $\pi$-$\zeta = \delta$ rad in order to obtain an approximate straight line parallel to the X-axis (Fig. 4.23).

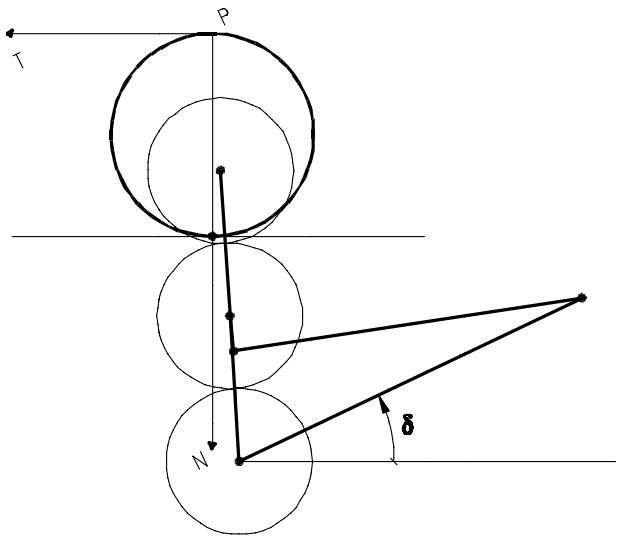


Fig. 4.23 Straight Line Parallel to X-Axis

Then, the resulting path of point E is shown in the Fig. 4.24.

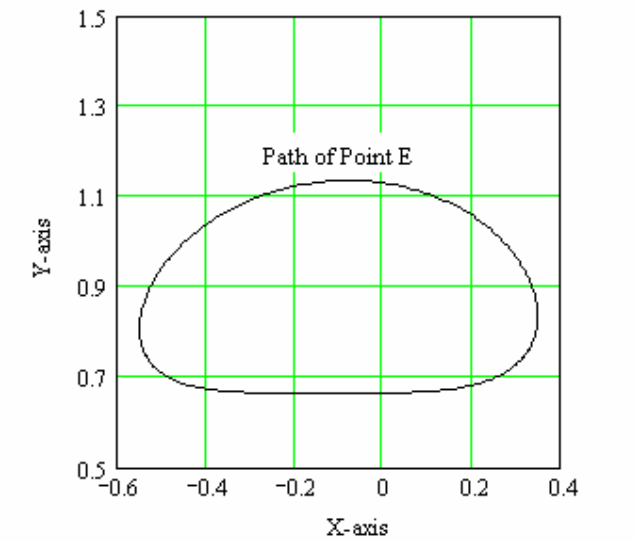


Fig. 4.24 The Resulting Path of the Point E

From centric slider-crank mechanisms it is known that the connecting rod does not affect the output stroke and for the other type of slider-crank mechanisms its effect to the output stroke is negligible. As the length of the connecting rod increases, the transmission angle improves. After several trials it is observed that the effect of connecting rod to the output stroke is also negligible for this type of mechanisms. Therefore, the connecting rod, $a_8$, is not a design parameter. It should be chosen large for better transmission characteristics (up to a link length ratio of 1/10).

The remaining parameter is the height of the slider axis, $c_{19}$, and it should be chosen due to design or working conditions, since its effect to the output stroke within the feasible design region is also negligible. However, $c_{19}$ has an important effect on the second transmission angle. From Fig 4.25, it is observed that the height of the slider axis can be chosen at several positions, around the path of point E. If it is chosen around the midpoint of the path of point E, the transmission angle deviation from $90^o$ would be approximately equal during the working and reverse cycle. If it is chosen around the apex or the lower part of the path of point E, the transmission angle deviation from $90^o$ would be very low during a cycle. However, the lower part (approximate straight line) of path of point E is the quick return cycle.

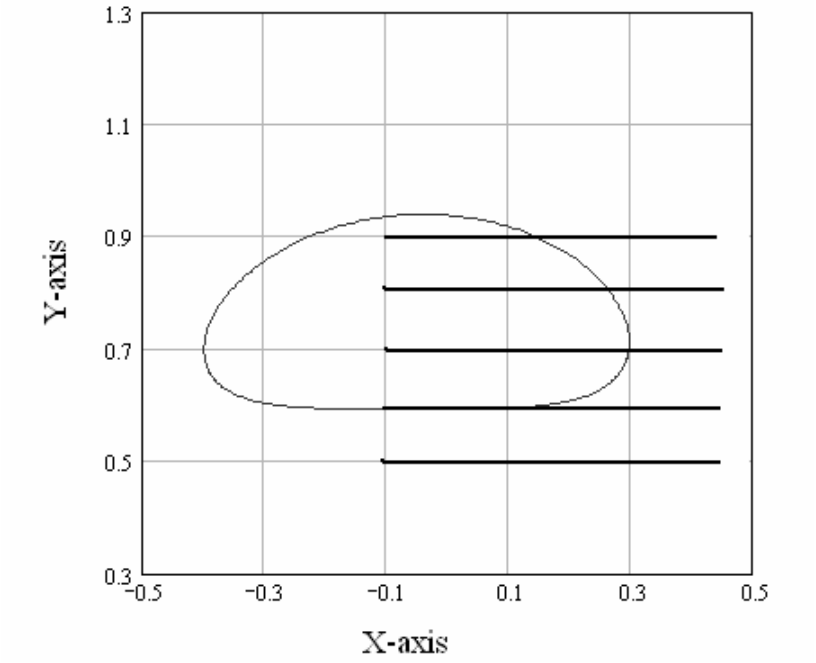


Fig. 4.25 Determination of the Height of the Slider Axis

**Design Example 4.2**

This example is to illustrate the synthesis of the GASM by using the inflection circle of link 7. Initially an optimum geared five-link mechanism is chosen ($R_1$ = 1, cw input rotation). The oscillation of the arm (link 2) is, $\phi = 35^o$, corresponding rotation of link 4 is $\psi = 10^o$ and $\lambda_{opt}$ = 0.45. Corresponding link lengths are: $a_1$ = 1, $a_2$ = 0.932, $a_3$ = 0.276, $a_4$ = 0.614 and the length of the arm, $d_2$ = 1.865 ($R_2$ = 1).

Motion of the arm is shown in Fig 4.26:

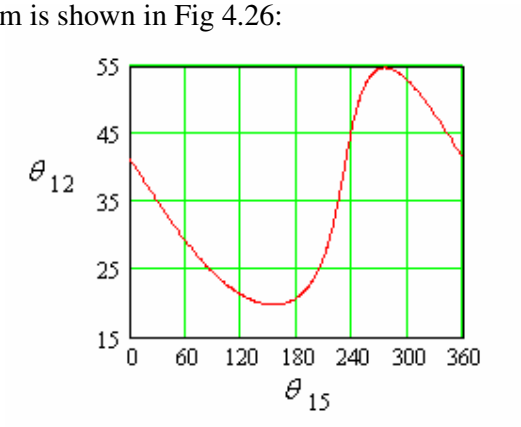


Figure 4.26 Motion of the Arm for Ex.4.2

Then, by applying the synthesis method, link length $a_7$, and phase angle $k_2$, are evaluated as:

$$a_7 = 1.484, \quad k_2 = 316.6^o$$

The slope of the centrodes is obtained as $103.9^o$, so adjustment angle can be determined as $76.1^o$. Consequently, from the path of point E, $s$, and $h$ are determined as:

$$s = 3.92 \qquad h = 2.89$$

$\frac{d_2}{s} = 0.476$, which means stroke is more than two times larger than the arm.

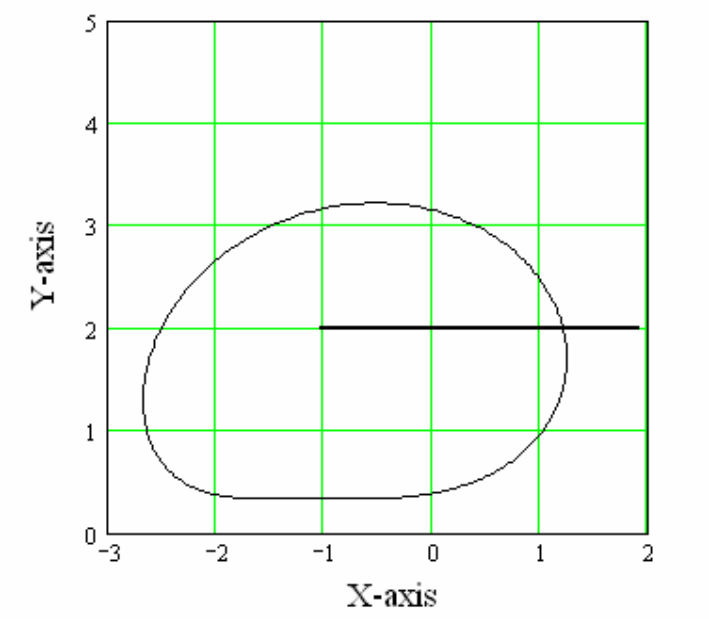


Figure 4.27 Choosing the Height of the Slider Axis ($c_{19}$)

The height of the slider axis is chosen as, $c_{19} = 2$, and connecting rod is chosen as, $a_8 = 2.7$.

Then, the output motion and the second transmission angle of the mechanism are plotted as:

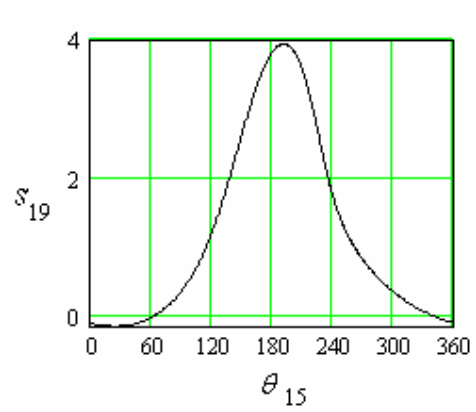


Figure 4.28 Displacement of the Output Link for Ex.4.2

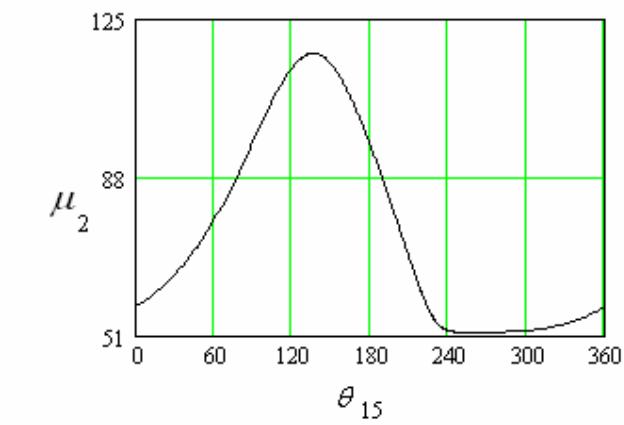


Figure 4.29 Second Transmission Angle of the Mechanism for Ex.4.2

The animation of the mechanism designed in Ex.4.2 is prepared and several positions are shown in the following figures.

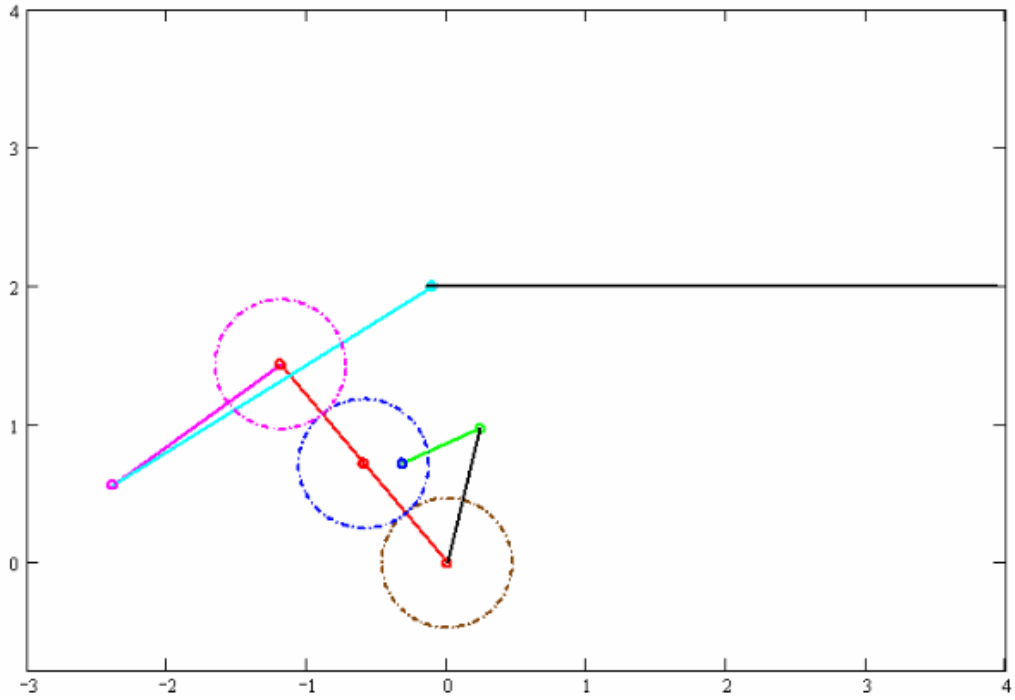


Figure 4.30 a. Input = $0^o$, Output = -0.1

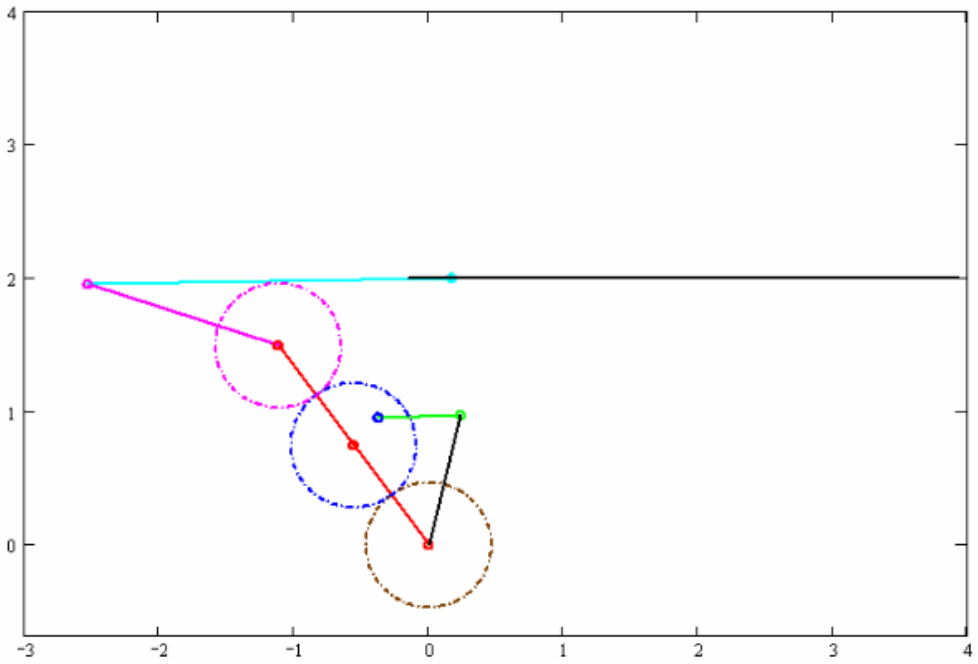


Figure 4.30 b. Input = 75°, Output = 0.11

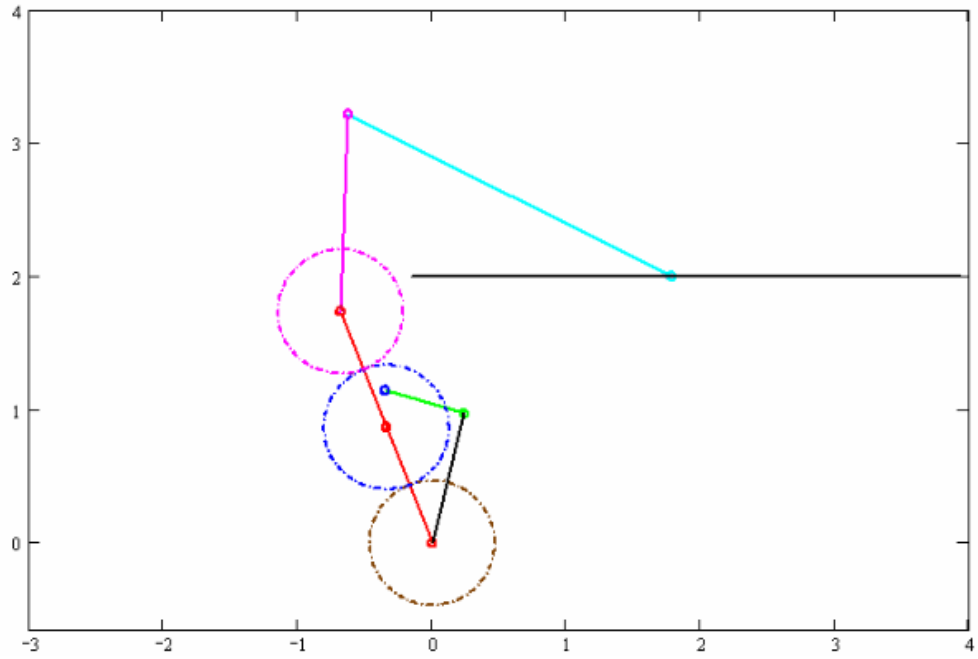


Figure 4.30 c. Input = 130°, Output = 1.695

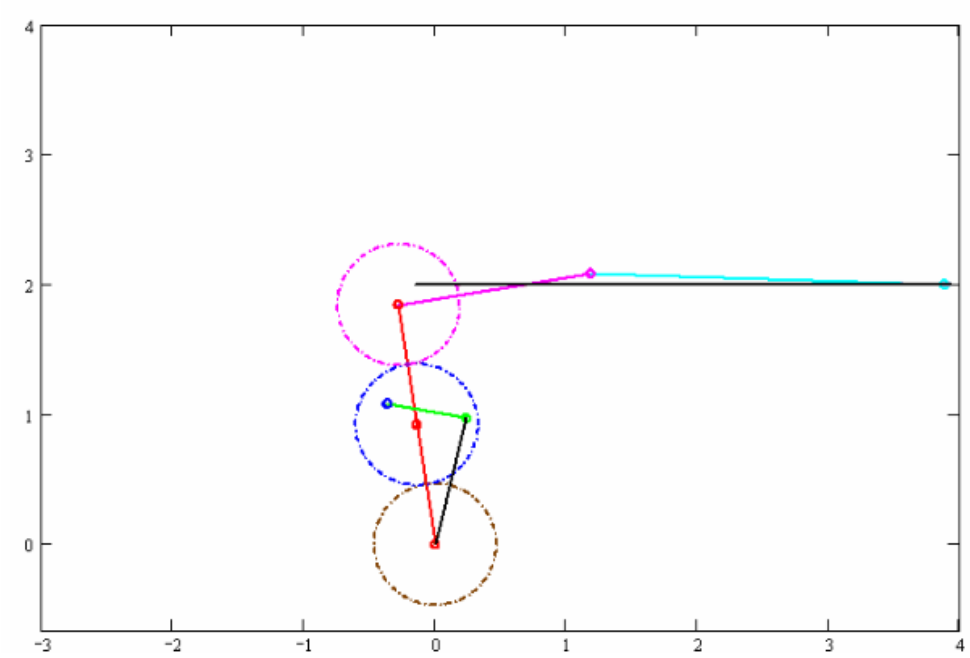


Figure 4.30 d. Input =180$^{o}$, Output = 3.8

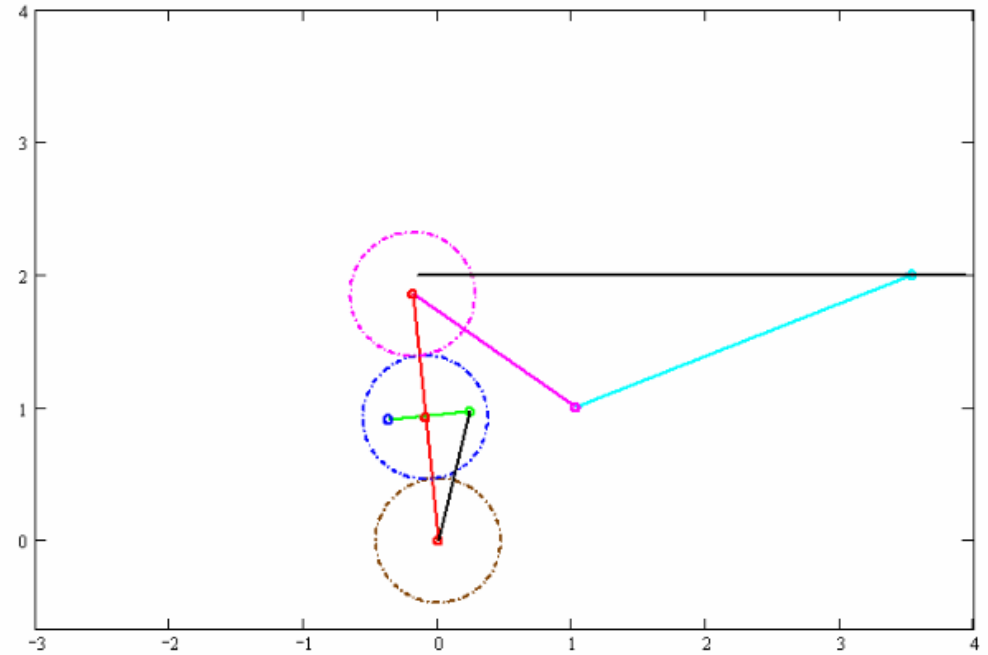


Figure 4.30 e. Input = 208$^{o}$, Output = 3.61

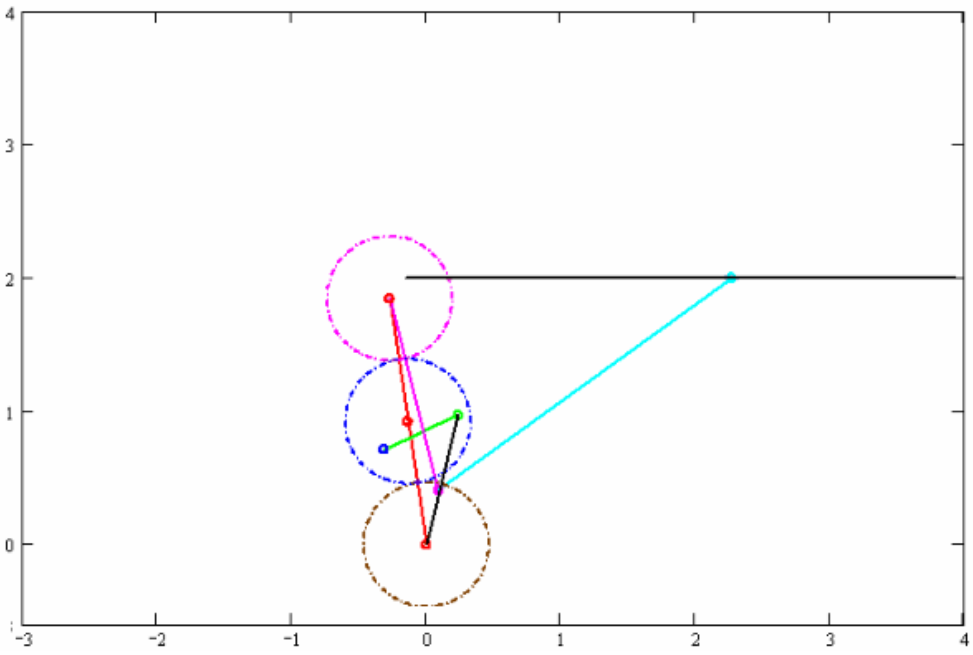


Figure 4.30 f. Input = 230$^{o}$, Output = 2.33

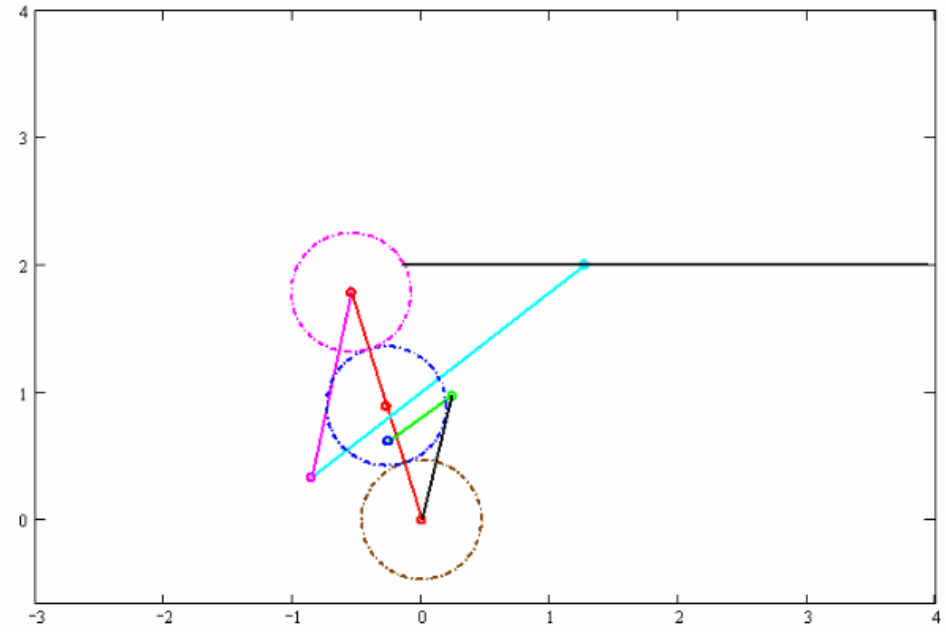


Figure 4.30 g. Input =250$^{o}$, Output = 1.32

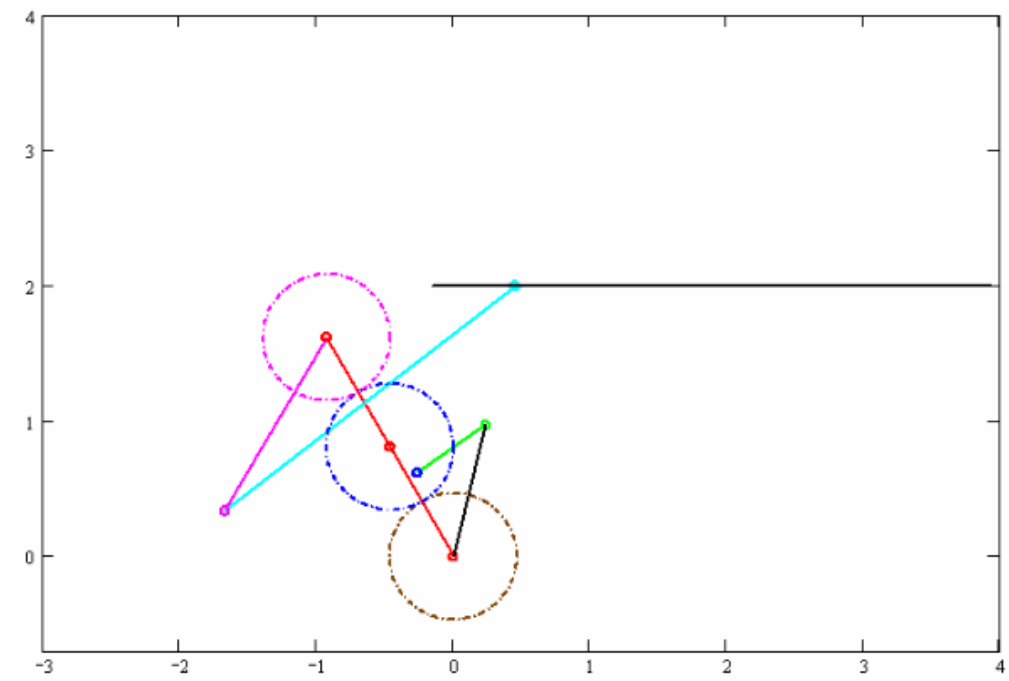


Figure 4.30 h. Input =290$^{o}$, Output = 0.46

By this approach, feasible results are obtained, but as the oscillation of the arm increases, diameter of the inflection circle increases, so link length 7 increases (point E is determined to be outside the gear as the oscillation of the arm increases). This condition is a constraint for the design. Moreover, this method may not yield the optimum configuration for maximum stroke.

### 4.10 Optimum Synthesis of the Geared Adjustable Stroke Mechanism

Initial design step is to choose an optimum GFLM from the design charts. Hence, link lengths $a_2$, $a_3$, $a_4$ are determined, when the gear ratios are specified, the length of the arm can also be determined ( $d_2 = r_5 + 2r_3 + r_7$ ). The arm performs an oscillating motion, the mechanism can be analyzed and the motion of the arm can be determined. Then, the midpoint of the oscillation of the arm can be obtained. The arm passes from the midpoint two times, but the position that the arm passes from the midpoint during the quick-return cycle should be chosen (i.e. $\theta_{13}>\pi$), because this position is approximately a symmetric position for the path of point E.

At that position the angle between X-axis and the arm is determined; $\theta_{12\text{average}}$ (Fig. 4.31 left). Then, the fixed link of the mechanism is rotated since $\theta_{12\text{average}}$ becomes $90^o$ (Fig. 4.31 right). Hence, the adjustment angle, $\delta$ can be determined as:

$$\delta = 90^\circ - \theta_{12avg} \tag{4.34}$$

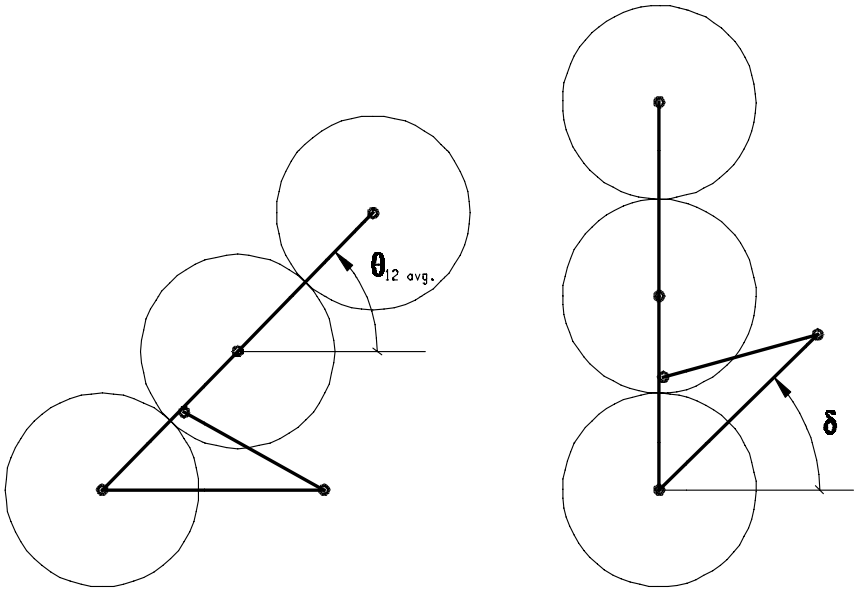


Fig. 4.31 Obtaining the Adjustment Angle, $\delta$

Then, simply any point on link 7, but inline with the arm is selected as point E as shown in Fig. 4.32.

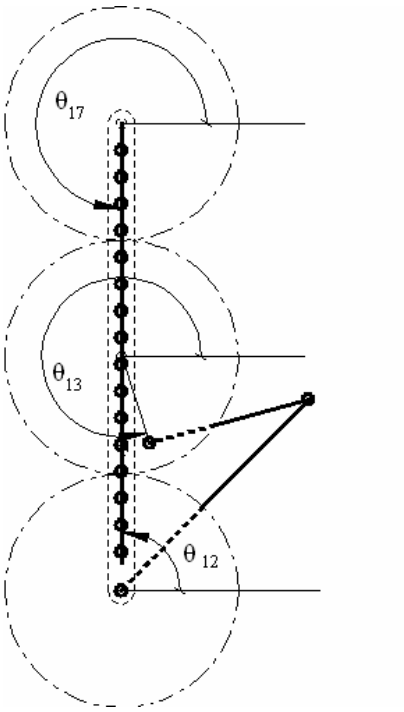


Fig. 4.32 Point E is Chosen Inline with the Arm

Choosing point E inline with the arm means that the angle of link 7 is $270^o$ ($\theta_{17}$ =$270^o$). At that instant, $\theta_{13}$ is obtained and $\theta_{12}$ = $90^o$, so the phase angle, $k_2$ is determined from Equation 4.3.

$$k_2 = \theta_3 + 270 - 180 \tag{4.35}$$

The parameters $\delta$ and $k_2$ determined by this method are not the optimum values, but are feasible solutions for any parametric optimization procedure.

Point E can be chosen anywhere on the vertical axis as shown in Fig. 4.32 and different paths are obtained for these points as shown in Fig. 4.33. As link length $a_7$ increases larger paths are obtained.

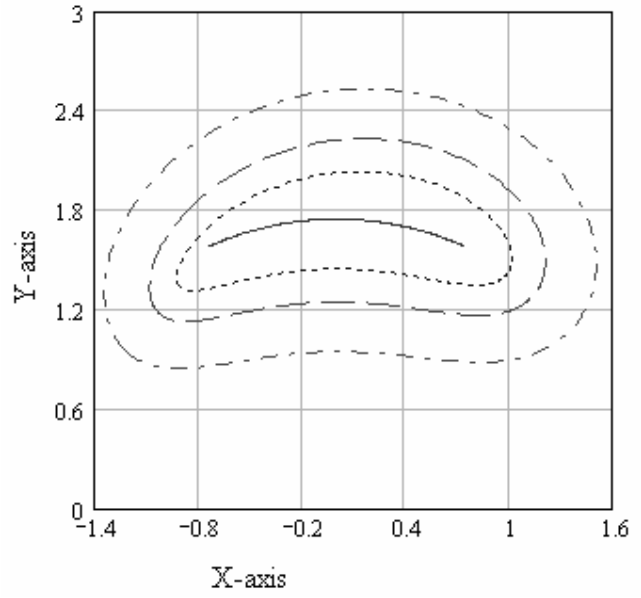


Figure 4.33 Larger Paths as Link 7 Increases

It can be easily observed that as link length $a_7$ is increased, the stroke also increases, but the transmission characteristics decreases. In other words, as the link length $a_7$ is increased, $d_2/s$ decreases, but h/s increases as shown in Fig. 4.34. Hence, the effect of link length $a_7$ is clear and it can be chosen due to design conditions.

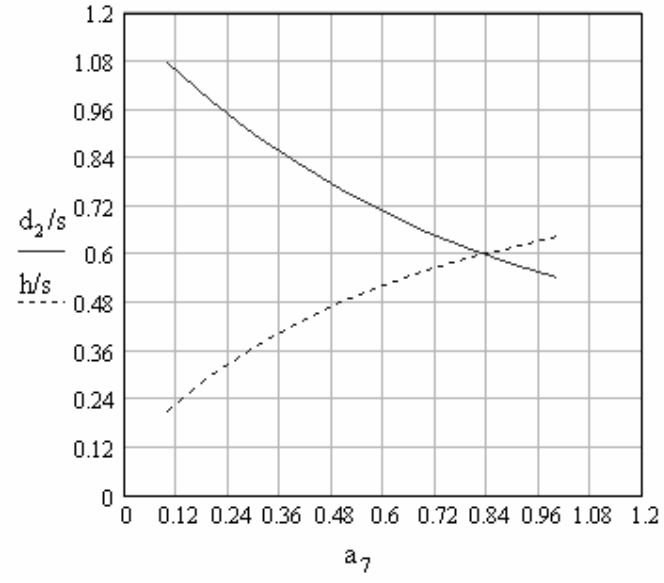


Figure 4.34 As $a_7$ Increases $s$ and $h$ Increases

It is explained that as the length of the connecting rod increases, the transmission angle improves. Therefore, the connecting rod, $a_8$, is not a design parameter. It is also explained that the height of the slider axis, $c_{19}$, can be chosen due to design conditions (Fig 4.35).

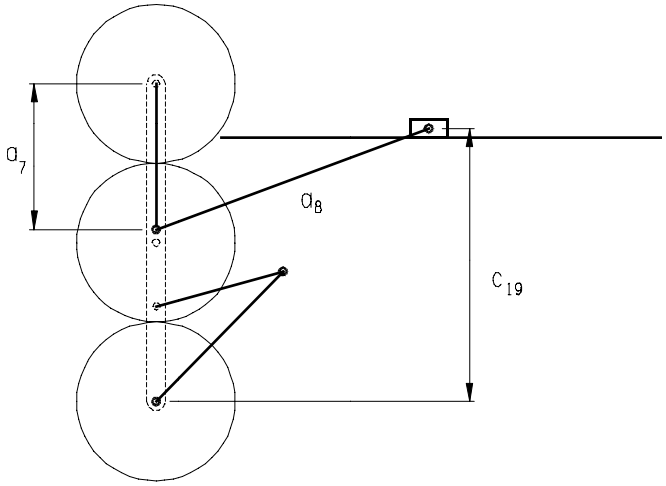


Figure 4.35 Link Length 7, the Slider Axis and the Connecting Rod

Therefore, the optimization parameters are the adjustment angle, $\delta$, and the phase angle, $k_2$, in other words the relative angular position of point E (Fig 4.36). Hence, $\delta$, and $k_2$ should be optimized for maximum stroke.

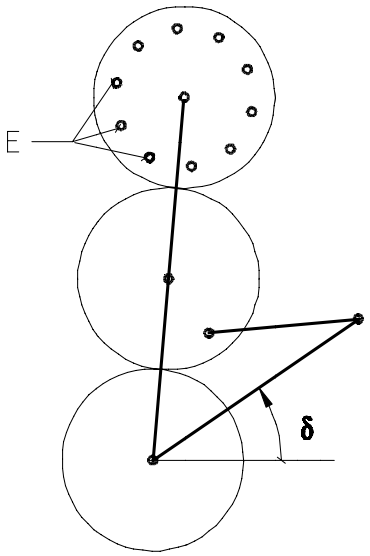


Figure 4.36 The Optimization Parameters: $\delta$ and $k_2$

### 4.11 Optimization Parameters

After choosing an optimum GFLM, the optimization parameters for the GASM are determined to be $\delta$, and $k_2$. These parameters should be optimized for maximum stroke. Initially, the adjustment angle $\delta$ is searched in a region $\pm 20^o$ around the value obtained by Eq. 4.34 and the phase angle $k_2$ is searched from 0 to $2\pi$. Link length 7 is chosen on the gear as: $a_7 = 0.9r_7$.

**Design Example 4.3:**

This example is to illustrate the preparation of a stroke chart and determining the optimum $\delta$ and $k_2$ values for a given $\phi$ and $\psi$. Initially an optimum GFLM is chosen from the design chat (gear ratios are equal to 1). The oscillation of the arm (link2) is, $\phi = 50^o$, corresponding rotation of link 4 is $\psi = 10^o$ and $\lambda = 0.505$. Corresponding link lengths are: $a_1 = 1$, $a_2 = 0.873$, $a_3 = 0.365$, $a_4 = 0.722$, the arm $d_2 = 1.746$, and $a_7 = 0.9r_7 = 0.393$.

The midpoint of the oscillation of the arm is obtained as:

$$\alpha = 45.61^o$$

Before the optimization, the adjustment angle $\delta$ and the phase angle $k_2$ can be evaluated from Eqs. 4.34-35 as:

$$\delta = 90^o - 45.61^o = 44.39^o$$

$$k_2 = 3^o$$

Then, for $\delta = 44.39^o - 20^o$ to $44.39^o + 20^o$ and for $k_2 = 0$ to $2\pi$, $s$ and $h$ are determined seen in Fig. 4.37. X-axis represents $k_2$ values and Y-axis represents $\delta$ values. Dotted curves represent $s$ and full lined curves represent the corresponding $h$.

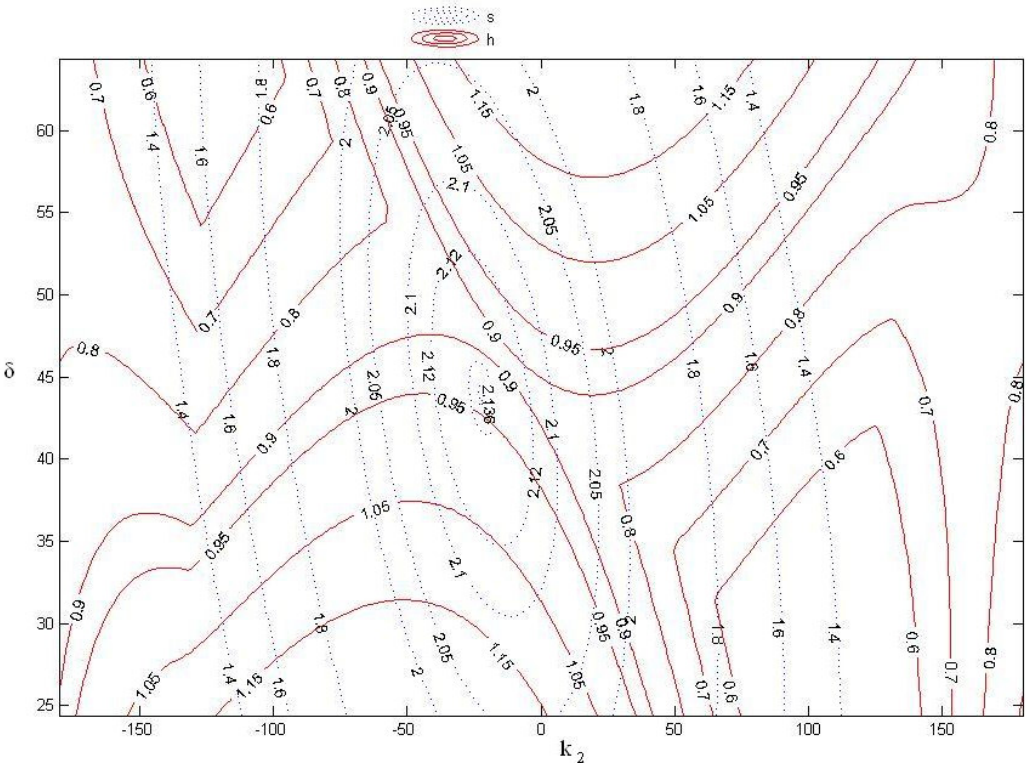


Figure 4.37 The Stroke Chart for $\phi = 50^o$, $\psi = 10^o$

As seen in Fig. 4.37 maximum $s$ is equal to 2.137 units and corresponding optimum $\delta$ and $k_2$ values are:

$$\delta_{opt} = 43.4^o,\ k_{2opt} = -22^o$$

Corresponding $h$ is equal to 0.94, and it is very small according to $s$ ($h/s$=0.44).

Note that $\delta_{opt}$ is very close to the value determined by Eq.4.34.

For every $\phi$ and $\psi$ a similar chart can be obtained. Therefore, a parametric optimization routine is developed to determine the optimum $\delta$ and $k_2$ values for every $\phi$ and $\psi$ for maximum stroke. After determining these optimum parameters, $a_7$, $a_8$, and $c_{19}$ can be chosen due to design conditions.

## 4.12 Optimization of the Geared Adjustable Stroke Mechanism for Maximum Stroke

For every $\phi$ and $\psi$, the optimum values of $\delta$ and $k_2$ for maximum stroke are determined by a parametric optimization routine which is performed via MATLAB. Initially for a given $\phi$ (swing angle of the arm) and $\psi$ (corresponding rotation of link 4) the GFLM is synthesized and the optimum with respect to the transmission angle is determined. Then, the method explained in section 4.10 is applied for gear ratios of unity, and preliminary feasible solutions are determined.

Note that according to the direction of rotation of the input there are two sets of optimum GFLM. Hence two design charts are determined for the GASM according to input rotation direction.

$\delta_{opt}$ and $k_{2opt}$ are searched for every $\phi$ and $\psi$. $\delta_{opt}$ is searched in a region $\pm 5^o$ from the value obtained by Eq. 4.34, and $k_{2opt}$ is searched from $-40^o$ to $10^o$, since after several attempts it is observed that the optimum values are located in these regions. The resulting design charts are shown in Fig. 4.38 in which the X-axis corresponds to $\psi$, Y-axis corresponds to $\phi$. Full lines represent $\delta_{opt}$ and dotted lines represent $k_{2opt}$.

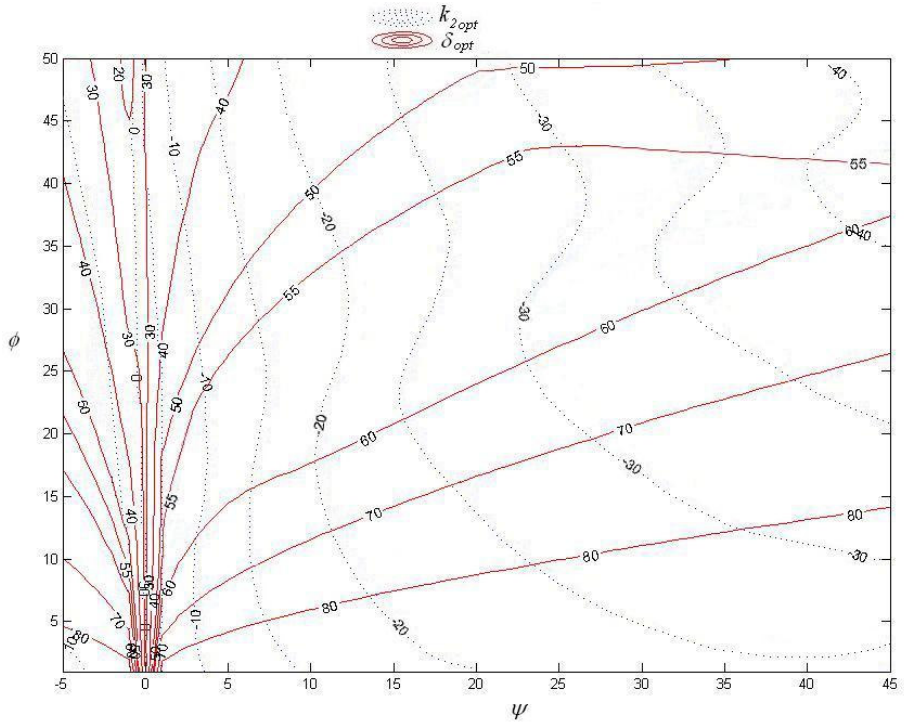


Fig. 4.38 a. The Design Chart for Maximum Stroke (Input cw)

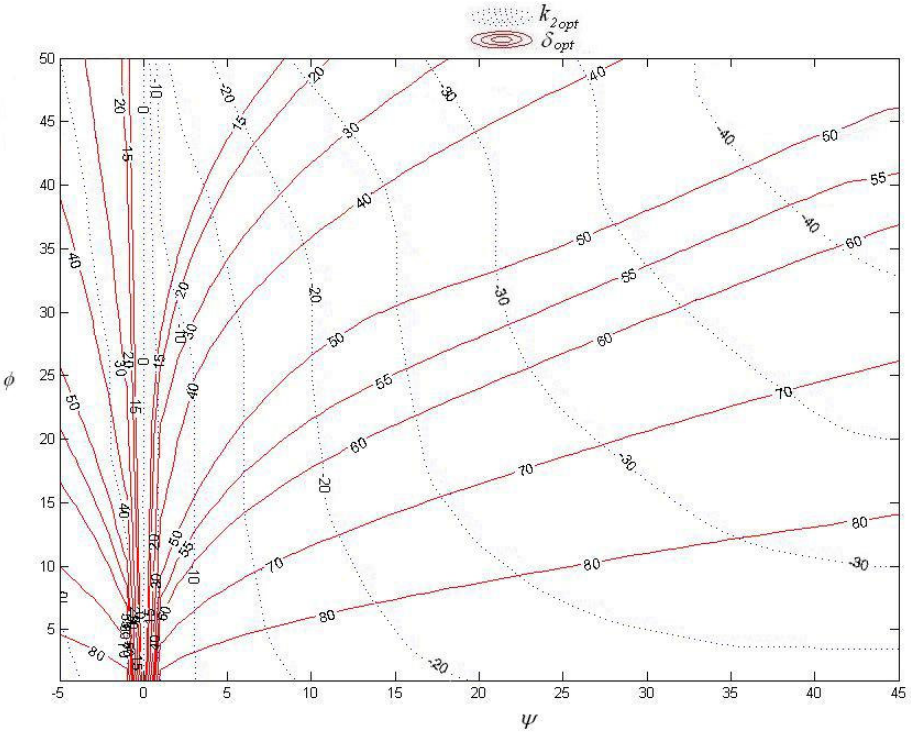


Fig. 4.38 b. The Design Chart for Maximum Stroke (Input ccw)

**Design Example 4.4**

This example is to illustrate the use of design chart for maximum stroke and determining the link lengths of the GASM for a given $\phi$ and $\psi$. From Fig.4.38, for $\phi$ = 50°, and $\psi$ = 10°, the optimum parameters for maximum stroke are determined as: $\delta_{opt}$ = 43.4°, $k_{2opt}$ = -22°. The link lengths are: $a_1$ = 1, $a_2$ = 0.873, $a_3$ = 0.365, $a_4$ = 0.722, and $d_2$ = 1.746.

Motion of the arm and the transmission angle of the GFLM will be given as:

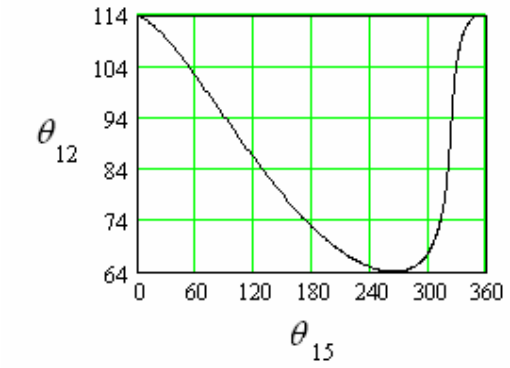


Figure 4.39 Motion of the Arm (link 2) for Ex. 4.4

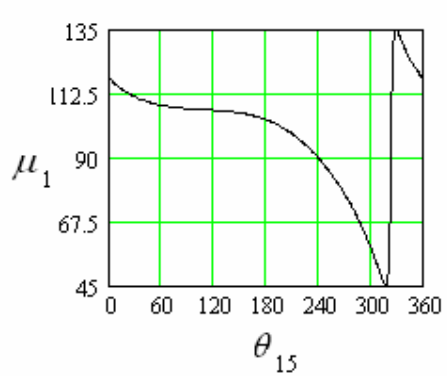


Figure 4.40 The Transmission Angle of the GFLM for Ex. 4.4

For a large stroke $a_7$ can be chosen equal to 1.2 units. Resulting path of point E is given in Fig.4.39. $s$ = 3.7 units which is 2.1 times larger than the arm. Note that the oscillation of the arm is 50° and the angle between the maximum X coordinate and

the minimum X coordinate of path of point E is $139^0$, which is 2.8 times larger than the oscillation of the arm (Fig.4.41).

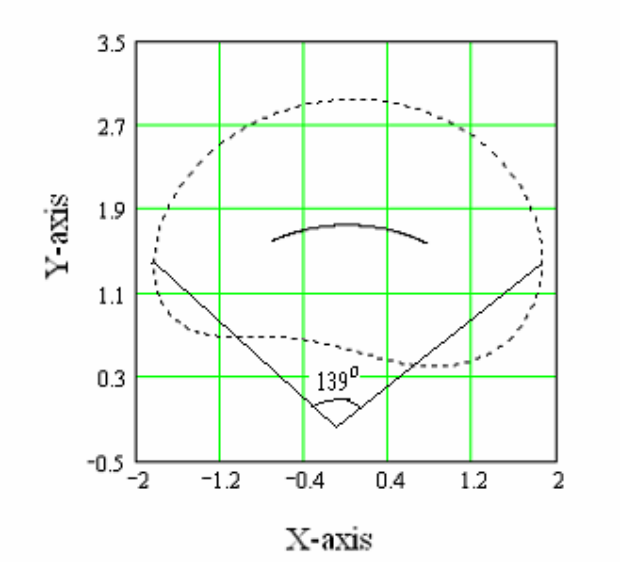


Figure 4.41 The Path of Point E and the Endpoint of the Arm for Ex. 4.4

The connecting rod, $a_8$, is chosen as; $a_8$ = 2.1 units (it can be increased up to 3.6 units, since the shortest link is $a_3$ = 0.365). The mechanism is a quick-return mechanism and the lower part of the path corresponds to quick-return cycle. Therefore, the slider axis $c_{19}$ can be chosen equal to 1.8 units to obtain better transmission characteristics during working cycle (Fig. 4.39). Then, the output motion of the mechanism is given in Figure 4.42. Note that output stroke is equal to 3.75 units ($d_2$/s=0.465).

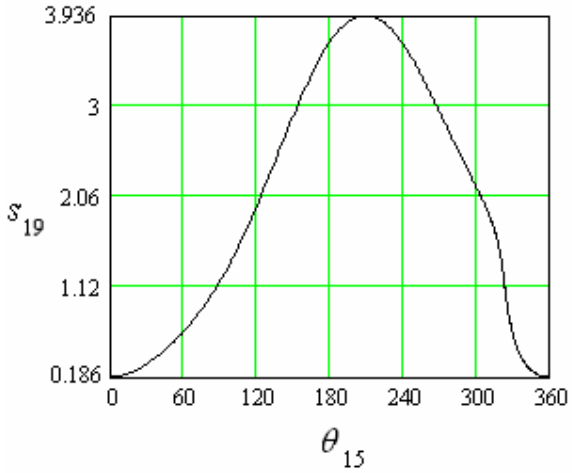


Figure 4.42 The Output Reciprocating Motion for Ex. 4.4

Second transmission angle of the mechanism is given in Fig.4.43. Note that during the working cycle maximum deviation of the transmission angle is 34°.

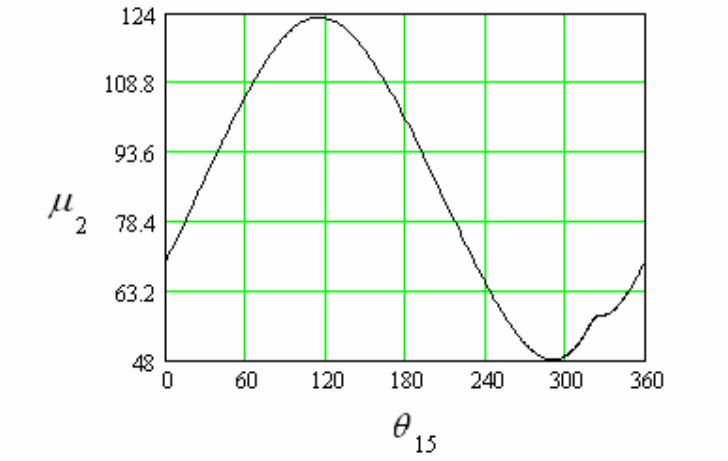


Figure 4.43 Second Transmission Angle of the Mechanism for Ex. 4.4

The animation of the mechanism designed in Ex.4.4 is prepared and several positions are shown in the following figures.

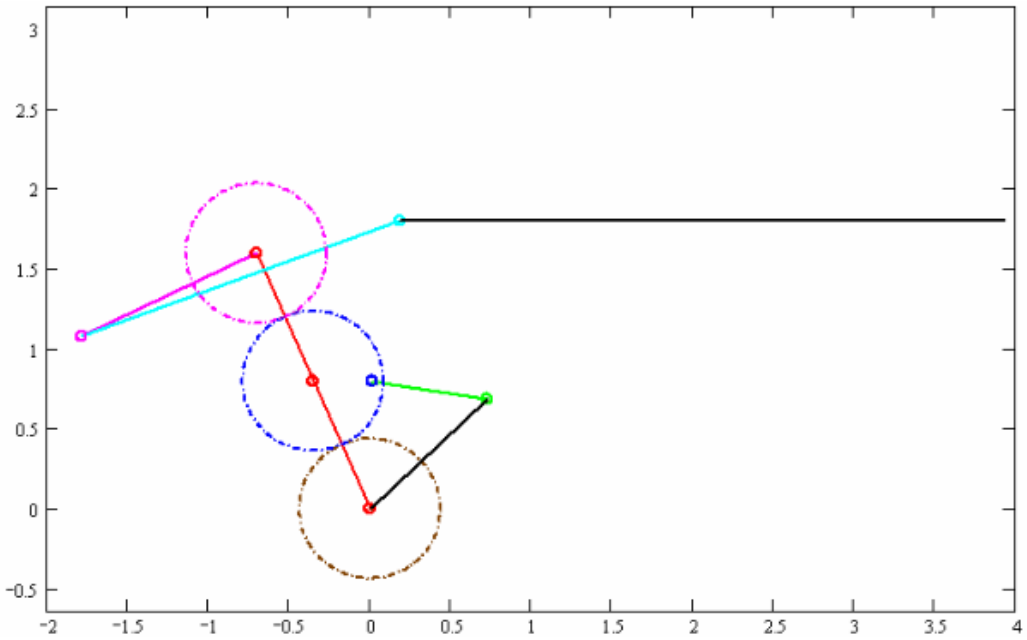


Figure 4.44 a. Input =0°, Output = 0.186

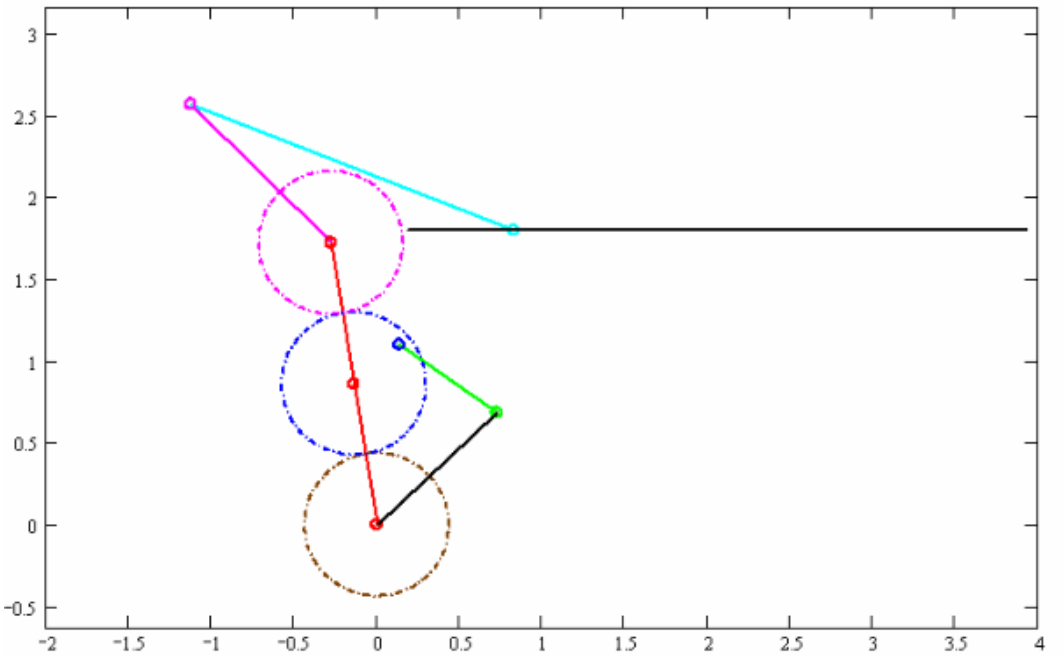


Figure 4.44 b. Input =75$^{o}$, Output = 0.9

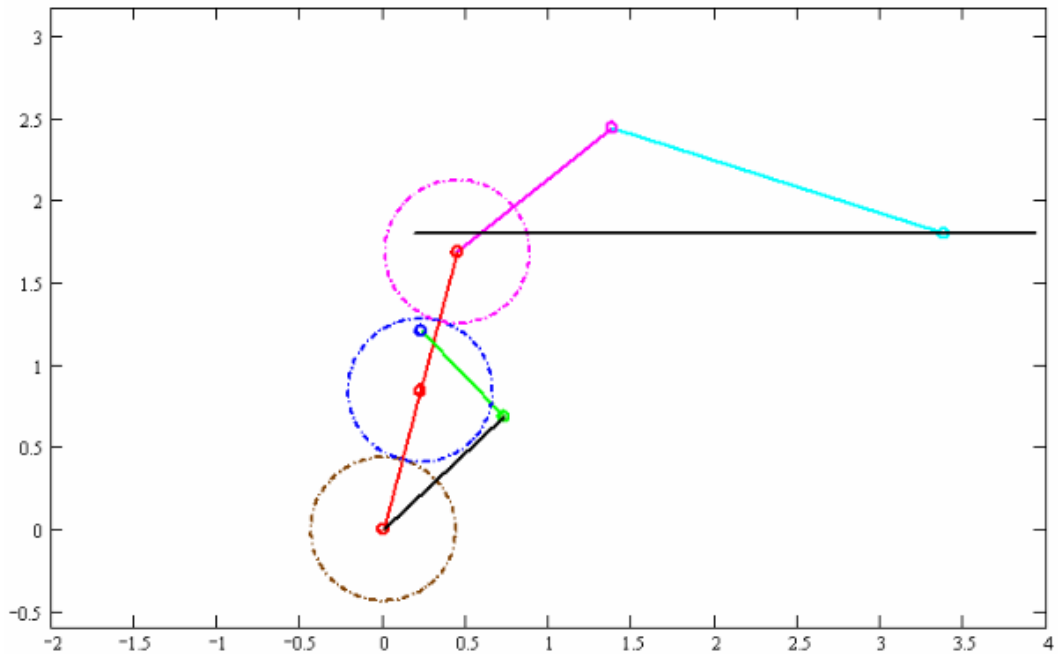


Figure 4.44 c. Input =167$^{o}$, Output = 3.4

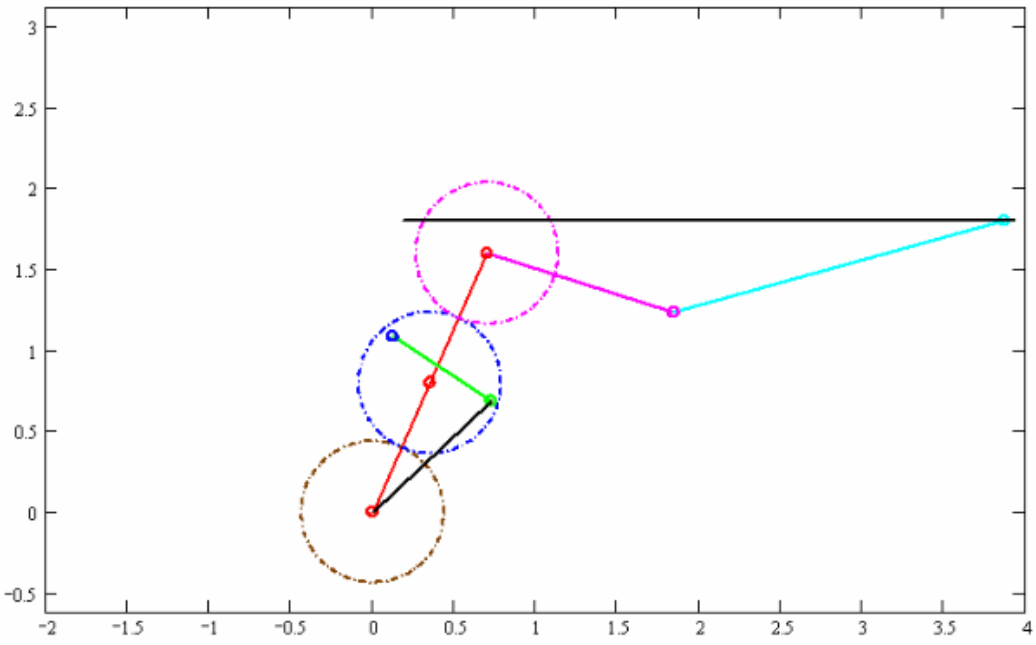


Figure 4.44 d. Input =230$^{o}$, Output = 3.78

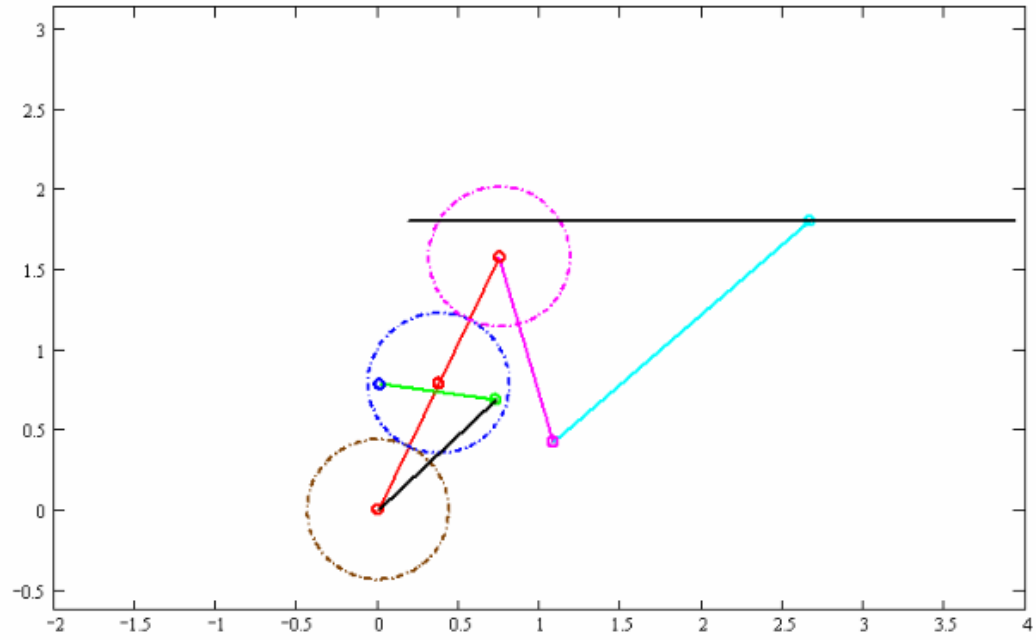


Figure 4.44 e. Input =278$^{o}$, Output = 2.7

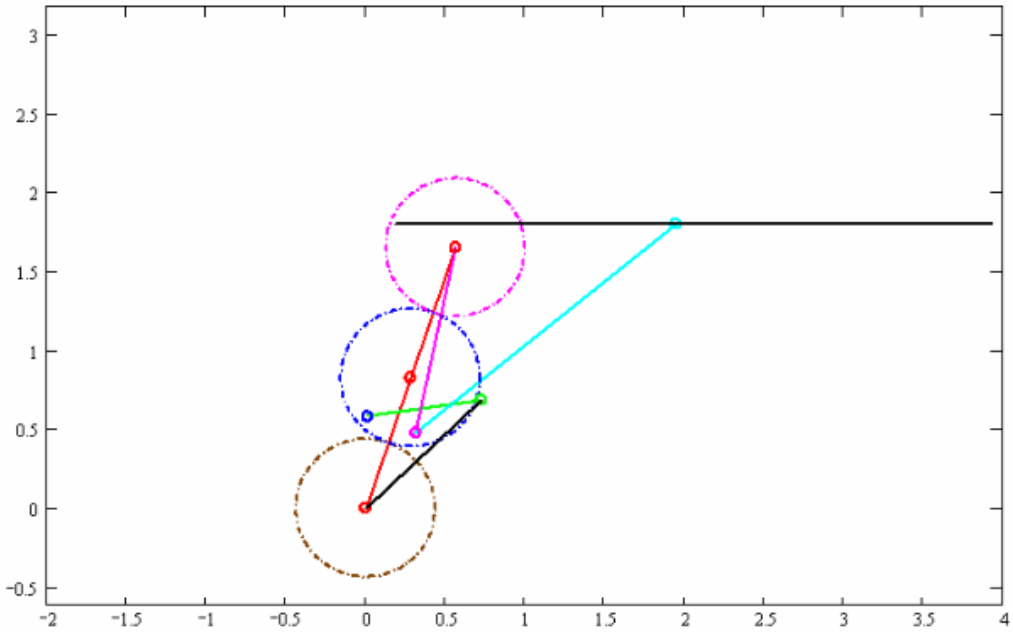


Figure 4.44 f. Input =309$^{o}$, Output = 1.91

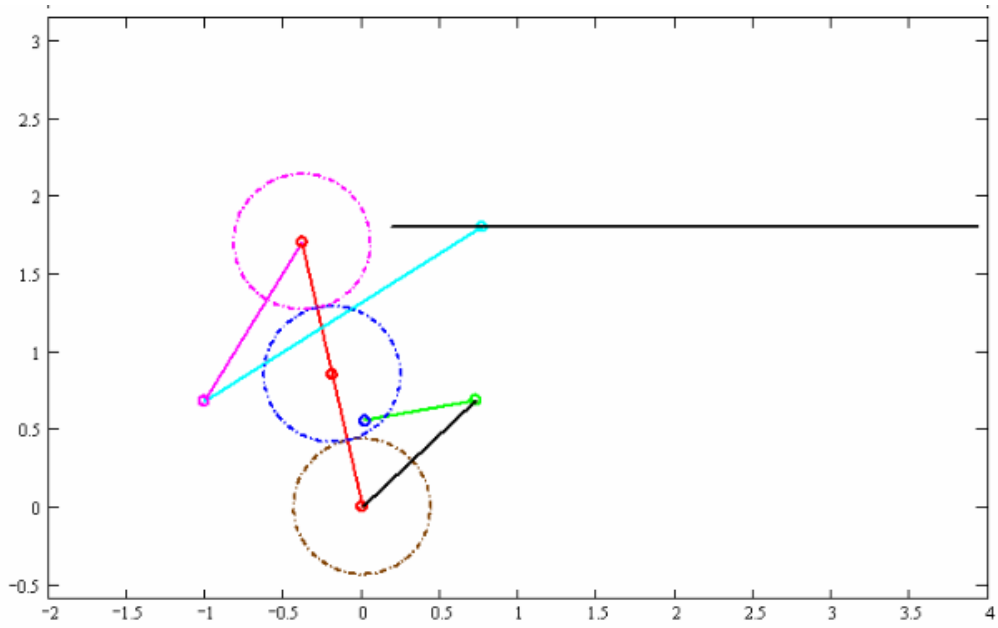


Figure 4.44 g. Input =326$^{o}$, Output = 0.78

## 4.13 Velocity and Acceleration Analysis of the Geared Adjustable Stroke Mechanism

The first derivatives of the loop closure equation and its complex conjugate (Eq. 4.4 and Eq. 4.5) are:

$$\dot{s}_{19} + ia_8 e^{i\theta_{18}}\omega_{18} = id_2 e^{i\theta_{12}}\omega_{12} + ia_7 e^{i\theta_{17}}\omega_{17} \tag{4.36}$$

$$\dot{s}_{19} - ia_8 e^{-i\theta_{18}}\omega_{18} = -id_2 e^{-i\theta_{12}}\omega_{12} - ia_7 e^{-i\theta_{17}}\omega_{17} \tag{4.37}$$

From Eq.4.36 and 4.37, the velocity of the output link is determined as:

$$\dot{s}_{19} = -\frac{d_2 \sin(\theta_{12} - \theta_{18})\omega_{12} + a_7 \sin(\theta_{17} - \theta_{18})\omega_{17}}{\cos\theta_{18}} \tag{4.38}$$

where, $\omega_{17} = \dfrac{\omega_{15} + (R-1)\omega_{12}}{R}$

Angular velocity of the coupler link can be determined as:

$$\omega_{18} = \frac{d_2\omega_{12}\cos\theta_{12} + a_7\omega_{17}\cos\theta_{17}}{a_8\cos\theta_{18}} \tag{4.39}$$

Then, from the second derivatives of the loop closure equation and its complex conjugate, accelerations of link 9 and link 8 are determined as:

$$\ddot{s}_{19} = -\frac{d_2\omega_{12}^{\,2}\cos(\theta_{12} - \theta_{18}) + d_2\alpha_{12}\sin(\theta_{12} - \theta_{18}) + a_7\omega_{17}^{\,2}\cos(\theta_{17} - \theta_{18}) - a_8\omega_{18}^{\,2}}{\cos(\theta_{18})} \tag{4.40}$$

$$\alpha_{18} = -\frac{d_2\omega_{12}^{\,2}\sin(\theta_{12}) - d_2\alpha_{12}\cos(\theta_{12}) + a_7\omega_{17}^{\,2}\sin(\theta_{17}) - a_8\omega_{18}^{\,2}\sin(\theta_{18})}{a_8\cos(\theta_{18})} \tag{4.41}$$

# CHAPTER 5

# STROKE ADJUSTMENT

## 5.1 Introduction

An optimum synthesis method is developed for maximizing the output stroke of the mechanism. Below, capability of the mechanism for stroke variation is investigated.

The mechanism has two prismatic joints; link 9 is the output link and link 6 is the adjustment link (Fig.5.1). Up to this point, link 6 has been fixed at a certain position. After synthesizing the mechanisms for a large stroke, now the effect of changing the position of link 6 on the stroke is investigated.

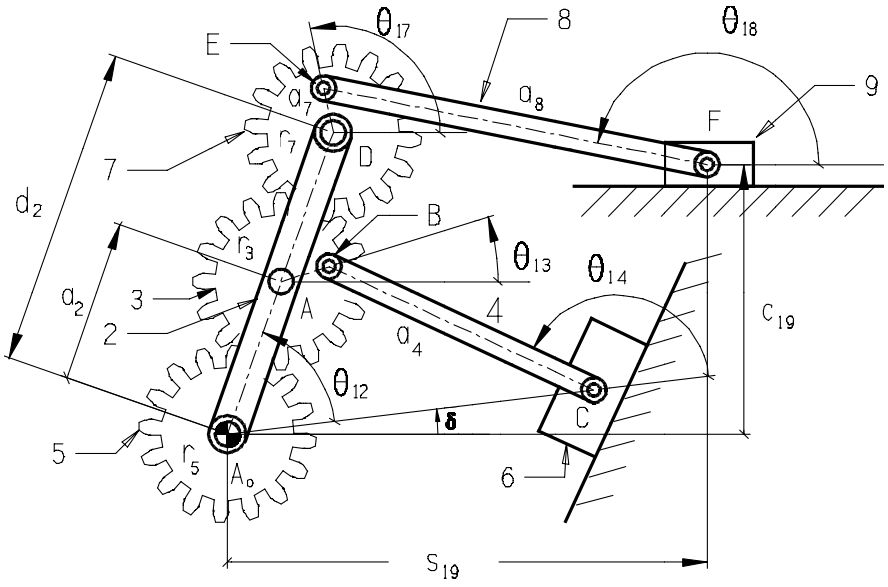


Figure 5.1 The Geared Adjustable Stroke Mechanism

### 5.2 Effects of Changing the Position of Link 6

If the position of link 6 is altered, then the orientation and the length of $A_oC$ changes. Initially, the oscillation change of the arm (link 2) of the GFLM is investigated. If the length of $A_oC$ is altered, then the oscillation of the arm changes. However, it is observed that the oscillation change of the arm is very small especially if the oscillation is desired to be decreased. The reason is; the length of the fixed link ($A_oC$) can be altered slightly, because the transmission angle of the GFLM is very sensitive to length of the fixed link. Also, the GFLM behaves as a double-rocker four bar mechanism. It is known that, the output swing angle of four-bar mechanisms can be changed slightly by altering the length of the fixed link; the major parameter is the length of the input crank. Hence, when the complete mechanism is considered, it is observed that the oscillation change of the arm has a negligible effect on the output stroke. Therefore, it is clear that the change in the output stroke of the mechanism is *not* due to the oscillation change of the arm. If the length of the fixed link is changed first transmission angle deteriorates, so only the orientation of $A_oC$ will be changed.

Hence, the stroke change can be revealed again by the path of point E. It was explained that, the distance between the maximum X coordinate and the minimum X coordinate, *s*, is the major parameter for the output stroke. The distance between the maximum Y coordinate and the minimum Y coordinate (*h)* significantly affects the second transmission angle. As, the mechanism is rotated clockwise or counter-clockwise about $A_o$, *s* decreases and *h* increases drastically (Fig.5.2 and 5.3).

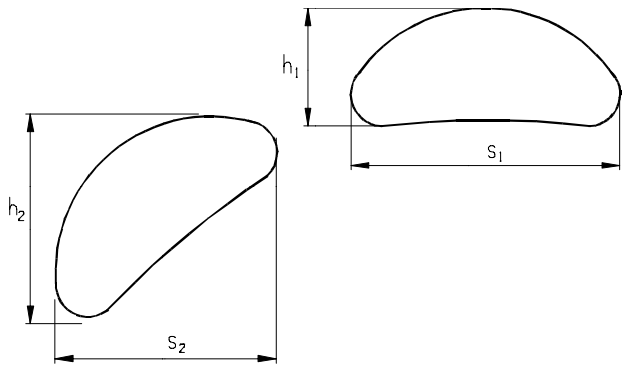


Figure 5.2 Decreasing the Stroke by Rotating the Mechanism about $A_o$

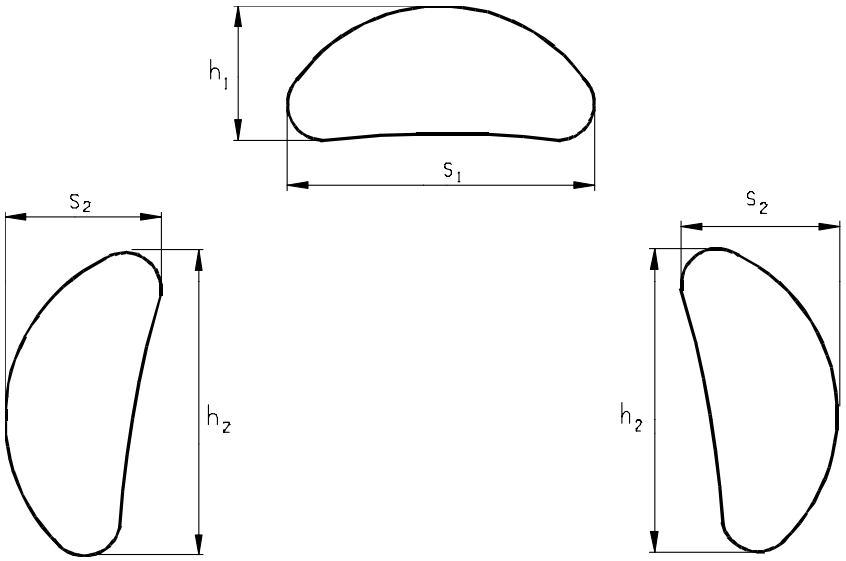


Figure 5.3 Path of Point E during First and Second Positions

Therefore, the adjustment angle, $\delta$ is changed in order to rotate the mechanism about $A_o$. This adjustment can be simply accomplished by moving the slider (link 6) in a circular slot. The center of the slot is $A_o$ and radius of the slot is equal to $A_oC$ as shown in Fig. 5.4.

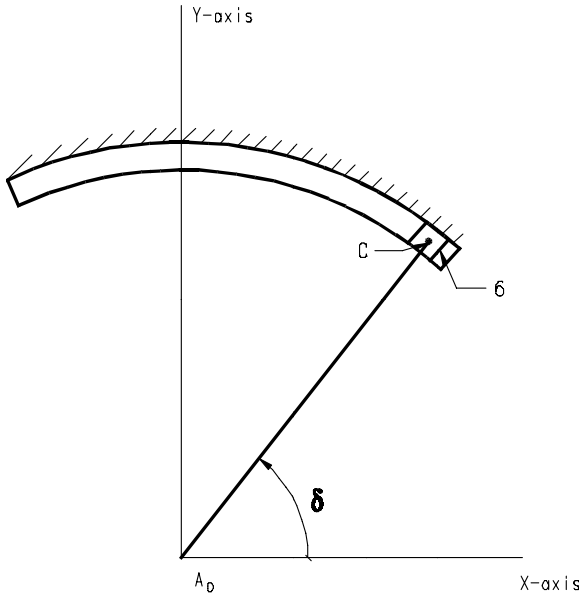


Figure 5.4 Changing the Adjustment Angle, $\delta$

After determining $\delta_{opt}$ and $k_{2opt}$ for maximum stroke, stroke can be decreased just by changing $\delta$. This property can also be observed in the stroke charts. Example 4.3 is considered and the stroke chart (Fig 4.37) is prepared again for a larger range of $\delta$. After determining $\delta_{opt}$ =43.4$^o$ and $k_{2opt}$ = -22$^o$ for maximum stroke, if $k_{2opt}$ (X-axis) is fixed and $\delta$ is changed (Y-axis), then $s$ decreases ($s$ can be decreased from 2.14 to 1) as shown in Figure 5.5.

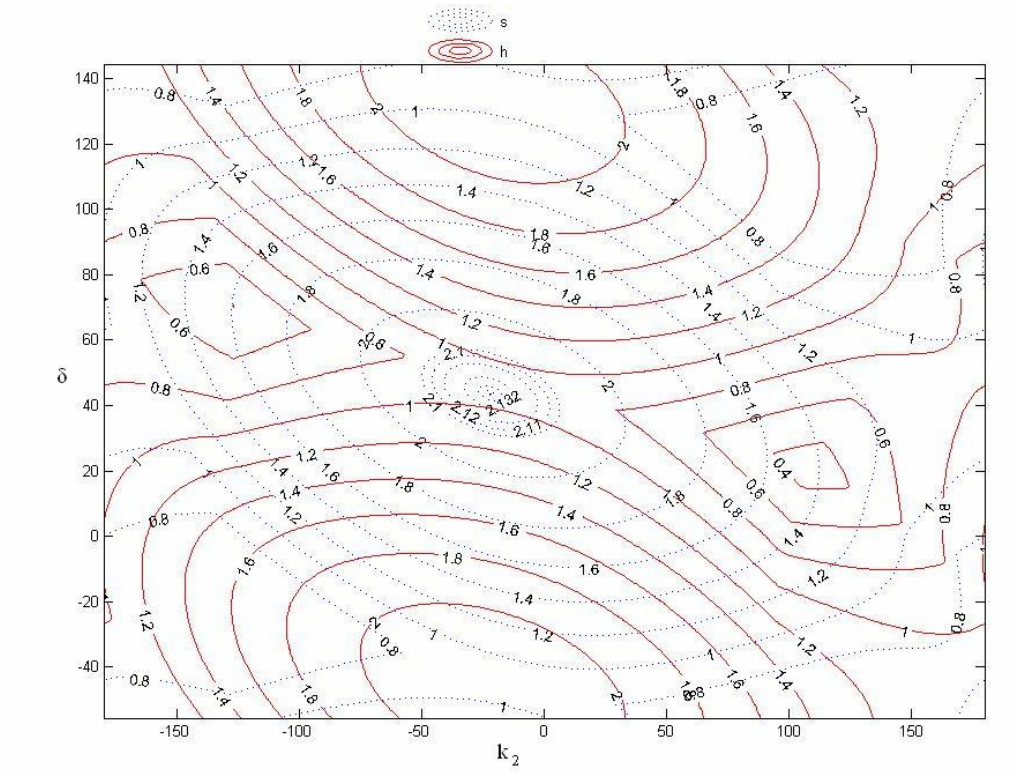


Figure 5.5 A Stroke Chart for Stroke Adjustment ($\phi$ = 50$^o$, $\psi$ = 10$^o$)

However, as $s$ decreases, $h$ increases. Consequently, $\delta$ should be changed in cw or ccw direction to minimize the stroke, but by checking the transmission angle.

In order to obtain appropriate transmission characteristics for the first and second positions, some conditions should be considered. If a very large stroke is desired at the first position, $a_7$ is chosen large as mentioned before, but at the second position, $s$ approaches to $h$, ($s_1 \rightarrow h_2$) and large $s_1$ ($h_2$) leads to deterioration of the transmission angle at the second position. In addition, at the first position if $s_1$ is increased by choosing a large $a_7$, $h_1$ also increases and during the adjustment $h_1$ approaches to $s_2$,

so large $h_1$ leads a large stroke at the second position (Fig.5-2, 5-3). Consequently, in order to obtain a short stroke with permissible transmission characteristics at the second position, initially $a_7$ should not be chosen very large. As a consequence, it is observed that more stroke change can be accomplished if point E is chosen on the gear (link 7).

During the synthesis of large stroke mechanisms, the height of the slider axis $c_{19}$ is selected around the path of point E just considering the transmission characteristics of the first position. However, during the synthesis of adjustable stroke mechanisms transmission angle of the second position must also be considered. If $c_{19}$ is selected just considering the first position, at the second position deviation of the transmission angle from $90^o$ becomes unacceptable (Fig. 5.6).

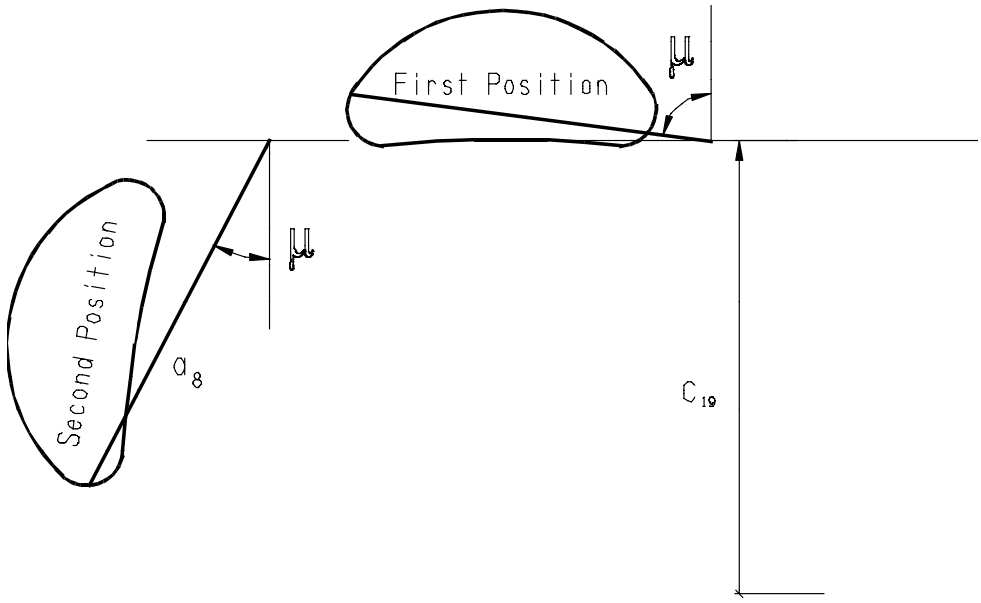


Figure 5.6 Unacceptable Transmission Angle at the Second Position

Therefore, the height of the slider axis $c_{19}$ must be chosen below the path of point E at the first position for an acceptable transmission angle during both of the positions as shown in Fig.5.7.

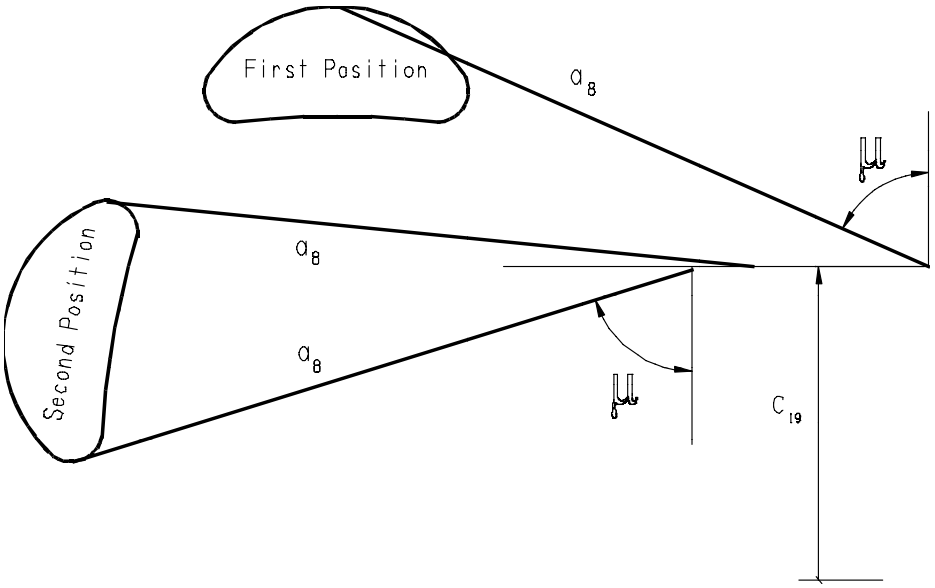


Figure 5.7 Selection of the Height of the Slider Axis

As mentioned before, the adjustment angle $\delta$ can be changed in cw or ccw direction. However, the output reciprocating motion differs according to direction of rotation of $\delta$. When $\delta$ is changed in cw direction, pilgrim step motions are obtained.

Consequently, value of $\delta$ for the desired stroke change can be determined from the stroke charts (code for stroke charts are given in Appendix F), but the link lengths $a_7$, $a_8$, $c_{19}$ and the direction of rotation of $\delta$ can be chosen according to design requirements.

**Design Example 5.1:**

This example is to illustrate the synthesis of a GASM where the stroke is decreased by using the stroke chart. The same mechanism as in the previous example (Ex.4.4) is chosen, oscillation of the arm, $\phi = 50^o$, corresponding rotation of link 4, $\psi = 10^o$. The resulting link lengths are:

$$a_1 = 1 \quad a_2 = 0.873 \quad a_3 = 0.365 \quad a_4 = 0.722 \quad d_2 = 1.746$$

$$k_{2opt} = -22^o \quad \delta_{opt} = 43.4^0 \quad r_5 = r_3 = r_7 = \frac{a_2}{2} = 0.436$$

This time point E is chosen on the gear (link 7),

$$a_7 = 0.9 r_7 = 0.393$$

Then, path of point E and endpoint of the arm is shown in the figure below. $s = 2.137$ units.

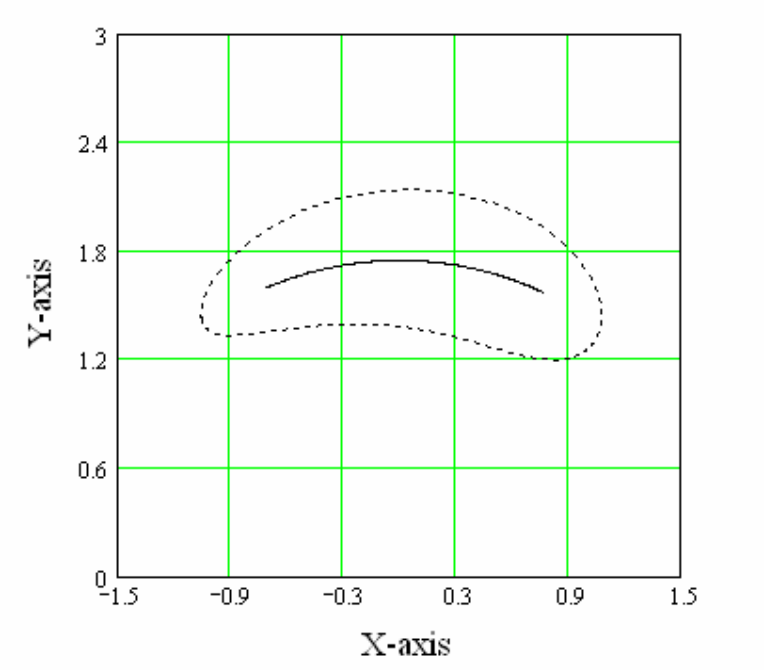


Figure 5.8 Path of Point E and Endpoint of the Arm for Ex 5.1

The height of the slider axis is chosen considering two positions as: $c_{19}$ = 0.5. Connecting rod is chosen as: $a_8$ = 2.6 (it can be increased up to 3.6). Then, the output stroke of the mechanism is 2.18 units, as shown in Fig 5.9. In the normalized form the output stroke is equal to 1.

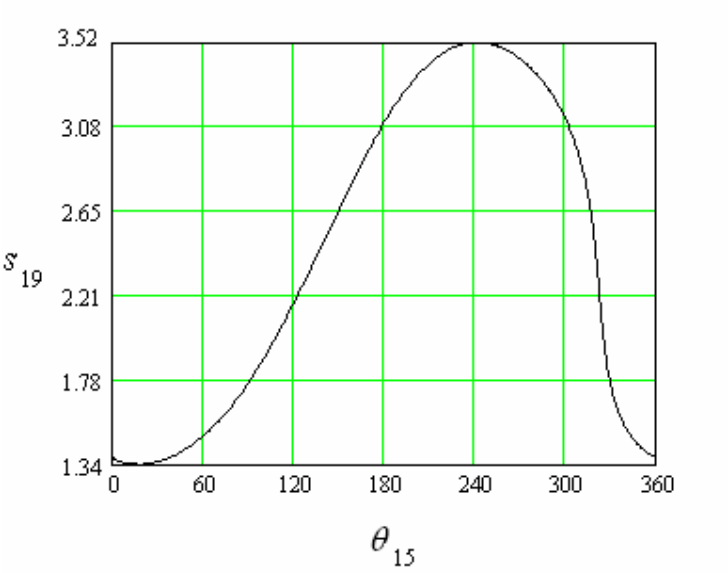


Figure 5.9 Output Reciprocating Motion at the first Position for Ex 5.1

The second transmission angle of the mechanism deviates 39.5$^o$ from 90$^0$ during working cycle as shown in Fig. 5.10.

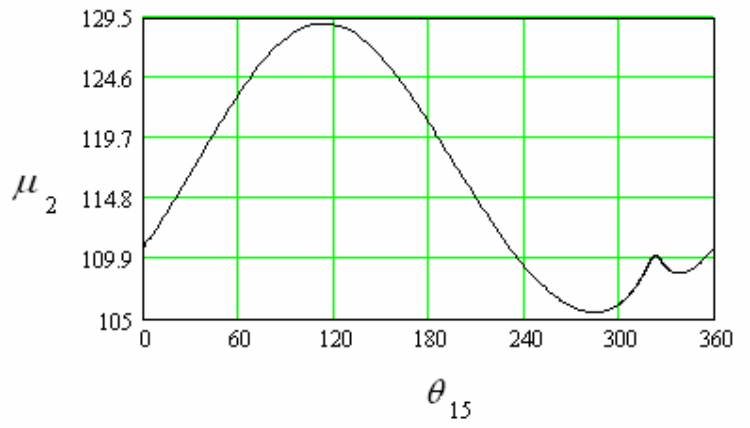


Figure 5.10 Second Transmission Angle of the Mechanism at the First Position for Ex 5.1

First position of the mechanism is shown in the figure below:

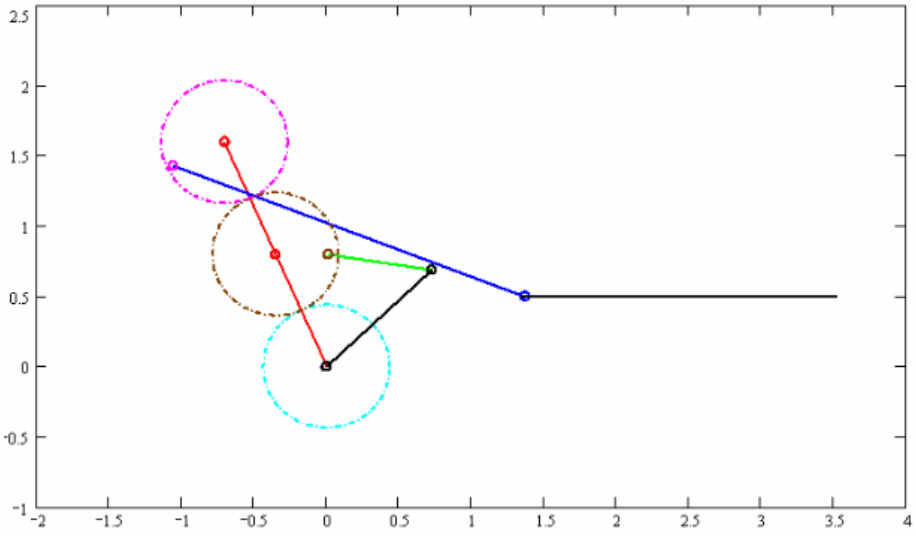


Figure 5.11 First Position of the Mechanism, where the Input = $0^o$ for Ex 5.1

If the adjustment angle is changed cw, the value of $\delta$ for a maximum decrease in the stroke is obtained from Fig.5.5 as $\delta = -42^o$.

Then, the output motion of the mechanism and the second transmission angle at the second position are shown in Fig. 5.12-13. Note that pilgrim step motion is obtained since the adjustment angle is changed cw.

The output stroke of the mechanism at the second position is 1.19 units. In the normalized form the output stroke is equal to: $\frac{1.19}{2.18} = 0.54$ units.

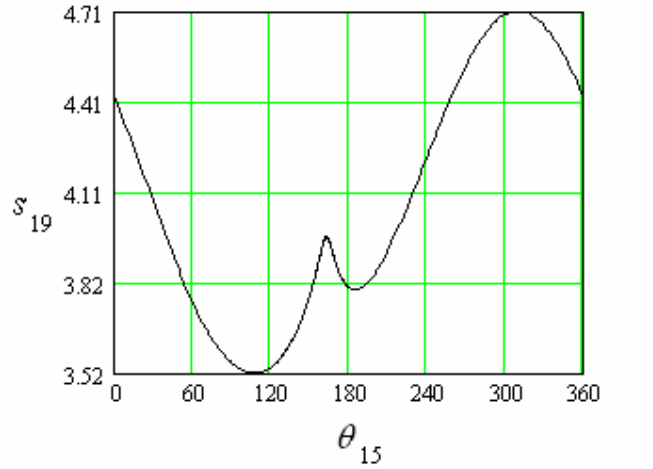


Figure 5.12 The Output Displacement at the Second Position (Pilgrim Step Motion) for Ex 5.1

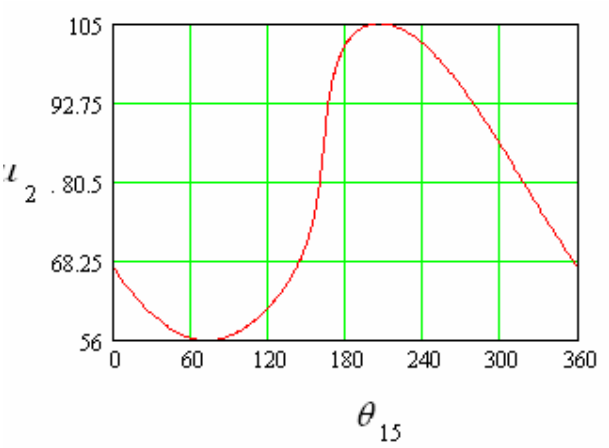


Figure 5.13 Second Transmission Angle at the Second Position for Ex 5.1

The mechanism at the second position ($\delta$cw) is shown in Fig.5.14:

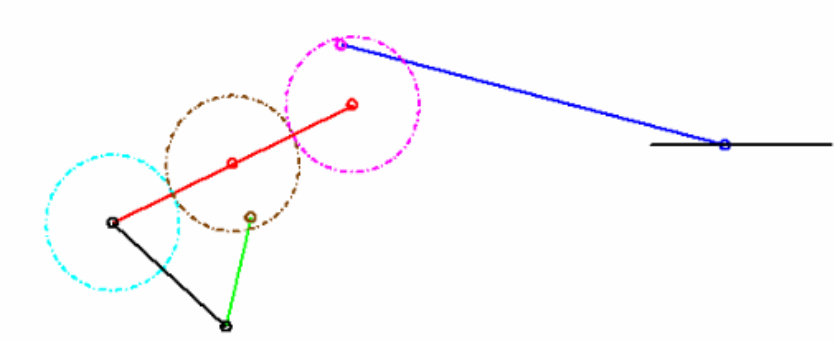

Figure 5.14 Second Position of the Mechanism ($\delta$cw) for Ex 5.1

If the adjustment angle is changed ccw, the value of $\delta$ for a maximum decrease in the stroke is obtained from Fig.5.5 as $\delta = 138^{o}$.

Then, the output motion of the mechanism and the second transmission angle at the second position are shown Fig. 5.15-16.

The output stroke of the mechanism at the second position is 0.99 units. In the normalized form the output stroke is equal to: $\frac{0.99}{2.18} = 0.45$ units.

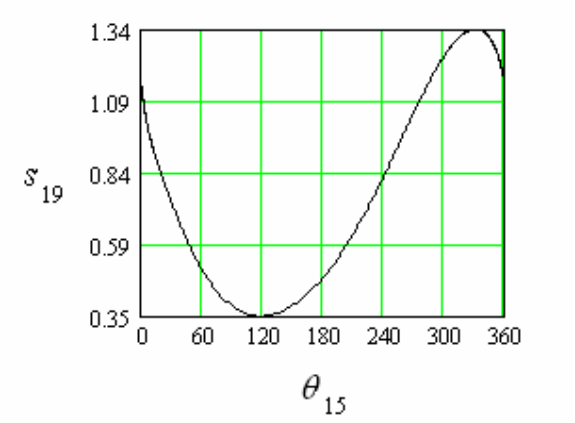


Figure 5.15 The Output Displacement at the Second Position for Ex 5.1

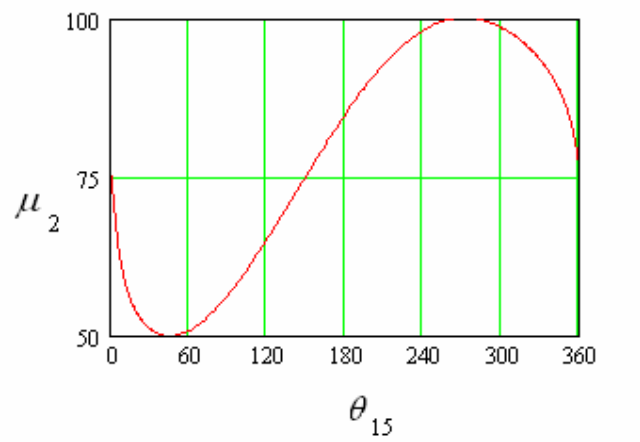


Figure 5.16 Second Transmission Angle at the Second Position for Ex 5.1

The mechanism at the second position ($\delta$ccw) is shown in Fig. 5.17.

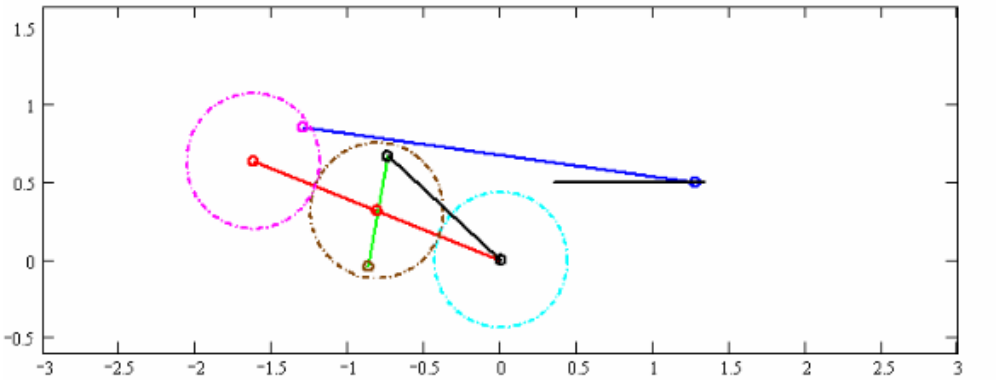


Figure 5.17 Second Position of the Mechanism ($\delta$ccw) for Ex 5.1

**Design Example 5.2:**

This example is to illustrate the synthesis of a GASM where the stroke is decreased by using the stroke chart and display the velocity and acceleration characteristics of the designed mechanism. An optimum GFLM of $\phi = 40^o$, $\psi = 0^o$, $\lambda_{opt} = 0.209$ is selected from the design chart (Fig.3.19). Link lengths can be evaluated as, $a_1 = 1$, $a_2$=0.53, $a_3$=0.181, $a_4$=0.867. Gear ratios are equal to unity, so, $r_5 = r_3 = r_7 = \frac{a_2}{2} = 0.265$, and the arm $d_2 = 1.106$. $a_7$ is chosen on the gear as: $a_7 = 0.9r_7 = 0.238$.

Stroke-chart of the mechanism is seen in Fig.5.18. The optimum parameters for maximum stroke are determined as: $k_{2opt} = -5^o$, $\delta_{opt} = 30^0$.

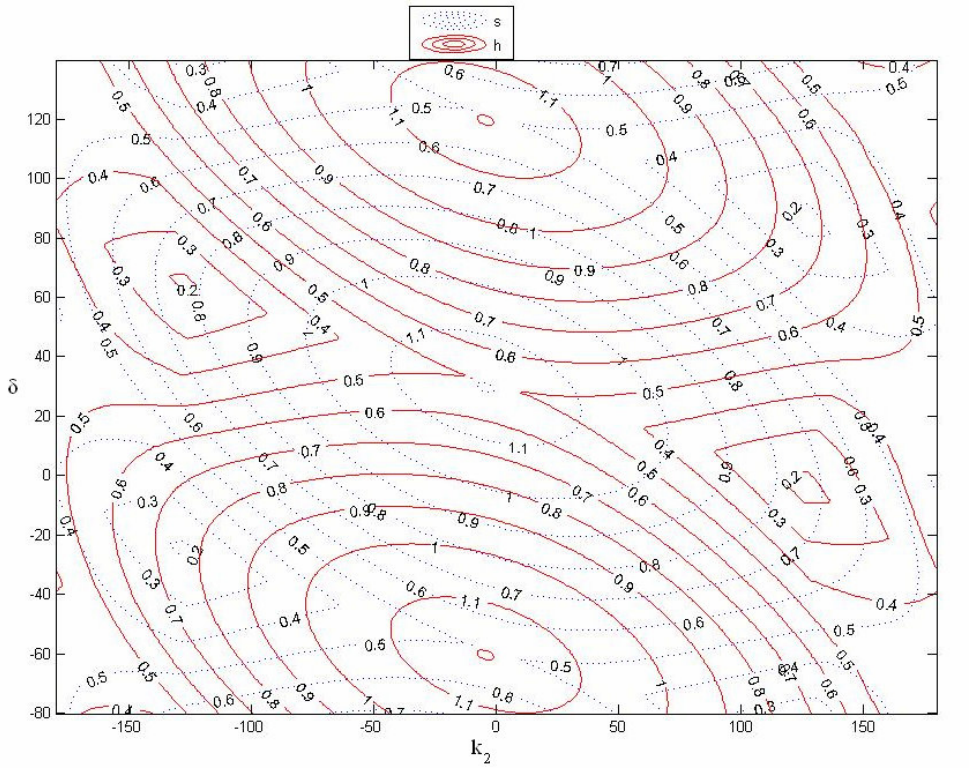


Figure 5.18 A Stroke Chart for Stroke Adjustment ($\phi = 40^o$, $\psi = 10^o$)

Resulting path of point E, and the endpoint of the arm are shown in Fig.5.19. $s$ = 1.14 units.

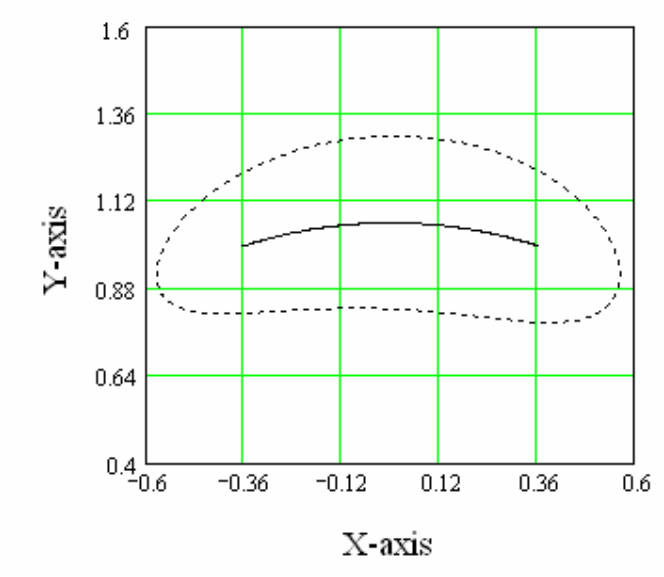


Figure 5.19 Path of Point E and Endpoint of the Arm for Ex 5.2

The height of the slider axis is chosen considering two positions as: $c_{19}$ = 0.3. Connecting rod is chosen as: $a_8$ = 1.7. The output stroke of the mechanism is 1.16 units as shown in Fig 5.20. In the normalized form the output stroke is equal to 1.

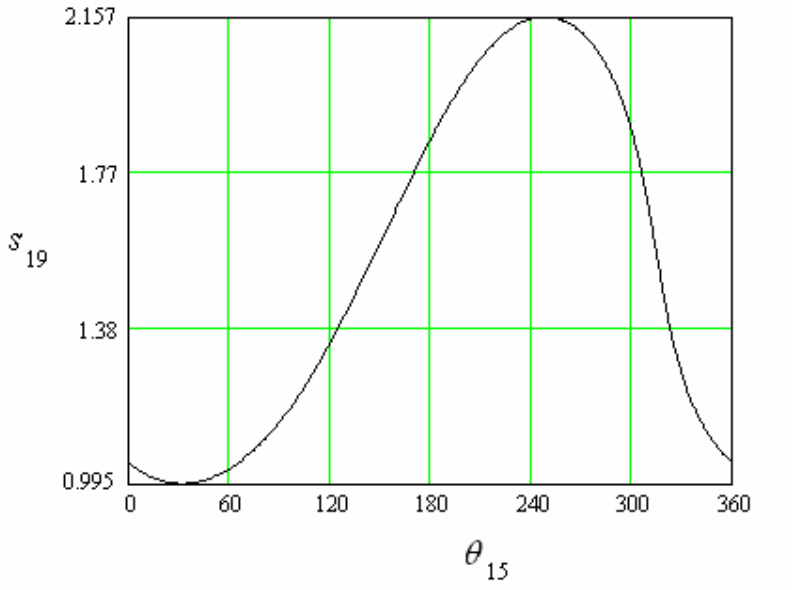


Figure 5.20 Output Reciprocating Motion at the First Position for Ex 5.2

Transmission angles of the mechanism are shown in Fig. 5.21. Second transmission angle deviates 37° from 90° during working cycle.

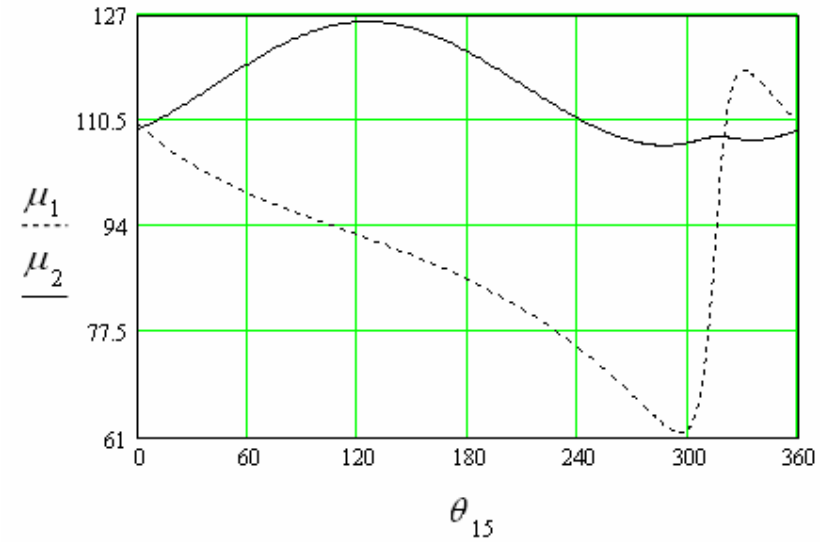


Figure 5.21 Transmission Angles of the Mechanism at the First Position for Ex 5.2

Output reciprocating motion and velocity of the output link are shown at the first position in Fig. 5.22.

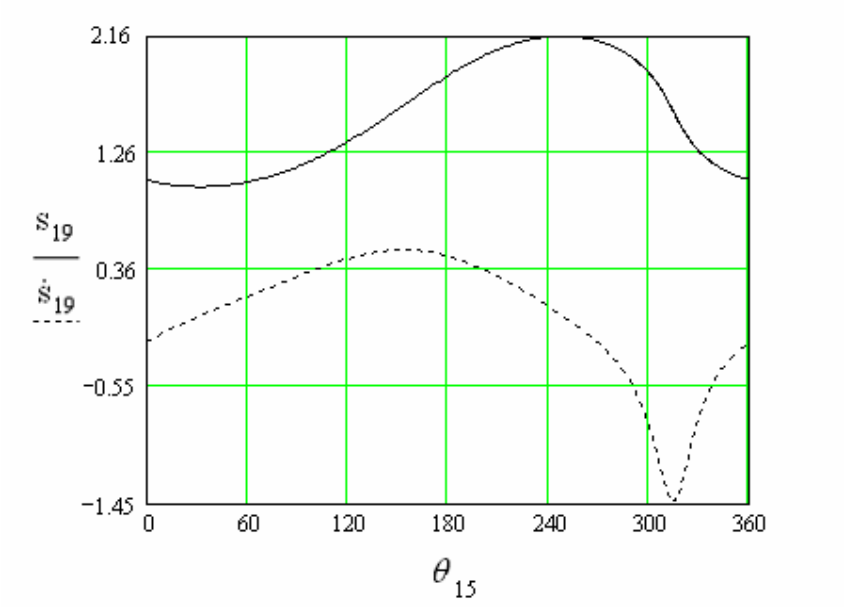


Figure 5.22 Output Reciprocating Motion and Velocity of the Output Link for Ex 5.2

Velocity and acceleration of the output link are shown at the first position in Fig. 5.23.

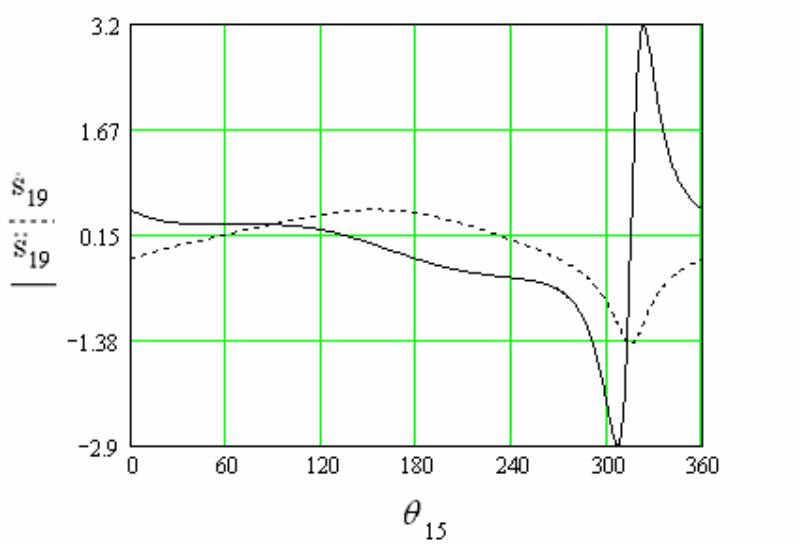


Figure 5.23 Velocity and Acceleration of the Output Link for Ex 5.2

Then, the adjustment angle is changed ccw, the value of $\delta$ for a maximum decrease in the stroke is obtained from Fig.5.18, as $\delta = 122^{o}$. The resulting output motion and the second transmission angle at the second position are shown Fig. 5.24-25.

The output stroke of the mechanism at the second position is 0.55 units. In the normalized form the output stroke is equal to: $\frac{0.55}{1.16} = 0.47$ units.

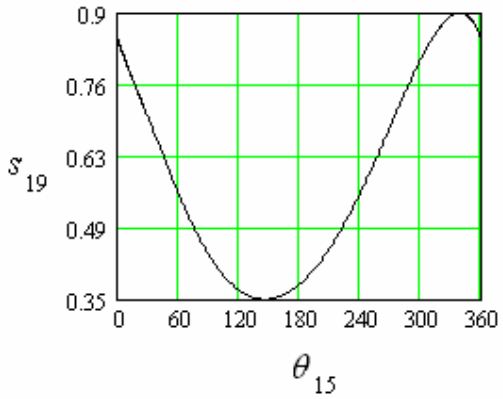


Figure 5.24 Output Reciprocating Motion at the Second Position for Ex 5.2

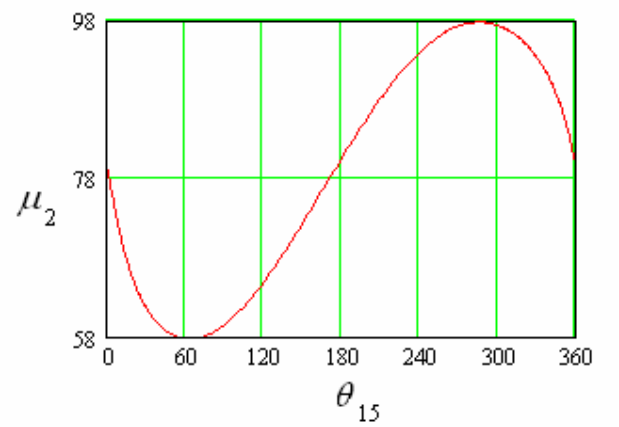


Figure 5.25 Second Transmission Angle at the Second Position for Ex 5.2

Output reciprocating motion, velocity, and acceleration of the output link are shown at the second position in Fig. 5.26.

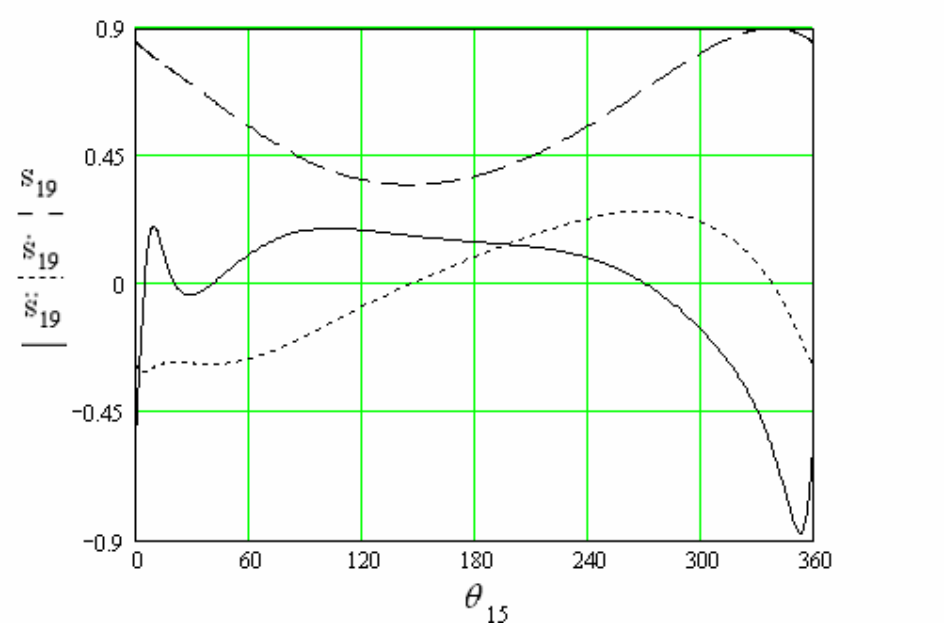


Figure 5.26 Displacement, Velocity, and Acceleration of the Output Link for Ex 5.2

# CHAPTER 6

# DISCUSSION, CONCLUSION and FUTURE WORK

## 6.1 Discussion and Conclusion

In this dissertation, two types of geared linkages are studied in detail. One of the mechanisms is a geared five link mechanism of a particular type. The other is a two degree-of-freedom nine-link mechanism which uses the geared five link mechanism in its structure. Neither of these mechanisms has been studied in the literature.

The geared five-link mechanism is a basic mechanism which has a planetary gear arrangement where the planet gear is connected to the ground by a link. Different types of input output relationships can be obtained from this type of mechanisms, which have found applications in industry generally for pilgrim step and dwell motions. However, in the present case the input is applied to the sun gear, and an output swing angle is obtained at the arm.

An initial attempt to obtain a relationship between the input and output led to a 4th order polynomial equation. A closed form relationship between the input and the output could not be reached by this method. In order to obtain a simpler analysis method for the GFLM, rotation of the planet gear is assumed to be the input. Continuous rotation of the sun gear results with a continuous rotation the planet gear. In such a case, the GFLM can be analyzed as a four-bar mechanism with the coupler link as the input. Then, the angular rotation of the arm can be determined in terms of the angular rotation of the coupler. The four-bar mechanism is double-rocker type according to Grasshof's rule.

In the classical sense, the transmission angle is a kinematic property of a mechanism which gives the designer the ease of force transmission to the output link. In case of

the GFLM the transmission angle is not easy to define as in the cases of four-bar and slider-crank mechanisms.

Neglecting the mass of the links, the force components acting on the output link are determined. Then, the transmission angle is expressed in terms of the link lengths and the angles. The expression obtained for the transmission angle is highly nonlinear, and an analytical expression for its extreme values could not be reached. Therefore, definite positions for the extreme values of the transmission angle could not be obtained. However, it is observed that these extreme values occur during the quick-return cycle; just after the folded position and just before the extended position or vice-versa according to the direction of rotation of the input link.

In the literature, no example where the transmission angle depended on the direction of rotation was found. However, for the GFLM discussed, if the direction of rotation of the input link is changed then, then the expression for transmission angle alters. A mechanism which has acceptable transmission angle values in one rotation direction can even lock if the direction of rotation of the input is reversed.

The synthesis of the GFLM is considered in two parts. The first part is the synthesis problem in which one must determine four-bar mechanisms with double-rocker proportions that must have a given swing angle ($\phi$) and a corresponding rotation of link 4 ($\psi$). There is an infinite set of solutions for this part of the problem. The second part of the problem is concerned with the optimization of the transmission angle. Out of the infinite possible set of solutions obtained in the first part, one must determine a particular mechanism whose maximum transmission angle deviation from $90^o$ is a minimum. A parametric optimization routine is developed and design charts for the optimum GFLM are prepared.

According to the direction of rotation of the input, there are two different optimum mechanisms which have same output swing angle and corresponding crank rotation. Therefore, transmission angle optimization is performed for both of the input directions of rotation and two sets of design charts are prepared. It is observed that

one of the input rotation direction do not have a significant advantage with respect to the other one. Furthermore, transmission angle optimization is performed for several gear ratios and design charts for them are also prepared.

It is observed that, for both input rotation directions and for all the gear ratios the transmission characteristics of the mechanisms deteriorate drastically for cw values of $\psi$. Therefore, it can be concluded that cw values of $\psi$ are not convenient.

The gear ratio significantly affects the transmission angle. It is observed that as the gear ratio ($r_3/r_5$) increases, the transmission angle improves. For a gear ratio of unity mechanisms up to $55^o$ output swing angle with permissible transmission angles could be obtained. However, as the gear ratio is increased up to 4, mechanisms with $70^o$ output swing angle can be obtained with acceptable transmission angles. Conversely, if the gear ratio is decreased the transmission characteristics deteriorate significantly.

It is also observed that for an acceptable transmission angle, centric mechanisms can be obtained for small swing angles only. When the gear ratio is equal to unity, up to $\phi \cong 12^o$, and when the gear ratio is equal to four, up to $\phi \cong 22^o$ centric mechanisms were achieved with a transmission angle deviation less then $45^o$. Therefore, it can be concluded that this type of geared five-link mechanisms are useful for quick-return motions.

Velocity and acceleration characteristics of the GFLM are also analyzed. During the velocity and acceleration analysis, a constant angular velocity equal to unity (rad/sec) is chosen for the input link. For a gear ratio of unity, maximum value of angular velocity and acceleration of the links during the quick-return cycle increases as output swing angle reaches $50^o$ for small values of $\psi$. However, initially larger $\psi$ values can be chosen for the same output swing angle in order to obtain mechanisms with lower maximum value of velocity and acceleration. This property is expected because, as $\psi$ increases mechanisms approaches centricity.

If the gear ratio of the mechanism is increased, then the angular velocity and acceleration of the links decrease. For example, if a gear ratio of two is chosen instead of one, the output will complete a cycle for two cycles of the input gear. Then, for the same input angular velocity, the mechanism operates slower.

As the gear ratio increases, larger output swing angles with acceptable transmission characteristics are obtained, but for these limiting output swing angles, maximum value of the angular acceleration of the output link during the quick-return cycle increases for small values of $\psi$. Similarly, initially larger $\psi$ values can be chosen for the same output swing angle in order to obtain mechanisms with lower maximum value of angular velocity and acceleration.

For all gear ratios ($R_1 \geq 1$) and all values of $\phi$ and $\psi$, small (smaller then unity) angular velocity and accelerations are determined during the working cycle. Moreover, approximately constant angular velocity at the output link during the working cycle is observed for small values of $\psi$ or for gear ratios more then unity.

The GFLM investigated is a basic mechanism similar to the four-bar mechanisms; simply a gear pair combined with a double-rocker four-bar mechanism. If the permissible maximum deviation of transmission angle from $90^o$ is assumed to be $45^o$, then output swing angles up to $90^o$ can be obtained by crank-rocker four-bar mechanisms. Similarly output swing angles up to $70^o$ can be obtained by this type of GFLM.

Transmission characteristics of crank-rocker four-bar mechanisms deteriorate rapidly when they get further away from centricity, but the geared five-link mechanisms studied are inherently quick-return mechanisms. Long working periods with suitable transmission, velocity and acceleration characteristics can be determined via this type of GFLM. Furthermore, if an approximately constant velocity is desired at the output link during the working cycle, this type of GFLM may provide a good solution.

The analysis and synthesis of the GFLM was the most important step in the analysis and synthesis of the GASM. After this step, an analytical analysis procedure is developed for the GASM

When the complete mechanism is considered, there are two critical transmission angles. One of the transmission angles is defined for the GFLM and the other transmission angle occurs between the output link and the coupler link, similar to that of the slider crank mechanisms.

In an adjustable stroke mechanism usually a large range for the stroke variation is desirable. As the stroke is enlarged the movability and the transmission angles of the mechanism become more critical. Also, it has been stated in literature [2] that the rotation of input gear causes a large-stroke reciprocating motion for the output link. Consequently, several methods have been devised for obtaining mechanisms having large strokes. Once a maximum stroke is obtained, a method for decreasing the stroke is developed by changing the position of the adjustment link.

A synthesis procedure is devised by employing the dead-centers of the geared adjustable stroke mechanism. Using this procedure, a closed-form solution is obtained for the link length proportions. However, the results show that solutions with permissible transmission characteristics can be determined in limited regions of $\phi$ and $\psi$. It was shown that the use of centric GFLM was not feasible because of small swing angles and/or low transmission angle values. And as the mechanisms get further away from centricity, it becomes harder to satisfy both of the dead-center positions with permissible transmission characteristics.

Connecting rod $a_8$ and slider axis $c_{19}$ are chosen as unknown design parameters in this procedure. However, it is also observed that the effect of connecting rod and height of the slider axis $c_{19}$ (within the feasible design region) to the output stroke is negligible. And, as the length of the connecting rod increases, transmission angle improves. The height of slider axis $c_{19}$ has also a very important effect on the second

transmission angle as discussed in Chapters 4 and 5. So, $a_8$ and $c_{19}$ can be chosen according to design specifications.

It is observed that the path of point E is very important, because shape of this path is the major parameter for the stroke. Then, a synthesis method is devised by use of inflection circle of link 7 at a specified position. The adjustment angle, $\delta$, the phase angle, $k_2$ and the length of link 7, $a_7$, are the design parameters. By this approach, feasible results are obtained, but as the oscillation of the arm increases, the diameter of the inflection circle also increases, so the length of link 7 increases (point E is determined to be outside the gear as the oscillation of the arm increases). This condition is a constraint for the design.

It is also observed that the effect of the length of link 7 is also clear; as it is increased larger paths of point E are obtained, so $s$ and $h$ increases. Consequently, it is decided that the adjustment angle, $\delta$, and the phase angle, $k_2$, should be optimized for maximum stroke.

For every $\phi$ and $\psi$, optimum values of $\delta$ and $k_2$ for maximum stroke are determined by a parametric optimization routine and a design chart is prepared. After determining the optimum values of $\delta$ and $k_2$, the length of link 7 can be increased or decreased according to design specifications. If length of link 7 is increased for a larger stroke, $h$ also increases. Then, the length of the connecting rod should also be increased in order to improve the second transmission angle of the mechanism.

The length of the connecting rod can be increased up to ten times the length of the shortest link, but about six times as larger as the shortest link is observed to be sufficient. The height of the slider axis has also a crucial effect on the second transmission angle. If the stroke adjustment is not required, and only a large stroke is desired, the height of the slider axis can be chosen close to the length of the arm.

For gear ratios of unity, maximum value of velocity and acceleration of the output link during the quick-return cycle increases as $\phi$ reaches $50^o$ for small values of $\psi$.

However, initially larger $\psi$ values can be chosen to obtain mechanisms with lower maximum value of velocity and acceleration. On the other hand, it is observed that velocity and acceleration of the links, during the working cycle are smaller then unity for $\omega_{input} = 1 rad/s$.

As the first gear ratio $R_1$ is increased, $\phi$ can be increased and larger output strokes with permissible transmission characteristics are obtained. But the maximum value of acceleration of the links during the quick-return cycle increases as $\phi$ increases. Also, as $R_1$ increases, radius of floating gears, length of the arm and length of the connecting rod increase, resulting in larger mechanisms.

When $R_1$ =1, it is observed that if the second gear ratio is $R_2$ = ½, a pilgrim step motion is obtained. If $R_2$ is not an integer and $R_2 \neq$ ½, then the output motion will complete a cycle after several cycles of the input link rotation. At each cycle of the input, the output stroke decreases, then after few cycles, for every cycle of the input, output stroke starts increasing and the mechanism completes a cycle after several cycles of the input. This property can also be used for stroke adjustment. The number of these cycles can be determined by a method given in Appendix E.

If $R_2$ is an integer greater than unity ($R_2$ = n, where n>1), then the output motion will complete a cycle after n*360$^o$ of the input link rotations, and a pilgrim step motion is obtained. Consequently, for the desired output reciprocating motion $R_2$ must be equal to unity.

If the position of link 6 is altered, then the orientation and the length of $A_oC$ (fixed link) changes. Initially, the oscillation change of the arm (link 2) of the GFLM is investigated. If the length of $A_oC$ is altered, then the oscillation of the arm changes. However, it is observed that the oscillation change of the arm is very small especially if the oscillation is desired to be decreased.

Length of the fixed link can be altered slightly, because the transmission angle of the GFLM is very sensitive to length of the fixed link. It is known that, the output swing

angle of four-bar mechanisms can be changed slightly by altering the length of the fixed link, the major parameter is the length of the input crank. Since the GFLM behaves as a double-rocker four-bar mechanism, that condition was expected. Hence, when the GASM is considered, it is observed that the oscillation change of the arm has a negligible effect on the output stroke. Therefore, it is clear that the change in the output stroke of the mechanism is *not* due to the oscillation change of the arm.

If the length of the fixed link is changed, first transmission angle of the mechanism deteriorates, so only the orientation of $A_oC$ is changed. Therefore, the adjustment angle, $\delta$ is changed in order to rotate the mechanism about $A_o$. This adjustment can be simply accomplished by moving the slider in a circular slot. As, the mechanism is rotated cw or ccw about $A_o$, $s$ decreases and $h$ increases drastically. Hence, after determining $\delta_{opt}$ and $k_{2opt}$ for maximum stroke, just by changing $\delta$, stroke is decreased.

In order to obtain appropriate transmission characteristics for the first and second positions, some conditions should be considered. It is observed that point E should be chosen on the gear (link 7), considering the second transmission angle during the second position. Also, the slider axis $c_{19}$ must be chosen below the path of point E for an acceptable transmission angle during the second position.

It is observed that if $\delta$ is rotated in cw direction, pilgrim step motions are obtained.

It is observed that the output stroke of the GASM can be decreased more then 50% (which is a significant value) with proper transmission, velocity and acceleration characteristics. Moreover, this adjustment can be achieved during the operation, which is the most important advantage of such mechanisms.

In this study, two types of geared linkages are investigated in detail and capabilities of these types of mechanisms are determined and explained. It is believed that the analysis and synthesis procedures developed, the design charts prepared and the codes generated can be very useful for applications of these types of mechanisms.

## 6.2 Future Work

It was explained that approximately constant angular velocity at the output link during the working cycle is observed for the GFLM. This property can be investigated in detail, since this is an important and desired condition for several applications.

For the GASM, different combinations of gear ratios can be analyzed in detail. For these combinations, larger output strokes or pilgrim step motions or output displacements which repeat itself after several cycles of the input are obtained and discussed previously in this study. However, these conditions can be investigated in detail.

## APPENDIX A

## DESIGN CHARTS for the GEARED FIVE-LINK MECHANISMS

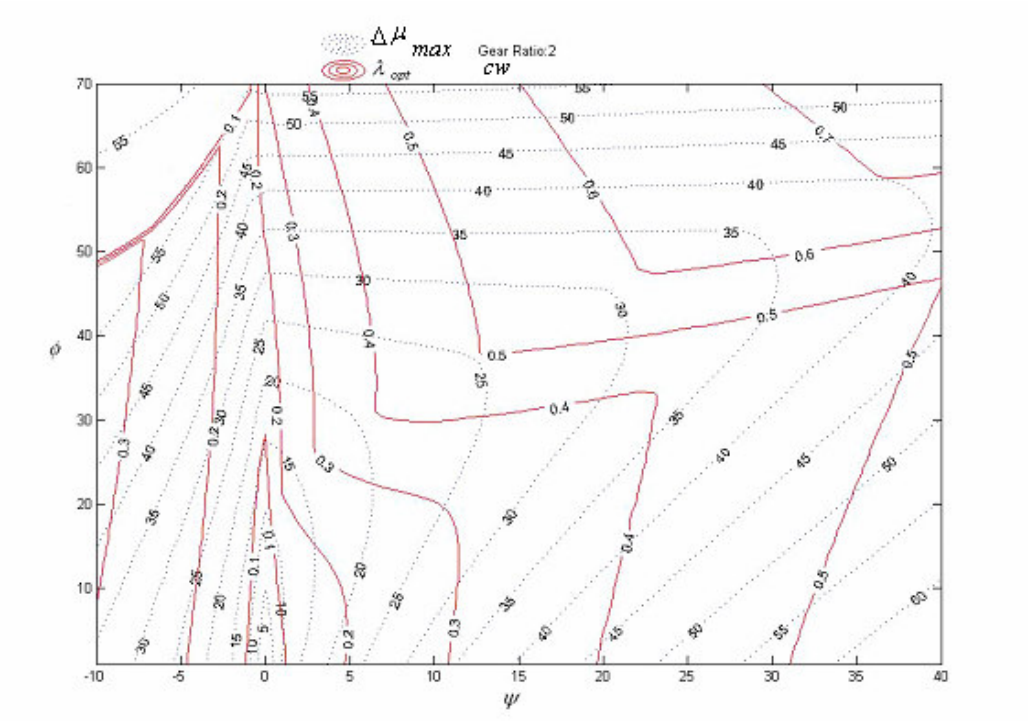


Figure A.1 Design Chart for Gear Ratio = 2, CW Input Rotation

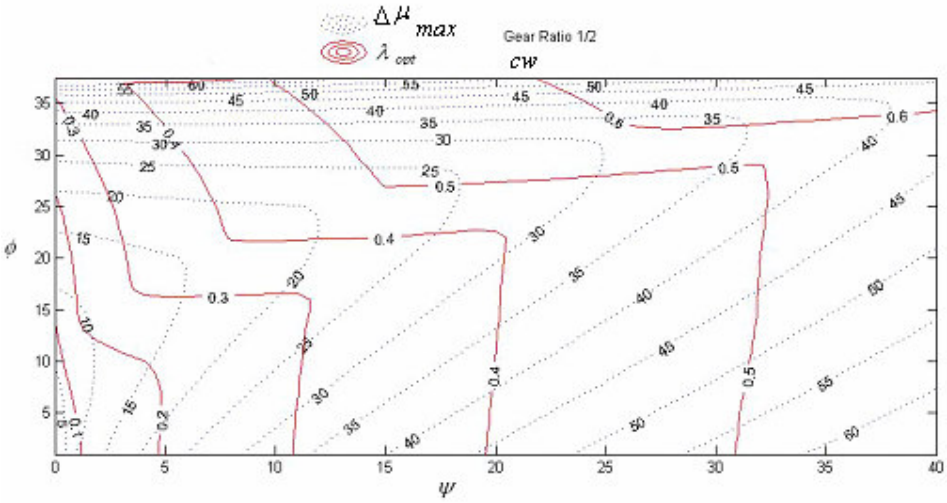


Figure A.2 Design Chart for Gear Ratio = 1/2, CW Input Rotation

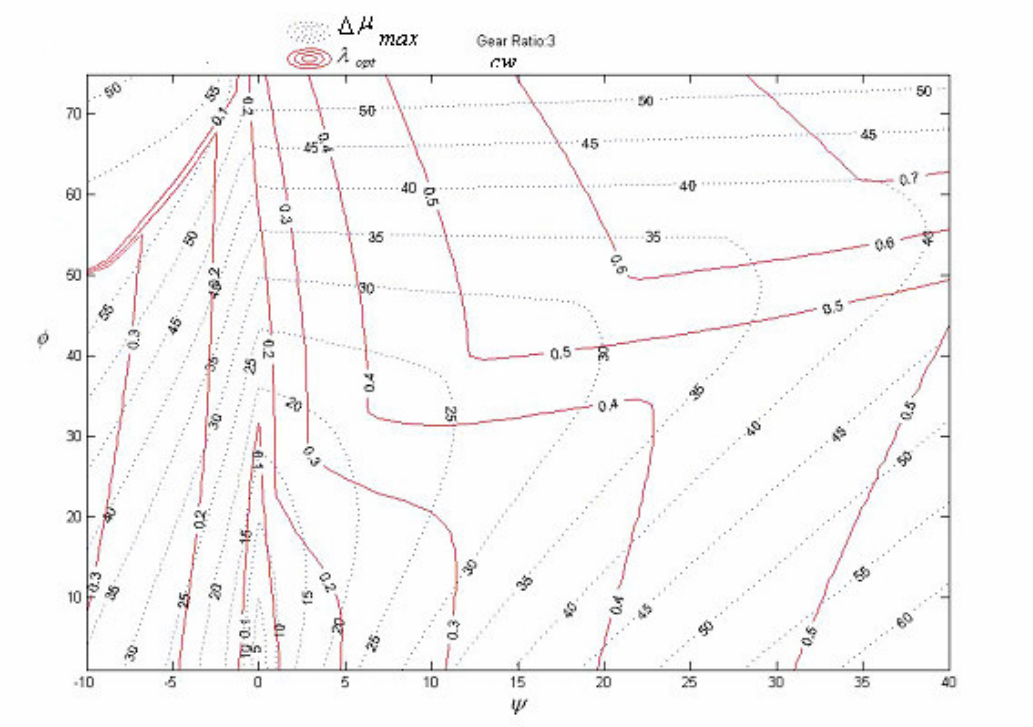


Figure A.3 Design Chart for Gear Ratio = 3, CW Input Rotation

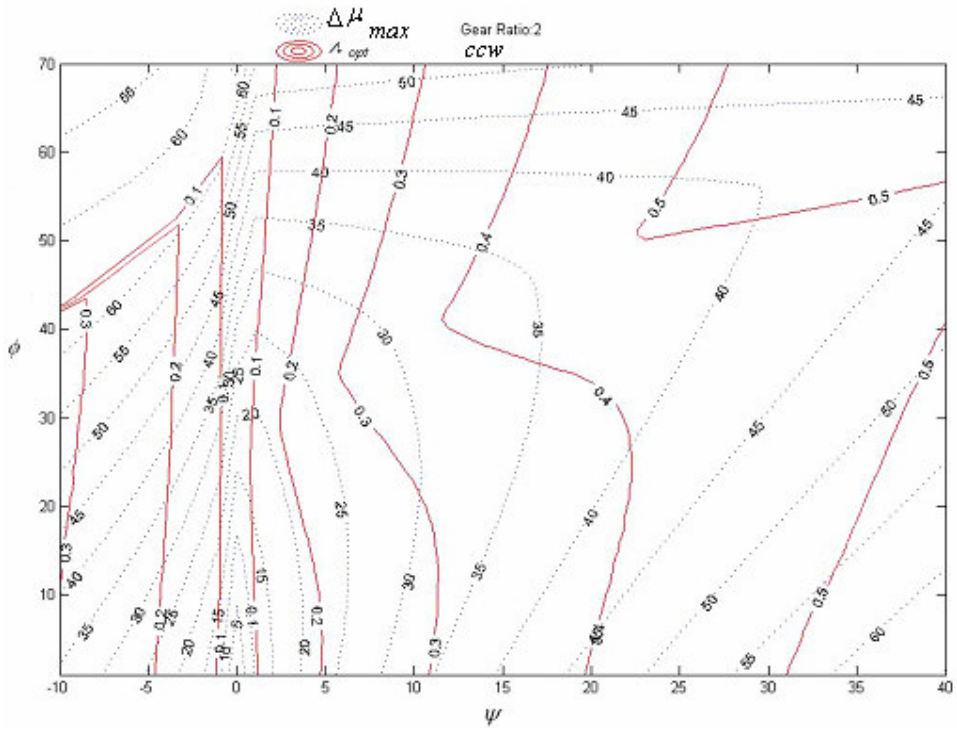


Figure A.4 Design Chart for Gear Ratio = 2, CCW Input Rotation

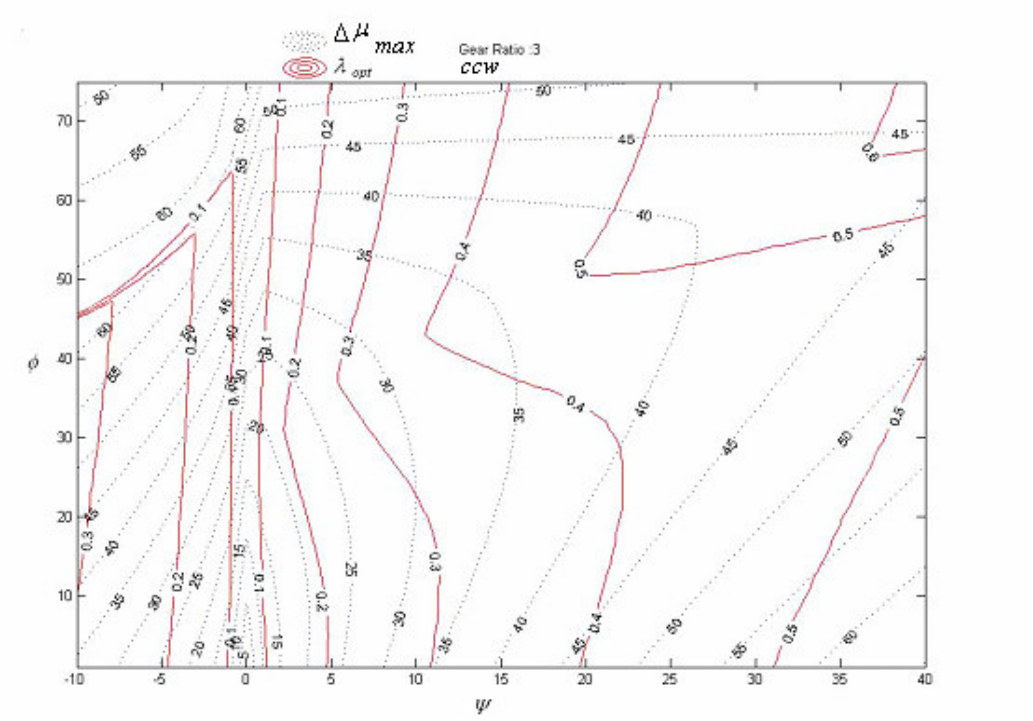


Figure A.5 Design Chart for Gear Ratio = 3, CCW Input Rotation

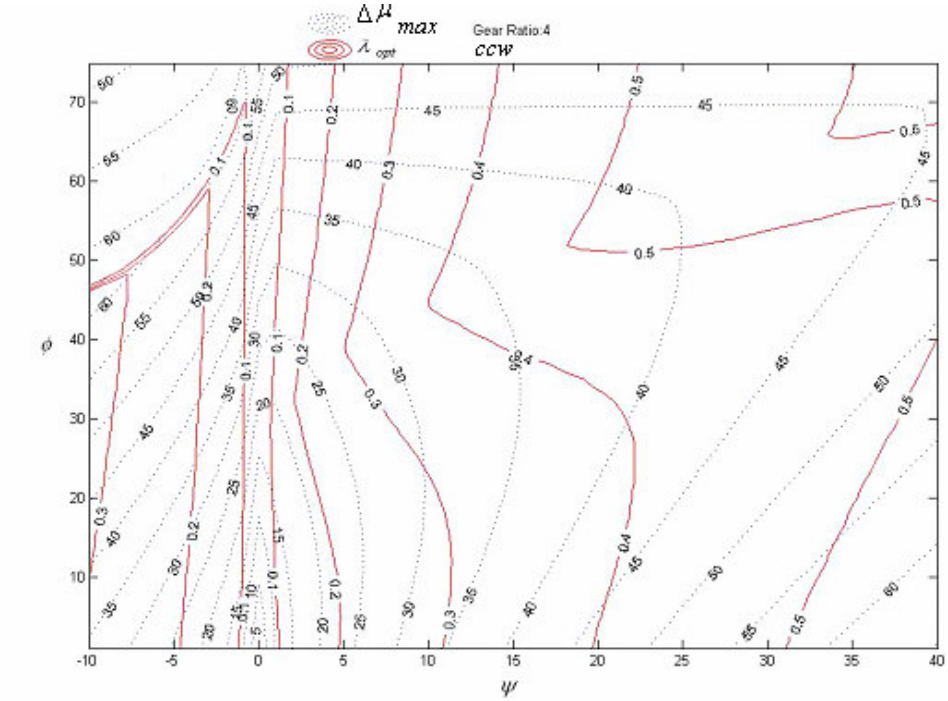


Figure A.6 Design Chart for Gear Ratio = 4, CCW Input Rotation

## APPENDIX B

## MOVING and FIXED CENTRODES of LINK 7

In order to obtain the moving and fixed centrodes of link 7, the fixed and moving coordinate axis should be established appropriately as shown in Figure B.1.

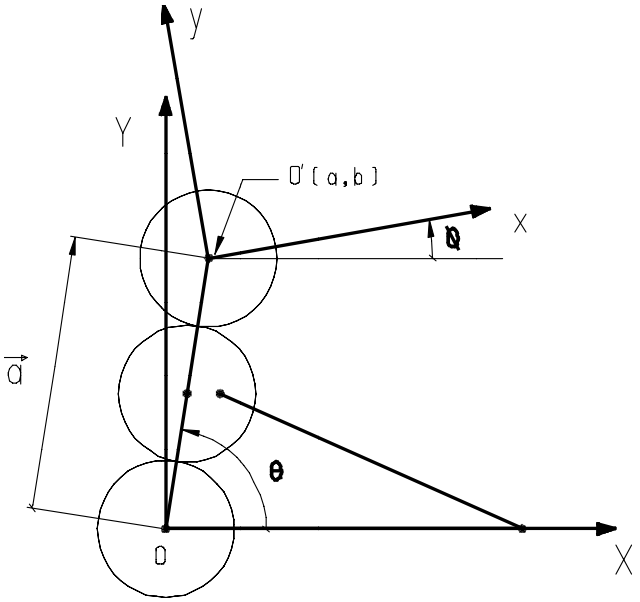


Figure B.1 Moving Coordinate Axis Attached to Link 7

The origin of the fixed axis, point O, is placed onto the center of link 5, and the origin of the moving axis, point O/, is placed onto the center of link 7.

Then, $\theta = \theta_{12}$ and $\phi = \theta_{17}$

the vector $\vec{a} = d_2 e^{i\theta_{12}}$

and

$$a = d_2 \cos\theta_{12}$$
$$b = d_2 \sin\theta_{12}$$

In polar coordinates, the moving and fixed centrodes are given as [37]:

$$\vec{z}_p = i\,\vec{a}_1\, e^{-i\phi}$$

$$\vec{Z}_p = i\,\vec{a}_1 + \vec{a}$$

$$\vec{a}_1 = \frac{d\,\vec{a}}{d\phi}$$

Then, the moving and fixed centrodes of link 7 can be determined in polar coordinates as:

$$\vec{a}_1 = \frac{d(d_2 e^{i\theta_{12}})}{d\theta_{17}} = i d_2 e^{i\theta_{12}} \frac{d\theta_{12}}{d\theta_{17}} \tag{B.1}$$

$$\vec{z}_p = -d_2 e^{i(\theta_{12}-\theta_{17})} \frac{d\theta_{12}}{d\theta_{17}} \tag{4.22}$$

$$\vec{Z}_p = d_2 e^{i\theta_{12}} (1 - \frac{d\theta_{12}}{d\theta_{17}}) \tag{4.23}$$

In cartesian coordinates the moving and fixed centrodes are given as [37]:

$$x_p = a_1 \sin\phi - b_1 \cos\phi = a_1 \sin\theta_{17} - b_1 \cos\theta_{17}$$

$$y_p = a_1 \cos\phi + b_1 \sin\phi = a_1 \cos\theta_{17} + b_1 \sin\theta_{17}$$

$$X_p = a - b_1$$

$$Y_p = b + a_1$$

Then, the moving and fixed centrodes of link 7 can be determined in cartesian coordinates as:

$$a_1 = \frac{da}{d\theta_{17}} = \frac{d(d_2 \cos\theta_{12})}{d\theta_{17}} = -d_2 \sin\theta_{12} \frac{d\theta_{12}}{d\theta_{17}} \tag{B.2}$$

$$b_1 = \frac{db}{d\theta_{17}} = \frac{d(d_2 \sin\theta_{12})}{d\theta_{17}} = d_2 \cos\theta_{12} \frac{d\theta_{12}}{d\theta_{17}} \tag{B.3}$$

$$x_p = -d_2 \frac{d\theta_{12}}{d\theta_{17}} cos(\theta_{12} - \theta_{17}) \tag{4.24}$$

$$y_p = d_2 \frac{d\theta_{12}}{d\theta_{17}} \sin(\theta_{17} - \theta_{12}) \tag{4.25}$$

$$X_p = d_2 cos\,\theta_{12} \left(1 - \frac{d\theta_{12}}{d\theta_{17}}\right) \tag{4.26}$$

$$Y_p = d_2 \sin\theta_{12} \left(1 - \frac{d\theta_{12}}{d\theta_{17}}\right) \tag{4.27}$$

The only unknown above is $\frac{d\theta_{12}}{d\theta_{17}}$. In order to obtain $\frac{d\theta_{12}}{d\theta_{17}}$, the relationship between $\theta_{12}$ and $\theta_{17}$ must be determined.

The velocity ratio between the gears 3, 7 and the arm (link 2) is:

$$-\frac{r_7}{r_3}=\frac{\omega_{13}-\omega_{12}}{\omega_{17}-\omega_{12}}=-R_2 \tag{4.2}$$

Integrating equation (3.2), $\theta_{17}$ can be determined as:

$$\theta_{17}=\frac{(R_2+1).(\theta_{12})-\theta_{13}+k_2}{R_2} \tag{4.3}$$

For a gear ratio of unity ($R_2 = 1$),

$$\theta_{13}=2\theta_{12}-\theta_{17}+k_2 \tag{B.4}$$

Another relationship is obtained from the geared five-link mechanism**.** The loop closure equation for the geared five-link mechanism is:

$$a_2.e^{i\theta_{12}}+a_3.e^{i\theta_{13}}-a_1=a_4.e^{i\theta_{14}} \tag{3.4}$$

and its complex conjugate is:

$$a_2.e^{-i\theta_{12}}+a_3.e^{-i\theta_{13}}-a_1=a_4.e^{-i\theta_{14}} \tag{3.5}$$

Multiplying (3.4) by (3.5) and rearranging terms:

$$K_1+K_2\cos(\theta_{12}-\theta_{13})-K_3\cos\theta_{12}-K_4\cos\theta_{13}=0 \tag{B.5}$$

where,

$$K_1 = a_1^2 + a_2^2 + a_3^2 - a_4^2$$

$$K_2 = 2a_2a_3$$

$$K_3 = 2a_1a_2$$

$$K_4 = 2a_1a_3$$

Then, from equations (B.4) and (B.5) the relationship between $\theta_{12}$ and $\theta_{17}$ can be detremined as:

$$K_1 + K_2\cos(-\theta_{12} + \theta_{17} - k_2) - K_3\cos\theta_{12} - K_4\cos(2\theta_{12} - \theta_{17} + k_2) = 0 \qquad \text{(B.6)}$$

Then, from equation (B.6), $\frac{d\theta_{12}}{d\theta_{17}}$ can be determined as:

$$\frac{d\theta_{12}}{d\theta_{17}} = \frac{K_2\sin(-\theta_{12} + \theta_{17} - k_2) + K_4\sin(2\theta_{12} - \theta_{17} + k_2)}{K_2\sin(-\theta_{12} + \theta_{17} - k_2) + K_3\sin\theta_{12} + 2K_4\sin(2\theta_{12} - \theta_{17} + k_2)} \qquad \text{(4.28)}$$

## APPENDIX C

## INFLECTION CIRCLE of LINK 7

The basic form of Euler-Savary equation is [37]:

$$\left(\frac{1}{r}-\frac{1}{r_c}\right)\sin\varphi=-\frac{d\theta}{ds}$$

This equation relates the point and its center of curvature, by means of differential coefficient $d\theta/ds$ which is a function of the moving plane. $d\theta/ds$ can be written as [37]:

$$\frac{d\theta}{ds}=\frac{d\theta/dt}{ds/dt}=\frac{w}{v_p}$$

$v_p$ is the speed with which the point of contact between the moving and fixed centrodes move (positive in PT direction). P is a stationary point (at that instant) on the moving plane.

Then, the kinematic form of Euler-Savary equation is [37]:

$$\left(\frac{1}{r}-\frac{1}{r_c}\right)\sin\varphi=-\frac{\omega}{v_p}$$

At each instant there are points, W, on the moving plane that have infinite radius of curvature, e.g C is at infinity. There is one point on each ray which has infinite radius of curvature and this point is called the inflection point for this ray.

Consider a ray that makes an angle $\varphi$, with PT. If PW = $r_w$ is a point on this ray with infinite radius of curvature; $1/r_c = 0$, then from Euler-Savary equation is [37]:

$$\frac{\sin\varphi}{r_w} = -\frac{d\theta}{ds}$$

If ,- $d\theta/ds = 1/\gamma$, then:

$$r_w = \gamma \sin\varphi$$

On each ray there is one point W. Hence this equation describes the locus of points which have infinite radius of curvature on the moving plane at the instant considered ($\gamma$ does not depend on the ray that is selected). If this equation is transformed in to cartesian coordinates [37]:

$$x_w^2 + \left(y_w - \frac{\gamma}{2}\right)^2 = \left(\frac{\gamma}{2}\right)^2$$

Which is the equation of a circle with center on y-axis (pole normal) and of diameter $\gamma$. This circle is known as the inflection circle. Its center is at (0, $\gamma/2$) and radius ($\gamma/2$) as shown in Fig C.1.

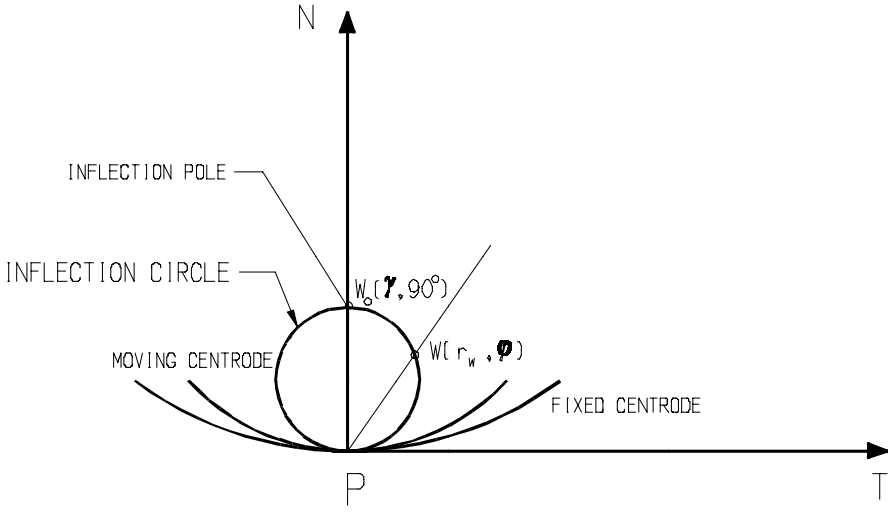


Figure C.1 The Inflection Circle and the Inflection Pole

Let O and O' be the centers of curvature of the fixed and moving centrodes. They will lie on the principal normal and will have polar coordinates $O(r_p,90^o)$ and $O'(r_\pi,90^o)$. The radii of curvature of the fixed and moving centrodes are $r_p$ and $r_\pi$ respectively Fig C.2. The inflection circle diameter, $\gamma$, can be determined if the radii of curvature of the fixed and moving centrodes are obtained. The inflection circle diameter can be determined as [37]:

$$\frac{1}{r_\pi} - \frac{1}{r_p} = \frac{1}{\gamma}$$

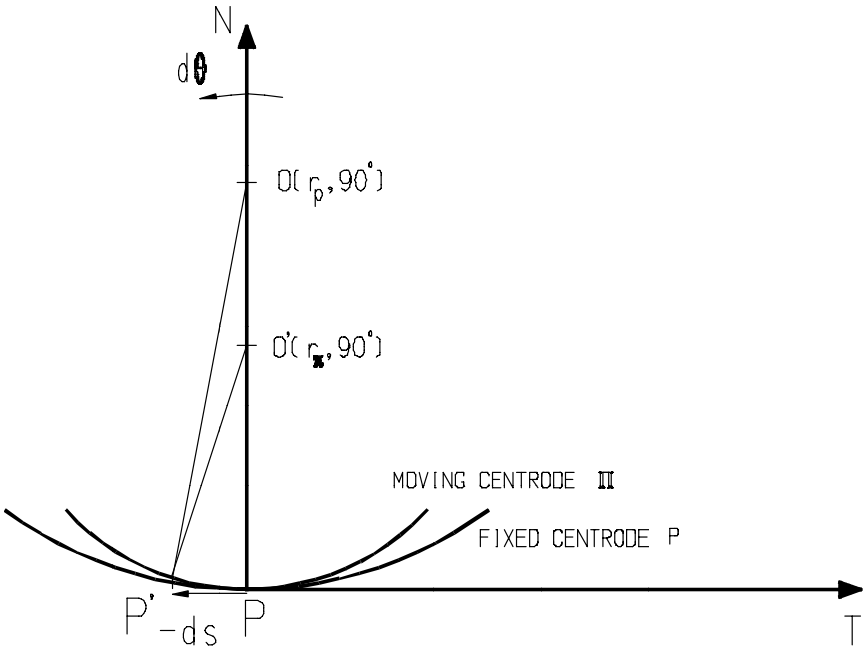


Figure C.2 Radii and Center of Curvature of the Fixed and Moving Centrodes

## APPENDIX D

### CENTER of CURVATURE of FIXED and MOVING CENTRODES

The radius of curvature of a point in cartesian form is given by the equation [37]:

$$\rho = \frac{\left(X'^2 + Y'^2\right)^{3/2}}{X''Y' - Y''X'}$$

The equations of the moving and fixed centrodes in cartesian coordinates are determined as:

$$x_p = -d_2 \frac{d\theta_{12}}{d\theta_{17}} co\,\mathrm{s}(\theta_{12} - \theta_{17}) \tag{4.24}$$

$$y_p = d_2 \frac{d\theta_{12}}{d\theta_{17}} \sin(\theta_{17} - \theta_{12}) \tag{4.25}$$

$$X_p = d_2 \cos\theta_{12}\left(1 - \frac{d\theta_{12}}{d\theta_{17}}\right) \tag{4.26}$$

$$Y_p = d_2 \sin\theta_{12}\left(1 - \frac{d\theta_{12}}{d\theta_{17}}\right) \tag{4.27}$$

First derivatives can be determined as:

$$x'_p = -d_2 \frac{d^2\theta_{12}}{d\theta_{17}{}^2}\left[\cos(\theta_{12} - \theta_{17})\right] - d_2 \frac{d\theta_{12}}{d\theta_{17}}\left[-\sin(\theta_{12} - \theta_{17})\left(\frac{d\theta_{12}}{d\theta_{17}} - 1\right)\right] \tag{D.1}$$

$$y'_p = d_2 \frac{d^2\theta_{12}}{d\theta_{17}^2}\left[\sin(\theta_{17}-\theta_{12})\right] + d_2 \frac{d\theta_{12}}{d\theta_{17}}\left[\cos(\theta_{17}-\theta_{12})\left(1-\frac{d\theta_{12}}{d\theta_{17}}\right)\right] \tag{D.2}$$

$$X'_p = -d_2 \sin\theta_{12}\left(\frac{d\theta_{12}}{d\theta_{17}} - \left(\frac{d\theta_{12}}{d\theta_{17}}\right)^2\right) - d_2 \cos\theta_{12}\frac{d^2\theta_{12}}{d\theta_{17}{}^2} \tag{D.3}$$

$$Y'_p = d_2 \cos\theta_{12}\left(\frac{d\theta_{12}}{d\theta_{17}} - \left(\frac{d\theta_{12}}{d\theta_{17}}\right)^2\right) - d_2 \sin\theta_{12}\frac{d^2\theta_{12}}{d\theta_{17}{}^2} \tag{D.4}$$

Second derivatives can be determined as:

$$x''_p = -d_2 \frac{d^3\theta_{12}}{d\theta_{17}^3}\left[\cos(\theta_{12}-\theta_{17})\right] + 2d_2 \frac{d^2\theta_{12}}{d\theta_{17}{}^2}\left[\sin(\theta_{12}-\theta_{17})\left(\frac{d\theta_{12}}{d\theta_{17}}-1\right)\right] -$$
$$d_2 \frac{d\theta_{12}}{d\theta_{17}}\left[-\cos(\theta_{12}-\theta_{17})\left(\frac{d\theta_{12}}{d\theta_{17}}-1\right)^2 - \sin(\theta_{12}-\theta_{17})\frac{d^2\theta_{12}}{d\theta_{17}{}^2}\right] \tag{D.5}$$

$$y''_p = d_2 \frac{d^3\theta_{12}}{d\theta_{17}^3}\left[\sin(\theta_{17}-\theta_{12})\right] + 2d_2 \frac{d^2\theta_{12}}{d\theta_{17}{}^2}\left[\cos(\theta_{17}-\theta_{12})\left(1-\frac{d\theta_{12}}{d\theta_{17}}\right)\right] +$$
$$d_2 \frac{d\theta_{12}}{d\theta_{17}}\left[-\sin(\theta_{17}-\theta_{12})\left(1-\frac{d\theta_{12}}{d\theta_{17}}\right)^2 - \cos(\theta_{17}-\theta_{12})\frac{d^2\theta_{12}}{d\theta_{17}{}^2}\right] \tag{D.6}$$

$$X''_p = -d_2 \cos\theta_{12}\left(\left(\frac{d\theta_{12}}{d\theta_{17}}\right)^2 - \left(\frac{d\theta_{12}}{d\theta_{17}}\right)^3 + \frac{d^3\theta_{12}}{d\theta_{17}{}^3}\right) - d_2 \sin\theta_{12}\left[\frac{d^2\theta_{12}}{d\theta_{17}{}^2} - 3\left(\frac{d\theta_{12}}{d\theta_{17}}\right).\frac{d^2\theta_{12}}{d\theta_{17}{}^2}\right] \tag{D.7}$$

$$Y_p'' = -d_2 \sin\theta_{12}\left(\left(\frac{d\theta_{12}}{d\theta_{17}}\right)^2 - \left(\frac{d\theta_{12}}{d\theta_{17}}\right)^3 + \frac{d^3\theta_{12}}{d\theta_{17}{}^3}\right) + d_2\cos\theta_{12}\left[\frac{d^2\theta_{12}}{d\theta_{17}{}^2} - 3\left(\frac{d\theta_{12}}{d\theta_{17}}\right).\frac{d^2\theta_{12}}{d\theta_{17}{}^2}\right]$$

(D.8)

From equation (B.6), $\frac{d^2\theta_{12}}{d\theta_{17}{}^2}$ can be obtained as:

$$\frac{d^2\theta_{12}}{d\theta_{17}{}^2} = \frac{K_2\cos(-\theta_{12}+\theta_{17}-k_2)\left(1-\frac{d\theta_{12}}{d\theta_{17}}\right)^2 - K_3\cos\theta_{12}\left(\frac{d\theta_{12}}{d\theta_{17}}\right)^2 - K_4\cos(2\theta_{12}-\theta_{17}+k_2)\left(2\frac{d\theta_{12}}{d\theta_{17}}-1\right)^2}{K_2\sin(-\theta_{12}+\theta_{17}-k_2)+K_3\sin\theta_{12}+2K_4\sin(2\theta_{12}-\theta_{17}+k_2)}$$

(D.9)

Then, $\frac{d^3\theta_{12}}{d\theta_{17}{}^3}$ can be obtained as:

$$\frac{d^3\theta_{12}}{d\theta_{17}{}^3} = -\frac{A+B+C}{K_2\sin(-\theta_{12}+\theta_{17}-k_2)+K_3\sin\theta_{12}+2K_4\sin(2\theta_{12}-\theta_{17}+k_2)} \qquad \text{(D.10)}$$

where,

$$A = -K_2\left[-\sin(-\theta_{12}+\theta_{17}-k_2)\left(1-\frac{d\theta_{12}}{d\theta_{17}}\right)^3 - 3\cos(-\theta_{12}+\theta_{17}-k_2)\left(1-\frac{d\theta_{12}}{d\theta_{17}}\right)\frac{d^2\theta_{12}}{d\theta_{17}{}^2}\right]$$

$$B = K_3\left[-\sin(\theta_{12})\left(\frac{d\theta_{12}}{d\theta_{17}}\right)^3 + 3\cos(\theta_{12})\left(\frac{d\theta_{12}}{d\theta_{17}}\right)\frac{d^2\theta_{12}}{d\theta_{17}{}^2}\right]$$

$$C = K_4\left[-\sin(2\theta_{12}-\theta_{17}+k_2)\left(2\frac{d\theta_{12}}{d\theta_{17}}-1\right)^3 + 6\cos\left(2\theta_{12}-\theta_{17}+k_2\right)\left(2\frac{d\theta_{12}}{d\theta_{17}}-1\right)\frac{d^2\theta_{12}}{d\theta_{17}{}^2}\right]$$

Then, the radius of curvature of the fixed and moving centrodes can be evaluated as:

$$\rho = \frac{\left(X_P'^2 + Y_P'^2\right)^{3/2}}{X_P'' Y_P' - Y_P'' X_P'} \tag{D.11}$$

Let O and O' be the centers of curvature of the fixed and moving centrodes. They will lie on the principal normal. The slope of the centrodes is $\zeta$, and it can be evaluated throughout the cycle since the equations of the centrodes are obtained (Fig.D.1). $\upsilon$ is the angle between the positive X-axis and pole normal, where:

$$\upsilon = \frac{\pi}{2} + \varsigma \tag{D.12}$$

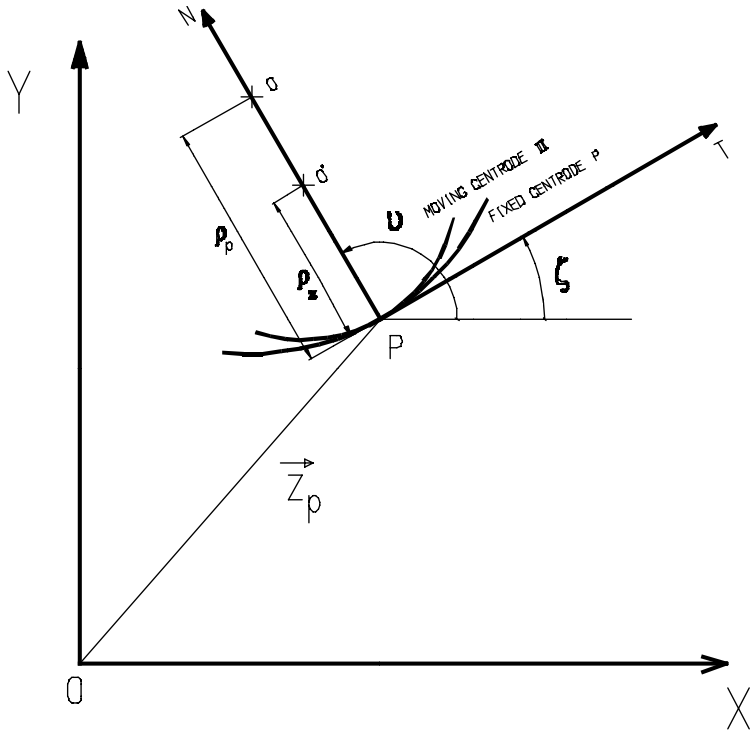


Figure D.1 Centers of Curvature of the Fixed and Moving Centrodes

The radii of curvature of the fixed and moving centrodes are $\rho_p$ and $\rho_\pi$ respectively. The center of curvature of a point is given by the equation [37].

$$r_c = \rho + r$$

Since the point is the pole, while evaluating the centers of curvature of the fixed and moving centrodes $r = 0$, then:

$$r_o = \rho_p \tag{D.13}$$

$$r_{o'} = \rho_\pi \tag{D.14}$$

Therefore, centers of curvature of the fixed and moving centrodes in cartesian coordinates are:

$$\vec{r}_\pi = \vec{Z}_p + \rho_\pi e^{iv} \tag{D.15}$$

$$\vec{r}_p = \vec{Z}_p + \rho_p e^{iv} \tag{D.16}$$

## APPENDIX E

## USE of NON-INTEGER GEAR RATIO

It was mentioned that, if $R_2$ is not an integer and $R_2 \neq ½$, then the output motion will complete a cycle after several cycles of the input link rotation. At each cycle of the input, the output stroke decreases, then after few cycles, for every cycle of the input, output stroke starts increasing and the mechanism completes a cycle after several cycles of the input. This property can also be used for stroke adjustment. The number of these cycles can be determined by a method.

Let the gear ratio between the gears 3 and 5, $R_1$ is equal to unity, and the gear ratio between gears 7 and 3, $R_2$ is not an integer (Fig. E.1).

Let $R_2 = 1.t$ (like 1.3, where $t$ is an integer), then the velocity ratio between the gears 5, 7 and the arm (link 2) is:

$$\frac{\omega_{17} - \omega_{12}}{\omega_{15} - \omega_{12}} = \frac{r_5}{r_7} = \frac{1}{1.t} \tag{E.1}$$

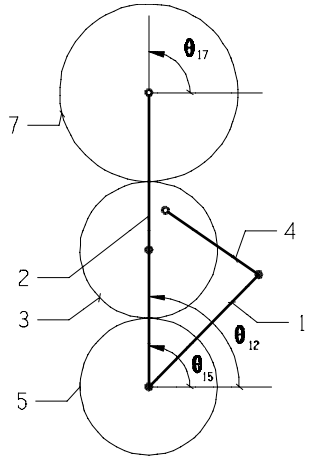


Figure E.1 A Mechanism where $R_2$ is not an Integer

Integrating Eq. E.1:

$$1.t\theta_{17} = \theta_{15} + 0.t\theta_{12} + k \tag{E.2}$$

If initially $\theta_{17i} = \theta_{15i} = \theta_{12i}$ like in Fig. E.1, then the integration constant $k = 0$, then:

$$1.t\theta_{17} = \theta_{15} + 0.t\theta_{12} \tag{E.3}$$

At the end of each cycle, the arm (link 2) comes to its initial position, so at the end of each cycle $\theta_{12} = \theta_{15i}$ . After $n$ cycles Eq. E.3 can be written as:

$$1.t\theta_{17} = (\theta_{15i} + n2\pi) + 0.t\theta_{15i} \tag{E.4}$$

Manupilating Eq. E.4:

$$\theta_{17} = \theta_{15i} + \frac{n}{1.t}2\pi \tag{E.5}$$

From equation E.5, it is clear that if $\frac{n}{1.t}$ is an integer, then $\theta_{17} = \theta_{15i}$, link 7 comes to its initial position.

Similarly if $R_2 = 0.t$ (where $t$ is an integer), $\theta_{17}$ can be detremined after $n$ cycles as:

$$\theta_{17} = \theta_{15i} + \frac{n}{0.t}2\pi \tag{E.6}$$

From equation E.6, it is clear that if $\frac{n}{0.t}$ is an integer, then $\theta_{17} = \theta_{15i}$, link 7 comes to its initial position.

For example, if $R_2$ = 1.1, then $\theta_{17}$ comes to its initial position after $n$ =11 cycles $\left(\frac{11}{1.1}=10\right)$. If $R_2$ = 1.2, then $\theta_{17}$ comes to its initial position after $n$ = 6 cycles $\left(\frac{6}{1.2}=5\right)$. If $R_2$ = 0.7, then $\theta_{17}$ comes to its initial position after $n$ =7 cycles $\left(\frac{7}{0.7}=10\right)$. If $R_2$ = 0.8, then $\theta_{17}$ comes to its initial position after $n$ = 4 cycles $\left(\frac{4}{0.8}=5\right)$. It is observed that if $R_2$ is an odd number, then number of cycles can be calculated as: $n = 10R_2$, if $R_2$ is an even number, then number of cycles can be calculated as: $n = 5R_2$.

If Example 4.4 is reconsidered with an only difference of $R_2$ = 1.1 instead of unity, then, the path of point E and endpoint of the arm are shown in Fig E.2. The output reciprocating motion is shown in Fig E.3 (Note that 3960/360=11).

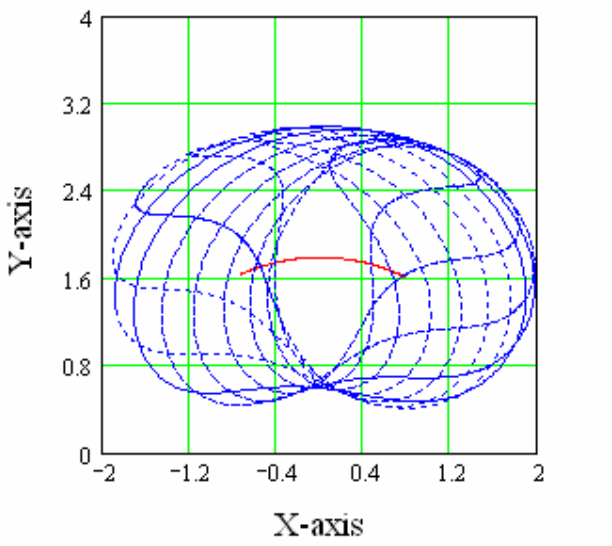


Figure E.2 The Path of Point E and Endpoint of the Arm where $R_2$ = 1.1

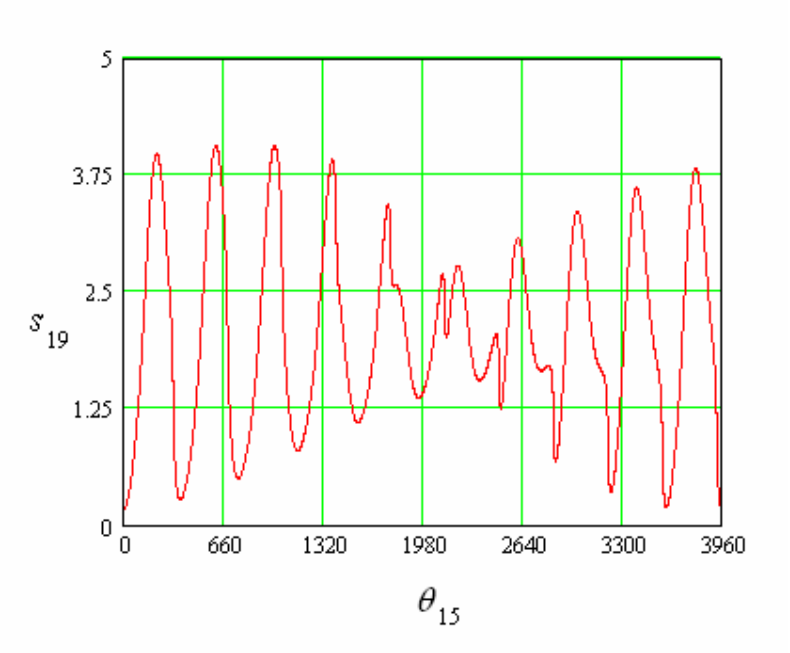


Figure E.3 The Output Reciprocating Motion where $R_2 = 1.1$

## APPENDIX F

## CODE for DESIGN CHARTS of the GFLM

```
clear
clc
for n=1:75;
fi=(n)*pi/180;
for m=1:51;
si=(m-11)*pi/180;
for k=1:850;
   lambda=k*0.001;
   Z1=((1-lambda)-(1+lambda)*exp(i*si))/((1-lambda)*exp(i*fi)-
(1+lambda)*exp(i*si));
   Z2=(1-exp(i*fi))/((1-lambda)*exp(i*fi)-(1+lambda)*exp(i*si));
   a1=1;
   a2=sqrt(Z1*conj(Z1));
   a4=sqrt(Z2*conj(Z2));
   a3=a4*lambda;
   K1=a1^2+a2^2+a3^2-a4^2;
   K2=2*a2*a3;
   K3=2*a1*a2;
   K4=2*a1*a3;
   alfa=(14.5)*pi/180;
   r2=4*a2/5;
   for j=1:361
      teta3=(j-1)*pi/180;
      A=K1-K2*cos(teta3)+K3-K4*cos(teta3);
      B=2*K2*sin(teta3);
```

```
        C=K1+K2*cos(teta3)-K3-K4*cos(teta3);
        teta2(j)=2*atan2((-B+sqrt(B^2-4*A*C)),(2*A));
        teta4(j)=angle(a2*exp(i*teta2(j))+a3*exp(i*teta3)-a1);
        transr(j)=atan2(-((a3/r2)*sin(teta4(j)-teta3)+sin(teta4(j)-
teta2(j))),((a3/r2)*tan(pi-alfa)*sin(teta4(j)-teta3)+cos(teta4(j)-teta2(j))));
        if transr(j)>0
        transr(j)=transr(j);
        else
        transr(j)=transr(j)+pi;
        end
    end
    [maxtransr,maxteta3r]=max(transr);
    [mintransr,minteta3r]=min(transr);
    if abs(maxtransr-(pi/2))>abs((pi/2)-mintransr)
        maxtransr=maxtransr;
        maxteta3r=maxteta3r;
    else
        maxtransr=mintransr;
        maxteta3r=minteta3r;
    end
    maxTRr(k)=maxtransr;
    maxTETA3r(k)=maxteta3r;
    deltaTRr(k)=abs(maxTRr(k)-pi/2);
end
[OptTRr,Optlamda]=min(deltaTRr);
OptimumTRr(n,m)=OptTRr*180/pi;
Optimumlamda(n,m)=Optlamda*0.001;
end
end
clf
%row
X=1:51;
```

```
x=(X-11);
%column
Y=1:75;
y=Y;
%data matrix
z=OptimumTRr;
%contour lines
v1=[5 10 15 20 25 30 35 40 45 50 55 60 65 70 75]
l=Optimumlamda;
v2=[0.1 0.2 0.3 0.4 0.5 0.6 0.7 0.8];
[C,h] = contour(x,y,z,v1,':b','LineWidth',1);
set(h,'ShowText','on','TextStep',get(h,'LevelStep')*2)
hold on
[C,h] = contour(x,y,l,v2,'-r','LineWidth',1);
set(h,'ShowText','on','TextStep',get(h,'LevelStep')*2)
```

## APPENDIX G

## CODE for OPTIMIZATION CHARTS of the GASM

```
clear
clc
for n=1:50;
fi=(n)*pi/180;
for m=1:51;
si=(m-6)*pi/180;
for k=1:600;
   lambda=k*0.001;
   Z1=((1-lambda)-(1+lambda)*exp(i*si))/((1-lambda)*exp(i*fi)-
(1+lambda)*exp(i*si));
   Z2=(1-exp(i*fi))/((1-lambda)*exp(i*fi)-(1+lambda)*exp(i*si));
   a1=1;
   a2=sqrt(Z1*conj(Z1));
   a4=sqrt(Z2*conj(Z2));
   a3=a4*lambda;
   K1=a1^2+a2^2+a3^2-a4^2;
   K2=2*a2*a3;
   K3=2*a1*a2;
   K4=2*a1*a3;
   alfa=(14.5)*pi/180;
   r2=a2/2;
   for j=1:361
      teta3=(j-1)*pi/180;
      A=K1-K2*cos(teta3)+K3-K4*cos(teta3);
```

```
        B=2*K2*sin(teta3);
        C=K1+K2*cos(teta3)-K3-K4*cos(teta3);
        teta2(j)=2*atan2((-B+sqrt(B^2-4*A*C)),(2*A));
        teta4(j)=angle(a2*exp(i*teta2(j))+a3*exp(i*teta3)-a1);
        transr(j)=atan2(-((a3/r2)*sin(teta4(j)-teta3)+sin(teta4(j)-
teta2(j))),((a3/r2)*tan(pi-alfa)*sin(teta4(j)-teta3)+cos(teta4(j)-teta2(j))));
        if transr(j)>0
        transr(j)=transr(j);
        else
        transr(j)=transr(j)+pi;
        end
    end
    [maxtransr,maxteta3r]=max(transr);
    [mintransr,minteta3r]=min(transr);
    if abs(maxtransr-(pi/2))>abs((pi/2)-mintransr)
        maxtransr=maxtransr;
        maxteta3r=maxteta3r;
    else
        maxtransr=mintransr;
        maxteta3r=minteta3r;
    end
    maxTRr(k)=maxtransr;
    maxTETA3r(k)=maxteta3r;
    deltaTRr(k)=abs(maxTRr(k)-pi/2);
end
[OptTRr,Optlamda]=min(deltaTRr);
Optimumlamda=Optlamda*0.001;
i=sqrt(-1);
Z1=((1-Optimumlamda)-(1+Optimumlamda)*exp(i*si))/((1-
Optimumlamda)*exp(i*fi)-(1+Optimumlamda)*exp(i*si));
Z2=(1-exp(i*fi))/((1-Optimumlamda)*exp(i*fi)-(1+Optimumlamda)*exp(i*si));
a1=1;
```

```
a2=sqrt(Z1*conj(Z1));
a4=sqrt(Z2*conj(Z2));
a3=a4*Optimumlamda;
r3=a2/2;
a7=r3*0.9;
arm=2*a2;
   K1=a1^2+a2^2+a3^2-a4^2;
   K2=2*a2*a3;
   K3=2*a1*a2;
   K4=2*a1*a3;
   Maximumstroke=0;
   for j=1:361
      teta3=(j-1)*pi/180;
      A=K1-K2*cos(teta3)+K3-K4*cos(teta3);
      B=2*K2*sin(teta3);
      C=K1+K2*cos(teta3)-K3-K4*cos(teta3);
      teta2(j)=2*atan2((-B+sqrt(B^2-4*A*C)),(2*A));
   end
      a=max(teta2);
      b=min(teta2);
      averageteta2=(max(teta2)+min(teta2))/2;
      delta=(pi/2-averageteta2);
      deltas=delta-6*pi/180;
   for u=1:11
      del=deltas+(u)*pi/180;
    for t=1:51
         k2=(t-41)*pi/180;
     for j=1:361
      teta3=(j-1)*pi/180;
      A=K1-K2*cos(teta3-del)+K3-K4*cos(teta3-del);
      B=2*K2*sin(teta3-del);
      C=K1+K2*cos(teta3-del)-K3-K4*cos(teta3-del);
```

```
        teta2=2*atan2((-B+sqrt(B^2-4*A*C)),(2*A))+del;
        teta7=2*teta2-teta3+k2;
        path(j)= arm*exp(i*teta2)+a7*exp(i*teta7);
        realpath(j)=real(path(j));
        impath(j)=imag(path(j));
       end
        [smax,ct3]=max(realpath);
        [smin,ct3]=min(realpath);
        [hmax,ct3]=max(impath);
        [hmin,ct3]=min(impath);
          stroke=smax-smin;
          if  stroke>Maximumstroke
              Maximumstroke=stroke;
              optimumk2(n,m)=k2*180/pi;
              optimumdelta(n,m)=del*180/pi;
          end
        end
    end
end
end
clf
%row
X=1:51;
x=(X-6);
%column
Y=1:50;
y=Y;
%data matrix
z=optimumk2;
%contour lines
l=optimumdelta;
v2=[15 20 30 40 50 55 60 70 80]
```

```
[C,h] = contour(x,y,z,':b','LineWidth',1);
set(h,'ShowText','on','TextStep',get(h,'LevelStep')*2)
hold on
[C,h] = contour(x,y,l,v2,'-r','LineWidth',1);
set(h,'ShowText','on','TextStep',get(h,'LevelStep')*2)
```

## APPENDIX H

### CODE for STROKE CHARTS of the GASM

```
clear
clc
fi=50*pi/180;
si=10*pi/180;
lamda=0.505;
i=sqrt(-1)
Z1=((1-lamda)-(1+lamda)*exp(i*si))/((1-lamda)*exp(i*fi)-(1+lamda)*exp(i*si));
Z2=(1-exp(i*fi))/((1-lamda)*exp(i*fi)-(1+lamda)*exp(i*si));
a1=1;
a2=sqrt(Z1*conj(Z1));
a4=sqrt(Z2*conj(Z2));
a3=a4*lamda;
r3=a2/2;
a7=r3*0.9;
arm=2*a2;
   K1=a1^2+a2^2+a3^2-a4^2;
   K2=2*a2*a3;
   K3=2*a1*a2;
   K4=2*a1*a3;
   for j=1:361
      teta3=(j-1)*pi/180;
      A=K1-K2*cos(teta3)+K3-K4*cos(teta3);
      B=2*K2*sin(teta3);
      C=K1+K2*cos(teta3)-K3-K4*cos(teta3);
      teta2(j)=2*atan2((-B+sqrt(B^2-4*A*C)),(2*A));
```

```
    end
       a=max(teta2);
       b=min(teta2);
       averageteta2=(max(teta2)+min(teta2))/2;
       delta=(pi/2-averageteta2);
       deltas=delta-101*pi/180;
    for k=1:201
       del=deltas+k*pi/180;
       for t=1:361
          k2=(t-181)*pi/180;
      for j=1:361
       teta3=(j-1)*pi/180;
       A=K1-K2*cos(teta3-del)+K3-K4*cos(teta3-del);
       B=2*K2*sin(teta3-del);
       C=K1+K2*cos(teta3-del)-K3-K4*cos(teta3-del);
       teta2=2*atan2((-B+sqrt(B^2-4*A*C)),(2*A))+del;
       teta7=2*teta2-teta3+k2;
       path(j)= arm*exp(i*teta2)+a7*exp(i*teta7);
       realpath(j)=real(path(j));
       impath(j)=imag(path(j));
      end
       [smax,ct3]=max(realpath);
       [smin,ct3]=min(realpath);
       [hmax,ct3]=max(impath);
       [hmin,ct3]=min(impath);
         stroke(k,t)=smax-smin;
         h(k,t)=hmax-hmin;
       end
    end
    clf
%row
X=1:361;
```

```
x=X-181;
%column
Y=1:201;
y=deltas*180/pi+Y;
%data matrix
z=stroke;
%contour lines
v1=[0.8 1 1.2 1.4 1.6 1.8 2 2.1 2.11 2.12 2.132 2.136 2.137 2.1371];
l=h;
v2=[0.6 0.65 0.7 0.75 0.8 0.85 0.9 0.95 1 1.05 1.1 1.15];
[C,h] = contour(x,y,z,v1,':b','LineWidth',1);
set(h,'ShowText','on','TextStep',get(h,'LevelStep')*2)
hold on
[C,h] = contour(x,y,l,'-r','LineWidth',1);
set(h,'ShowText','on','TextStep',get(h,'LevelStep')*2)
```

## REFERENCES


[1] Ingenious Mechanisms for Designers and Inventors, Vol.3, p.237, 1956.

[2] Chironis, N., P., "Mechanisms, Linkages, and Mechanical Controls", McGraw-Hill Book Company, 1965.

[3] Neumann, R., "Einstellbare fünfgliedrige Raderkoppelgetriebe", Maschinenbautechnik, Vol. 28, pp. 211-215, 1979.

[4] Neumann, R., "Bauelemente Auslegung von Getrieben Berechnung von Getrieben mit grossem Schwingwinkel", Maschinenbautechnik, Vol. 29, pp. 405-406, 1980.

[5] Neumann, R., "Kinematische und kinetische Untersuchungen eines Raderkoppelgetriebes mit grossem Schwingwinkel", Maschinenbautechnik, Vol. 29, pp. 399-404, 1980.

[6] Volmer, J., Riedel, H., Rissman, E., "Bauelemente Auslegung von Getrieben Berechnung von Schritt und Pilgerschrittgetrieben", Maschinenbautechnik, Vol. 29, pp. 121-124, 1980.

[7] Volmer, J., "Rationalisierungsmittel für den konstrukteurarbeitsblaetter zur auslegung von getrieben", Maschinenbautechnik, Vol. 29, pp. 125-127, 1980.

[8] Volmer, J., Meiner, C., "Bauelemente Auslegung von Getrieben Berechnung von Schritt und Pilgerschrittgetrieben", Maschinenbautechnik, Vol. 27, pp. 219-220, 1978.

[9] Yüksel, Ş., Söylemez, E., "Dişli Çubuk Mekanizmalarının Bilgisayar Yardımıyla Tasarımı", Yüksek Lisans Tezi, G.Ü, 1988.

[10] Erdman, A.G., Sandor, G.N., “Kinematic synthesis of a geared five-bar function generator”, Journal of Engineering for Industry, Trans. ASME, Vol. 93, pp. 11-16, 1971.

[11] Oleska, S.A., Tesar, D., “Multiply seperated position design of the geared five-bar function generator”, Journal of Engineering for Industry, Trans. ASME, Vol. 93, pp. 74-84, 1971.

[12] Mohanrao, A.V., Sandor, G.N., “Extension of Freudenstein’s equation to geared linkages”, Journal of Engineering for Industry, Trans. ASME, Vol. 93, pp. 201-210, 1971.

[13] Lin, C.K., Chiang, C.H., “Synthesis of planar and spherical geared five-bar function generators by the pole method”, Mechanisms and Machine Theory, Vol.27, Issue 2, pp.131-141, 1992.

[14] Lee, T.W., Freudenstein, F., “Design of geared 5-bar mechanisms for unlimited crank rotations and optimum transmission”, Mechanisms and Machine Theory, Vol.13, Issue 2, pp.235-244, 1978.

[15] Rao, A.C., “Synthesis of geared planar 4-bar linkages and cams to generate function of two variables”, Mechanisms and Machine Theory, Vol.15, Issue 2, pp.137-143, 1980.

[16] Li, T., Cao, W., “Kinematic Synthesis of Planar Geared Four-BarLinkages with Prescribed Dwell Characteristics” Proceedings of the 11th World Congress in Mechanism and Machine Science April 1-4, 2004, Tianjin, China.

[17] Erdman, A., G., Hong, B., “A Method for Adjustable Planar and Spherical Four-Bar Linkage Synthesis” J. of Mechanical Design, Transactions of ASME, Vol. 127, pp.456-462, May 2005.

[18] Sodhi, R.S., Russell, K., "Kinematic synthesis of planar four-bar mechanisms for multi-phase motion generation with tolerances" Mechanic Based Design of Structures and Machines, Volume 32, Issue 2, May 2004, Pages 215-233.

[19] Russell, K., Sodhi R. S. "Kinematic synthesis of adjustable RRSS mechanisms for multi-phase motion generation." Mechanism and Machine Theory, 36 (8), pp. 939-952, 2001.

[20] Russell,K., Sodhi,R.S. "Kinematic synthesis of RRSS mechanisms for multi-phase motion generation with tolerances" Mechanism and Machine Theory, 37 (3), pp. 279-294, 2002.

[21] Russell,K., Sodhi,R.S. "Kinematic synthesis of planar five-bar mechanisms for multi-phase motion generation" JSME International Journal, Series C: Mechanical Systems, Machine Elements and Manufacturing 47 (1), pp. 345-349, 2004.

[22] Russell,K., Sodhi,R.S. " On the design of slider-crank mechanisms. Part I: Multi-phase motion generation " Mechanism and Machine Theory 40 (3), pp. 285-299, 2005.

[23] Russell,K., Sodhi,R.S. " On the design of slider-crank mechanisms. Part II: Multi-phase path and function generation " Mechanism and Machine Theory 40 (3), pp. 301-317, 2005.

[24] J.F. McGroven, G.N. Sandor, "Kinematic synthesis of adjustable mechanisms (Part 1: function generation)", ASME Journal of Engineering for Industry 95 (2), 417–422, 1973.

[25] J.F. McGroven, G.N. Sandor, "Kinematic synthesis of adjustable mechanisms (Part 2: path generation)", ASME Journal of Engineering for Industry 95 (2) 423–429, 1973.

[26] A. Ahmad, K.J. Waldron, “Synthesis of adjustable planar 4-bar mechanisms”, Mechanism and Machine Theory 14 (3), 405–411, 1979.

[27] H. Zhou, Kwun-Lon Ting, “Adjustable slider–crank linkages for multiple path generation”, Mechanism and Machine Theory 37, 499–509, 2002.

[28] Kohli, D., Soni, A. H., “Synthesis of Seven Link Mechanisms”, Journal of Engineering for Industry, Trans. ASME, pp. 533-540, May 1973.

[29] Mruthyunjaya, T. S., “A Note on Synthesis of the General, Two-Degree-of-Freedom Linkage”, Mechanism and Machine Theory (10), pp.77–88, 1975.

[30] Handra-Luca V., “The Study of Adjustable Oscillating Mechanisms", Journal of Engineering for Industry, Trans. ASME, pp. 677-680, August 1973.

[31] Akmeşe, A., Söylemez, E., “Two Degrees of Freedom Adjustable Mechanisms Design", M.S Thesis, METU, 1999.

[32] Tanık, E., Söylemez, E “Variable Structure Mechanisms Design”, The Ninth IFToMM International Symposium on Theory of Machines and Mechanisms, 2005.

[33] Kireççi, A., Dülger, C., Gültekin, M., “Design of Hybrid Actuator” 8. International Machine Design and Production Conference Proceedings, pp. 65-74, September 1998.

[34] Long, M., “Variable Dwell Cycloidal Indexing Device”, Patent no: US5692986, 2001

[35] Dizioğlu, B. “Mekanizma Tekniği”, İTÜ Kütüphanesi, 761, İstanbul, 1969.

[36] F.Freudenstein, F. P. Primrose, “The Classical Transmission Angle Problem”, The Institution of Mechanical Engineers, C96/72, Mechanisms 1972, London.

[37] R.Beyer, “The Kinematic Synthesis of Mechanisms”, Chapman and Hall, 1963, London.

# CURRICULUM VITAE

**PERSONAL INFORMATION**

Surname, Name: Parlaktaş, Volkan
Nationality: Turkish (TC)
Date and Place of Birth: 1 June 1974 , Ankara
Marital Status: Single
Phone: +90 532 2949297
email: pvolkan@metu.edu.tr

**EDUCATION**

| Degree | Institution | Year of Graduation |
|---|---|---|
| MS | METU Mechanical Engineering | 2001 |
| BS | G.U Mechanical Engineering | 1998 |

**WORK EXPERIENCE**

| Year | Place | Enrollment |
|---|---|---|
| 2005- | METU Department of Mechanical Engineering | Instructor |
| 2000-2005 | METU Department of Mechanical Engineering | Teaching Assistant |

**FOREIGN LANGUAGES**

Advanced English

**PUBLICATIONS**

Parlaktaş V., Söylemez E. “Beklemeli Hareket Yapan Uzaysal Mekanizmaların Tasarımı”, MATİM, Cilt:8, Sayı:2, Kasım 2006.

Söylemez E., Parlaktaş V. "Use of Spatial Four-Bar Mechanism for the Synthesis of Mechanisms with Large Dwell", Proceedings IFToMM on 11th Congress in Mechanisms and Machine Science, Nisan 2004, Tianjin (Çin), s.1103-1008.

Parlaktaş V., Söylemez E. “Uzaysal Dört Çubuk Mekanizması Kullanılarak Beklemeli Mekanizma Tasarımı”, UMTS 2001, 10. Ulusal Makina Teorisi Sempozyumu, Eylül 2001, Konya.